UNIVERSITY OF CYPRUS

DEPARTMENT OF BIOLOGICAL SCIENCES

ELUCIDATION OF THE MECHANISM OF PROOXIDANT AND CYTOTOXIC ACTIVITIES OF THE OLIVE SECOIRIDOID OLEUROPEIN

ELENA M. ODIATOU

PhD THESIS

JUNE 2013

BOARD OF EXAMINERS

Andreas Constantinou, Professor, University of Cyprus

Constantinos Deltas, Professor, University of Cyprus

Pantelis Georgiades, Assistant Professor, University of Cyprus

Ourania Tsitsiloni, Assistant Professor, National and Kapodistrian University of Athens

Andreas Hadjisavvas, Scientist, The Cyprus Institute of Neurology and Genetics

ABSTRACT

The ability of the olive secoiridoid oleuropein and its metabolite hydroxytyrosol to produce hydrogen peroxide (H_2O_2) under standard culture conditions has been previously reported by others [1,2,3]. However, the exact conditions and the mechanism of H_2O_2 production remain unknown. Specifically, it is not known whether the H_2O_2 production is strictly dependent on the chemical properties of the compound, the culture media components, other cell culture conditions, or a combination of these. More importantly, it is unknown if the cell-killing effects of the olive polyphenol-generated H_2O_2 are limited to cancer cells, or affect equally normal cells.

The aims of this study were to identify the precise conditions that lead to the H_2O_2 production by oleuropein and hydroxytyrosol, to determine if cancer cells are more susceptible to the deleterious effects of the produced H_2O_2 and elucidate the precise molecular mechanism of cell death. We have explored the capacity of oleuropein to produce H_2O_2 in the most commonly used culture media (i.e. DMEM, MEM and DMEM/F12). We have also evaluated the contribution of the MEM medium components to the production of H_2O_2, as well as the contribution of the culture conditions (i.e. pH). Moreover, the implication of many apoptotic and necrotic proteins were investigated in order to clarify the exact pathway that leads to cell death.

The precise factors responsible for the H_2O_2 production and the conditions promoting or retarding it are critical for the interpretation of the *in vitro* results. In this study, a systematic evaluation of the components of the most commonly used culture media revealed that sodium bicarbonate by stabilizing the medium pH at values above 7, is the defining cause for the production of H_2O_2 by these phenols.

The produced H_2O_2 caused extensive oxidative DNA damage and significant decrease in cell viability of cancer (MDA-MB-231) and normal (MCF-10A, STO) cells alike. Sodium pyruvate and the antioxidant N-acetyl cysteine (NAC) reversed these effects. Therefore, we conclusively identified the culture conditions that promote H_2O_2 production by these polyphenols, producing artifacts that may be misinterpreted as a specific anticancer activity. Our findings raise considerable questions regarding the use of culture media with sodium bicarbonate or sodium pyruvate as components, for the *in vitro* study of these and possibly other plant polyphenols.

Furthermore, we have elucidated the exact molecular mechanism of cell death in the breast cancer cell line MDA-MB-231. Oleuropein was shown to promote the MAPK and PARP-1 activation, PAR production and necrosis through mitochondrial and lysosomal membrane destabilization. This mode of cell death is common in cells treated with H_2O_2.

Our data give a complete description of the *in vitro* behavior of oleuropein with a detail characterization and explanation of the observed cytotoxicity in the molecular level. These results may enable cancer researchers to control the levels of H_2O_2 produced during the *in vitro* testing of plant polyphenols, and to design more meaningful *in vitro* and *vivo* studies.

ΠΕΡΙΛΗΨΗ

Η ικανότητα της πολυφαινόλης ολευροπαΐνης που συναντάται στο δέντρο της ελιάς όπως και του μεταβολίτη της υδροξυτυροσόλης να παράγουν υπεροξείδιο του υδρογόνου (H_2O_2) σε κανονικές συνθήκες καλλιέργειας έχει ήδη καταδειχθεί από άλλους ερευνητές. Οι υπεύθυνες συνθήκες όμως καθώς κι ο συγκεκριμενος μηχανισμός της παραγωγής H_2O_2 παραμένουν άγνωστα. Πιο συγκεκριμένα, είναι άγνωστο αν η παραγωγή του H_2O_2 είναι αυστηρά εξαρτώμενη από τις χημικές ιδιότητες της ολευροπαΐνης, από τα συστατικά του θρεπτικού καλλιέργειας, από τις συνθήκες καλλιέργειας ή συνδιασμό αυτών. Είναι επίσης άγνωστο αν η κυτταροτοξική επίδραση του παραγόμενου H_2O_2 περιορίζεται στα καρκινικά κύτταρα ή επηρεάζει εξίσου και τα φυσιολογικά κύτταρα.

Οι στόχοι της παρούσας εργασίας ήταν να ταυτοποιήσουμε τις συγκεκριμένες συνθήκες που οδηγούν σε παραγωγή H_2O_2 από την ολευροπαΐνη και την υδροξυτυροσόλη, να προσδιορίσουμε αν τα καρκινικά κύτταρα είναι πιο ευάλωτα στην τοξική επίδραση του H_2O_2 και να διασαφηνίσουμε τον ακριβή μοριακό μηχανισμό κυτταρικού θανάτου. Διερυνήσαμε την ικανότητα της ολευροπαΐνης να παράγει H_2O_2 στα πιο κοινώς χρησιμοποιούμενα θρεπτικά καλλιέργειας (DMEM, MEM και DMEM/F12). Αξιολογήσαμε επίσης τη συνεισφορά των συστατικών του MEM στην παραγωγή του H_2O_2, όπως επίσης και την συνεισφορά των συνθηκών καλλιέργειας (pH). Επιπλέον, διερευνήσαμε βιοχημικά και φαινοτυπικά χαρακτηριστικά των επωασμένων με ολευροπαΐνη κυττάρων καθώς και τη συμβολή αποπτωτικών και νεκρωτικών πρωτεϊνων με στόχο να διαλευκάνουμε τον ακριβή μηχανισμό που οδηγεί στον κυτταρικό θάνατο.

Οι ακριβείς παράγοντες υπεύθυνοι για την παραγωγή H_2O_2 και οι συνθήκες που την προάγουν ή αναστέλλουν, είναι σημαντικοί για την επεξήγηση των *in vitro* αποτελεσμάτων. Σε αυτή τη μελέτη, μια συστηματική αξιολόγηση των συστατικών των θρεπτικών καλλιέργειας κατέδειξε ότι το διττανθρακικό νάτριο με την σταθεροποίηση του pH σε τιμές μεγαλύτερες του 7, είναι η καθοριστική αιτία για την παραγωγή H_2O_2 από την ολευροπαΐνη και τον μεταβολίτη της υδροξυτυροσόλη

Το παραγόμενο H_2O_2 προκάλεσε εκτενή οξειδωτική βλάβη στο DNA και σημαντική μείωση στην κυτταρική βιωσιμότητα τόσο των καρκινικών (MDA-MB-231) όσο και των φυσιολογικών (MCF-10A, STO) κυττάρων. Το πυροσταφυλικό νάτριο το οποίο δεσμεύει και καταστρέφει το H_2O_2 καθώς και το αντιοξειδωτικό N ακέτυλ-κυστεϊνη (NAC) εμπόδισαν αυτά τα φαινόμενα. Επομένως, έχουμε ταυτοποιήσει τις συνθήκες καλλιέργειας που προωθούν την παραγωγή H_2O_2 από την ολευροπαΐνη και τον μεταβολίτη της υδροξυτυροσόλη, προκαλώντας επιδράσεις στα κύτταρα που παρερμηνεύονται σαν εξειδικευμένη αντικαρκινική δράση. Τα αποτελέσματα μας εγείρουν σημαντικά ερωτήματα σχετικά με τη χρήση θρεπτικών υποστρωμάτων που περιέχουν διττανθρακικό νάτριο και

πυροσταφυλικό νάτριο σαν συστατικά για την *in vitro* μελέτη των συγκεκριμένων αλλά και άλλων φυτικών πολυφαινολών.

Επιπλέον έχουμε διαλευκάνει τον ακριβή μηχανισμό κυτταρικού θανάτου στην καρκινική σειρά μαστού MDA-MB-231. Η ολευροπαΐνη φάνηκε ότι ενεργοποιεί τις MAPK κινάσες και την πρωτεΐνη PARP-1, με αποτέλεσμα την παραγωγή PAR πολυμερών και τη νέκρωση μέσω αποσταθεροποίησης της μιτοχονδριακής και λυσοσωμικής μεμβράνης. Ο κυτταρικός θάνατος φάνηκε να αναστέλλεται παρουσία της σιδηροδεσμευτικής ουσίας deferoxamine mesylate (DFO). Ο συγκεκριμένος μηχανισμός κυτταρικού θανάτου είναι κοινός στα κύτταρα που επωάζονται με H_2O_2.

Τα αποτελέσματα μας, δίνουν μια ολοκληρωμένη περιγραφή της *in vitro* συμπεριφοράς της ολευροπαΐνης με λεπτομερή χαρακτηρισμό και επεξήγηση σε μοριακό επίπεδο της παρατηρούμενης κυτταροτοξικότητας. Τα αποτελέσματα μας επιτρέπουν στους ερευνητές να ελέγχουν τα παραγόμενα επίπεδα H_2O_2 κατά τον *in vitro* έλεγχο φυτικών πολυφαινολών και τη σχεδίαση πιο αξιόπιστων *in vitro* και *in vivo* μελετών.

ACKNOWLEDGEMENTS

My biggest gratitude goes to my supervisor Prof. Andreas Constantinou first of all for giving me the opportunity to work in his laboratory. I am deeply grateful to him for accepting me working in his laboratory at different working hours than the usual and provided me with all the necessary funds needed for the completion of this work. I would also like to thank him for his supervision, his advices and his support throughout this project and also his open minded and critical way of thinking, that helped me develop initiatives and love science.

I thank Dr Constantinos Deltas, Dr Pantelis Georgiades, Dr Rania Tsitsiloni and Dr Andreas Hadjisavvas for their time and interest to participate in my committee.

I would also like to thank our collaborator Dr Alexis Leandros Skaltsounis who was kind enough to supply us with the olive constituents, necessary for this work and also for his grate help in designing the possible chemical pathway that we have proposed.

In addition I would like to thank Dr Pantelis Georgiades for providing us the STO mouse embryonic fibroblasts and the fluorescence microscope, Dr Maria Rikkou for the electronic design of the proposed mechanism and Dr Panayiotis Koutentis and Dr Nikos Chronakis for evaluating the proposed mechanism. Special thanks go to my brother Christophoros for his great help with the immunofluorescence stainings.

Many thanks for their help go to all the current and past members of the Cancer Biology and Chemoprevention Laboratory. Even though I did not have the chance to work many hours with them, they were always willing to help and discuss experimental problems that were met. I would also like to thank them for the friendship that was developed and will definitely continue to exist. A big thank you goes also to all the members of the other laboratories for any help they have provided.

This work is dedicated to my family that was always there for me supporting my decisions. I want to deeply thank them for their love and their support.

Table of Contents

LIST OF FIGURES

LIST OF TABLES

LIST OF ABBREVIATIONS

3-ABA: 3-Aminobenzamide

8-oxo-dG: 7,8-dihydro-8-oxo-2′-deoxyguanosine

ADP: adenosine 5'-diphosphate

AIF: Apoptosis Inducing Factor

Amplex® Red reagent: 10-acetyl-3,7-dihydroxyphenoxazine

ANT: Adenine nucleotide translocator

ATP: Adenosine Triphosphate

CIS: Carcinoma *in situ*

COX-2 : Cyclooxygenase 2

CypD: Cyclophilin D

DAPI: 4,6-diamidino-2-phenylindole

DFO: Deferoxamine mesylate

DMEM: Dulbrecco's Modified Eagle Medium

DMEM/F12: Dulbrecco's Modified Eagle Medium-F12 mixture

DMSO: Dimethylsulfoxide

DOLE: Dry olive leaf extract

DPQ: 3,4-Dihydro-5-[4-(1-piperidinyl)butoxyl]-1(2H)-isoquinolinone

DTT: Dithiothreitol

EBSS: Earle's balanced salt solution

EGF: Epidermal Growth Factor

ERα: Estrogen Receptor alpha

ERβ: Estrogen Receptor beta

FBS: Foetal Bovine Serum

FCS: fetal calf serum

FOX: ferrous oxidation-xylenol orange

G418: Geneticin

GLY: Glycine

GSH: Glutathione

H_2O_2: Hydrogen Peroxide

HS: Horse serum

JC1: 5,5',6,6'-tetrachloro-1,1',3,3'-tetraethyl-benzimidazolylcarbocyanine iodide

JNK: c-Jun amino-terminal kinases

LMP: Lysosomal membrane permeabilization

MAPK: Mitogen activated protein kinase

MEF: Mouse Embryonic Fibroblasts

MEM: Minimal Essential Medium

MNNG: N-methyl-N'-nitro-N-nitrosoguanidine

mPT : Mitochondrial permeability transition

MPTP: Mitochondrial permeability transition pore

MSDH: O-methyl-serine dodecylamine hydrochloride

NAC: N acetyl Cysteine

NAD: Nicotinamide adenine dinucleotide

$NaHCO_3$: sodium bicarbonate

NEAA: Non essential aminoacids

NMDA: N-methyl-D-aspartate

OLE: Oleuropein

PAR: Poly (ADP-ribose)

PARG: Poly(ADP-ribose) glycohydrolase

PARP -1: Poly (ADP-ribose) polymerase 1

PBS: Phosphate Buffer Saline

ROS: Reactive Oxygen Species

RPMI: Roswell Park Memorial Institute

SOD: Superoxide dismutases

SP: Sodium Pyruvate

TBE: Tris-Borate-EDTA

TBS-T: Tris Buffered Saline-Tween 20

Topo I: Topoisomerase I

Topo I RB: Topoisomerase I reaction buffer

Topo II: Topoisomerase II

VOO: Virgin olive oil

1. INTRODUCTION

1.1 Breast cancer

Breast cancer is a malignant tumor that starts in the cells of the breast. A malignant tumor is a group of cancer cells that can grow into (invade) surrounding tissues or spread (metastasize) to distant areas of the body. Breast cancer is the most commonly diagnosed form of cancer affecting women worldwide and the second (1.38 million new cases in 2008) after lung cancer affecting men and women [4]. The American Cancer Society's estimates for breast cancer in the United States for 2013 are: about 232,340 new cases of invasive breast cancer will be diagnosed in women, about 64,640 new cases of carcinoma in situ (CIS) will be diagnosed (CIS is non-invasive and is the earliest form of breast cancer) and about 39,620 women will die from breast cancer. In Cyprus, approximately 400 new cases of breast cancer are diagnosed annually with family history being the strongest predictor of risk and late menarche and breastfeeding displaying a strong protective effect [5]. Postmenopausal Greek Cypriot women with high consumption of fish, olive oil, vegetables and legumes, all characteristics of the Mediterranean diet, were shown to have a lower risk for developing breast cancer [6].

1.2 Olive oil

The world production of olive oil every year reaches the 2,000,000 tons with the contribution of the Mediterranean countries to be more than 95% [7]. Virgin olive oil (VOO) differs in that it is obtained directly from the olive fruit with mechanical extraction and no further treatment. Virgin olive oil consists of the major components that are 98% of the weight and include glycerols (monounsaturated fatty acids) and the minor components that are 2% and include more than 230 compounds [8]. The quality of the olive oil is mainly dependent on the volatile compounds which are carbonyl compounds, alcohols, esters and hydrocarbons and contribute to the aroma profile of olive oil. These are highly affected by the geographic region, the cultivar, the ripeness of the fruit, the harvest and processing methods and the storage time [9]. The phenolic fraction of VOO consists of a heterogeneous mixture of compounds belonging to several families with varying chemical structures. These are phenolic acids like gallic and caffeic acid, phenolic alcohols like hydroxytyrosol and tyrosol, secoiridoids like oleuropein and lingstroside, lignans like (+)-1-Pinoresinol, (+)-1-hydroxypinoresinol and (+)-1-acetoxypinoresinol and flavonoids like apigenin and luteolin.

There have been several studies about the metabolism of the olive oil polyphenols (mainly oleuropein, hydroxytyrosol and tyrosol) in human plasma and urine after oral uptake, although the information is still limited. It seems that these polyphenols become conjugated in the small intestine and in the liver. The resulting metabolites are mainly glucuronate and sulfate conjugates with or without methylation of the catechol group [9].

1.3 Oleuropein - Hydroxytyrosol

Oleuropein belongs to the group of secoiridoids. Secoiridoids derive from iridoids by removal of the 7-8 link. Iridoids are a wide group of monoterpenes whose structure may be considered as originating from iridane (Figure 1) [10].

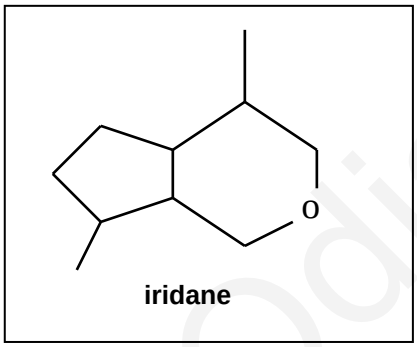

Figure 1: Chemical structure of iridane

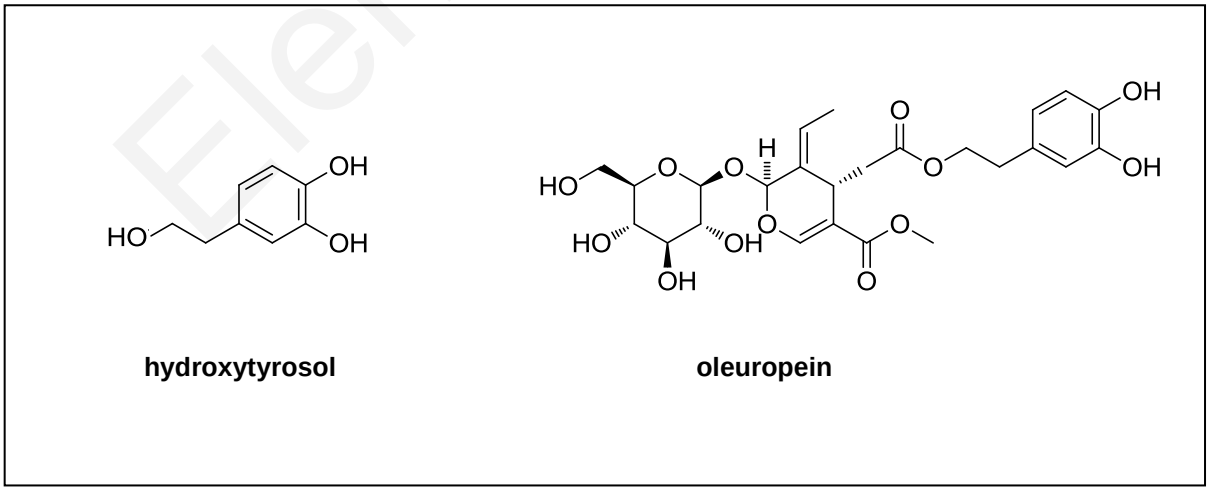

Figure 2: Chemical structures of hydroxytyrosol and oleuropein.
Designed with ChemDraw.

Oleuropein was discovered in 1908 [11] in *Olea europaea* and its chemical structure (Figure 2) along with its hypotensive activity were reported in 1960 [12]. Oleuropein, is the glycosylated ester of hydroxytyrosol (3,4-dihydroxyphenylethanol) to elenolic acid (Figure 2) and is the main polyphenol of olive fruit, oil and leaf, producing the bitter taste [13]. It is easily transformed by the β-glycosidase enzyme into glucose and oleuropein aglycone. Further esterolysis of the aglycone compound produces hydroxytyrosol and elenolic acid [14]. Oleuropein's levels are decreased with the ripening of the fruit [15]. It has been reported to possess strong antioxidant and free radical scavenger activity [16], antimicrobial [17], hypoglycemic [18,19], anti-toxoplasmosis [20], antiviral [21,22,23], antimycoplasmal [24], platelet anti-aggregant [25] and hypolipidimic [26] activities.

Hydroxytyrosol, the metabolite of oleuropein has also been reported to possess similar activities [27,28,29,30,31]. Oleuropein and hydroxytyrosol have also been reported to act as potent selective anticancer compounds in both cancer cell lines and mouse tumor models [32,33]. In differentiated Caco-2 cells used as the model system it was found that hydroxytyrosol enters the intestine quantitatively through passive diffusion and bidirectional. The only metabolite detected in this system was the methylated form 3-hydroxy-4-methoxyphenylethanol [34].

1.3.1 Antibacterial activity

The antimicrobial activity of oleuropein was shown *in vitro* against both gram negative and positive bacteria [35]. In addition, oleuropein and hydroxytyrosol were shown to inhibit or delay *in vitro* the growth of highly pathogenic bacteria of the human intestinal or respiratory tract. The bacteria tested were clinical isolates and standard reference strains (ATCC) [28]. It is interesting to note that in a study, the antibacterial activity of oleuropein was attributed to hydrogen peroxide production as a result of tryptone oxidation in the underlying medium [36].

1.3.2 Antiviral activity

The antiviral effect of oleuropein against Hepatitis B virus was demonstrated *in* vitro by ELISA in the human HBV-transfected HepG2 cell line cultured in DMEM. According to the authors, oleuropein (80 mg/kg, twice daily) reduced viremia in Duck Hepatitis B Virus-infected ducks without signs of toxicity [21]. Oleuropein (up to 54 μg/ml) inhibited the *in vitro* infectivity of the viral haemorrhagic septicaemia virus (VHSV), a salmonid rhabdovirus. Incubation of virus with olive leaf extract or oleuropein before infection in RPMI supplemented with sodium pyruvate, reduced the viral infectivity to 10 and 30%, respectively [37].

1.3.3 Antioxidant activity

Hydroxytyrosol and oleuropein exhibited strong radical scavenging activity with EC_{50} of 0.26 μM and 36.3 μM respectively by measuring the reduction of 2,2-diphenyl-1-picrylhydrazyl radical (DPPH). The antioxidant activity measured was comparable to those of known antioxidants like α tocopherol, ascorbate and BHT. The scavenging activity was also evident with superoxide anion, in cell free and neutrophil based methods [38]. Oleuropein at concentration of 10 μM was able to protect low density lipoprotein (LDL) oxidation by copper sulphate, indicating its antioxidant potential [39]. The antioxidant effect towards LDL was also demonstrated *in vivo*. In rabbits fed with oleuropein enriched diet (7 mg /kg), LDL was protected from oxidation and the plasmatic levels of total, free, and ester cholesterol were reduced (-15, -12, and -17%, respectively) [40].

Human promyelocytic leukemia cells (HL60) and peripheral blood mononuclear cells (PBMC), exposed to H_2O_2 in the presence of olive polyphenols at concentrations ranging from 1 to 10 μM, indicated a DNA damage protective effect as measured by the comet assay. This was further demonstrated in phorbole 12-myristate 13-acetate (PMA)-activated monocytes. Hydroxytyrosol and tyrosol were more effective than oleuropein [41].

The protective effect of the olive polyphenols was investigated in the Jurkat cells by the comet assay exposed to the continuous generation of H_2O_2 by the enzyme glucose oxidase. It was interesting that although hydroxytyrosol protected cells from DNA damage, oleuropein did not. Instead, oleuropein at concentrations over 100 μg/ml caused DNA damage and cell toxicity. Tyrosol did not have any effect [42].

1.3.4 Anticancer activity

In a study, the *in vitro* anticancer effect of oleuropein was demonstrated in a variety of tumor cell lines derived from advanced-grade human tumors (TF-1a, 786-O, T-47D, RPMI-7951, and LoVo) and also on normal human fibroblasts. The authors declared a strong anti-proliferative effect against cancer cells without toxicity on normal cells. The *in vivo* anti tumor effect was also assessed with the authors supporting that oleuropein totally regressed the tumors in 9-12 days [32]. Following studies tried to elucidate the anticancer effect of oleuropein in more cancer lines. The results are categorized here according to the cancer type studied.

1.3.4.1 Breast cancer

Oleuropein (200 μg/mL) and hydroxytyrosol (50 μg/mL) were shown to decrease the viability of the MCF-7 breast cancer cells grown in DMEM, by causing cell cycle arrest and apoptosis. Cell death was dependent on the initial number of the adherent cells, with the polyphenols being more cytotoxic at the lowest cell number tested (2000 cells/well) [43]. The growth inhibition of MCF-7 breast cancer cells grown in the RPMI medium was also shown for the hydroxytyrosol rich olive leaves extract, through the cell cycle arrest in the G0/G1. The levels of c-jun were elevated in treated cells and cyclin D and Pin levels were decreased [44].

The effect of oleuropein (200 μM) was further demonstrated in MDA-MB-231 and MCF-7 cells cultured in the RPMI medium. The median lethal concentrations (LC_{50}) for MCF-7 and MDA-MB-231 cells were 110 μM and 160 μM, respectively. However, at 200 μM of oleuropein, MDA-MB-231 showed much higher sensitivity than MCF-7. MCF-10A cells cultured in DMEM/F12 medium were resistant to oleuropein. Interestingly, cell death was evident after 72h and was mainly through apoptosis and to a lesser extent due to necrosis and cell cycle arrest. The molecules upregulated were bax and p21 while NF-κB, survivin and Bcl-2 were downregulated [45].

The uptake and metabolism of the phenolic compounds from the olive-leaf extract were assessed in the breast cancer cell line SKBR3 in the DMEM medium. The major compounds found within the cells were oleuropein, luteolin-7-O-glucoside and its metabolites luteolin aglycone and methyl-luteolin glucoside, as well as apigenin, and verbascoside. Interestingly, neither hydroxytyrosol nor any of its metabolites were found within the cells at any incubation time (15 min, 1, 2, 24, and 48 h). It was therefore proposed that the major compounds responsible for the cytotoxic activity of the olive-leaf extract in SKBR3 cells, were oleuropein and the flavones luteolin and apigenin, since these compounds showed high uptake and their antitumor activity has been previously reported [46].

1.3.4.2 Prostate cancer

The effect of oleuropein at concentrations 100 and 500 μg/ml, were tested on the prostate cancer cell lines LNCaP and DU450 and on the non-malignant BPH-1 [47]. The authors supported that exposing cell cultures to oleuropein, induced an antioxidant effect on BPH-1 cells and a pro-oxidant effect on cancer cells. BPH-1 and LNCaP cells were cultured in the RPMI-1640 medium and LNCaP cells in the Earle's Minimal Essential Medium (EMEM). Oleuropein reduced the cell viability and induced thiol group

modifications, γ-glutamylcysteine synthetase, reactive oxygen species, pAkt and heme oxygenase-1. The effects were more evident in the DU450 cells. The highest oleuropein concentration (500 μM) induced necrosis in all three cell types, although it was more evident in the DU145 cell line.

1.3.4.3 Colon cancer

Treatment of the colon adenocarcinoma cell lines SW480 and HT29 with crude phenolic extracts from extra virgin olive oil (VOO) in DMEM, caused inhibition of proliferation accompanied by apoptosis. The main phenols of the extracts found in the cytoplasm, were hydroxylated luteolin and decarboxymethyl oleuropein aglycone [48]. In another study with colon cancer cell lines, oleuropein caused anti-proliferative effect only on SW620 cells, while the HT29 cell line was found to be resistant. SW620 cells were cultured in DMEM while HT29 were cultured in McCOY'S 5A supplemented with sodium pyruvate. This differential effect was attributed by the authors to the differences in the genetic or morphological make-up of the cells. Hydroxytyrosol was found to have anti-proliferative effect on both cell lines after 72h. In SW620 cells, the Fatty acid synthase, a key anabolic enzyme of biosynthesis of fatty acids that plays an important role in colon carcinoma development was downregulated by hydroxytyrosol [49].

1.3.4.4 Leukemia

Two compounds isolated from the VOO phenol extract, the dialdehydic forms of elenolic acid linked to hydroxytyrosol (3,4-DHPEA-EDA) and to tyrosol (pHPEA-EDA), inhibited HL60 human promyelocytic leukemia cell proliferation and induced apoptosis in a time- and concentration-dependent manner [50]. In another study, HL60 cells were used to assess the cytotoxic effects of the olive leaf extract, oleuropein and luteolin. In a dose-dependent study, the cytotoxic effect was determined and found to be 170 μM for oleuropein and 40 μM for luteolin. DNA fragmentation patterns and cell staining with acridine orange and ethidium bromide indicated that the mechanism for the cytotoxic effect of oleuropein and luteolin was the apoptotic pathway [51].

A further investigation of hydroxytyrosol on proliferation, cell cycle progression, apoptosis, and differentiation of HL60 cells, cultured in RPMI 1640, indicated a potent inhibitory activity on DNA synthesis and induction of apoptosis at 100 μM. Hydroxytyrosol was also able to inhibit the progression of the cell cycle in synchronized HL60 cells, which accumulated in the G0/G1 phase of the cell cycle after 25 h of treatment. Furthermore,

hydroxytyrosol induced differentiation on HL60 cells with a maximum effect (22% of cells) at 100 μM. Hydroxytyrosol reduced the level of cyclin-dependent kinase (CDK) 6 and increased that of cyclin D3. With regard to the CDK inhibitors, p15 was not altered by 3,4-DHPEA treatment, whereas the expression of p21WAF1/Cip1 and p27Kip1 was increased at both protein and mRNA levels [52].

1.3.4.5 Melanoma

The highly malignant mouse skin cancer cell line B16 was treated with the dry olive leaf extract (DOLE). DOLE contained oleuropein, total flavonoids, including luteolin-7-O-glucoside and quercetin, as well as tannins and caffeic acid. Cells were blocked at the G0/G1 phase of the cell cycle, underwent apoptosis and died by late necrosis. *In vivo* injection of B16 cells in mice and intraperitoneal treatment with DOLE caused a significant reduction of solid melanomas [53].

1.4 H_2O_2

Hydrogen peroxide (H_2O_2) together with superoxide anion radical (·O2−) and hydroxyl radicals (·OH) belong to the group of the Reactive Oxygen Species (ROS). H_2O_2 is a weaker oxidizing agent than the free radical ·O2−. However, in the presence of transition metals like iron or copper, H_2O_2 can be oxidized into the reactive and toxic ·OH *via* the well-known Fenton reaction. In the cellular systems, ROS are normally removed by the cellular antioxidant proteins, such as superoxide dismutase (SOD), catalase, glutathione (GSH) peroxidase, thioredoxin, glutaredoxin, and GSH. For example, SOD can convert ·O2− into H_2O_2, whereas catalase and GSH peroxidase can reduce H_2O_2. When ROS exceeds the cellular defense system, oxidative stress occurs [54].

H_2O_2 is believed to regulate cell development, cell proliferation, cell death and signal transduction. It enters cells through the aquaporins which are diffusion facilitators for non-charged and partially polar solutes such as glycerol, urea, CO_2, polyols, purines, pyrimidines, NH3 and trivalent inorganic forms of arsenic and antimony [55,56].

Excessive production of H_2O_2 causes damage to the cellular components including DNA, protein, and lipid membranes. DNA damage includes oxidized bases (e.g., 8-oxo-dG), DNA strand breaks, DNA intra-strand adducts, and DNA–protein crosslinks. Mitochondrial DNA (mtDNA) is also vulnerable to damage by ROS. Cell death mediated by H_2O_2 can be through apoptosis, necrosis or their combination [57].

1.5 Production of H_2O_2 by polyphenols

The production of H_2O_2 in the culture medium seems to be a common phenomenon which is often misinterpreted as specific anticancer activity of the agents being studied. Most of the compounds evaluated for their anticancer activity, are unstable in the culturing conditions, producing significant amounts of H_2O_2. Examples of compounds producing H_2O_2 in the culture media are among others: ascorbate, green tea, L-dopa, dopamine, apple phenolics, gallic acid, grape seed extract, epigallocatechin gallate, and myricetin [58]. It is interesting that some polyphenols produce high levels and others lower levels of H_2O_2. Specifically, polyphenols like gallic acid, epigallocatechin gallate (EGCG), epigallocatechin and phenolic acids, were demonstrated to generate high levels of H_2O_2 in DMEM. Catechin and quercetin were observed to produce lower, but still significant, levels of H_2O_2 in the culture medium [59,60,61].

Other polyphenols of tea, apples and wine have also been found to be unstable in the culture media and produce significant levels of H_2O_2. Green tea in DMEM caused PC12 cell cytotoxicity through H_2O_2 production. Red wine cytotoxicity was partially attributed to H_2O_2, since lower levels of H_2O_2 were generated [62]. Apple extracts or phenolics of apple extracts and other flavonoids like quercetin, gallic acid, and caffeic acid, produced H_2O_2 time and dose dependently in the culture medium causing cytotoxicity to HepG2 cells. These effects were reversed by catalase and myoglobin [63]. In another study, apple juice extracts and polyphenols generated H_2O_2 dose dependently in DMEM, with the compounds bearing the catechol moiety producing the highest concentrations. Sodium bicarbonate and pH over 7 were found to accelerate H_2O_2 generation by the polyphenols. Interestingly, in DMEM/F12, polyphenols did not produce H_2O_2, something that was attributed to the HEPES buffer that replaced sodium bicarbonate [61]. Similar results were evident with apple extracts in culture media that included HEPES buffer, which also lacked H_2O_2 production, but nevertheless, induced cytotoxicity to HepG2 and Caco-2 cells. This cytotoxicity was not reversed by catalase [64].

Hydroxytyrosol (100 μM) was identified recently to generate H_2O_2 in the RPMI medium that was responsible for the induction of apoptosis in HL-60 cells. The pro-apoptotic effect of hydroxytyrosol towards the HL-60 cells was shown to be the result of this extracellular production of H_2O_2 in the RPMI medium. This effect was inhibited by the antioxidants catalase, tocopherol, ascorbate and NAC. The $^{\bullet}OH$ ions were not involved in apoptosis, since the Fe (II) chelating reagent o-phenantroline did not prevent apoptosis. The percentage of apoptosis and the concentration of the generated H_2O_2 were found to be inversely correlated to the cell number. The maximum accumulation of H_2O_2 was observed in the medium without FCS. When hydroxytyrosol was incubated in medium with FCS or in

the presence of HL60 cells, the levels of H_2O_2 were reduced [1]. A thorough evaluation of many phenolic compounds with respect to H_2O_2 production and induction of apoptosis in HL60 cells, indicated that there were three categories of phenols: (1) those that were unable to produce H_2O_2 and induce apoptosis (tyrosol, homovanillic alcohol and protocatechuic, vanillic, o-coumaric, homovanillic, ferulic and syringic acids); (2) those that induced apoptosis mediated in part by the production of H_2O_2, (3,4-DHPEA, dopamine, 3,4-dihydroxyphenylacetic, 3,4-dihydroxy-hydrocinnamic, caffeic and gallic acids); and (3) those that induced apoptosis without producing H_2O_2 (the secoiridoid derivatives of both hydroxytyrosol and tyrosol). Oleuropein however, was shown to possess a peculiar behavior; although it produced significant amounts of H_2O_2, its pro-apoptotic effect on HL-60 cells was rather weak [2]. The instability of hydroxytyrosol and the generation of H_2O_2 was further demonstrated in other commonly used culture media like Minimum Essential Medium (MEM) and Dulbecco's Modified Eagle Medium (DMEM) [3].

Further investigation showed that RPMI with HEPES as a buffering system produced half the H_2O_2 concentration being produced in the absence of HEPES while DMEM formulated with sodium pyruvate prevented completely H_2O_2 production. Hydroxytyrosol suppressed the growth of breast (MDA-MB-231 and MCF-7), prostate (PC3 and LNCap) and colon (SW480 and HCT116) cancer cell lines with catalase and sodium pyruvate preventing this effect. The H_2O_2 production was abolished in the absence of oxygen, but no medium component was found to be responsible for this production [65].

1.6 Mitogen Activated Protein Kinases (MAPK)

There are three main groups of MAPK: the ERK, the JNK, and the p38 kinases. MAPK are protein kinases that are sequentially phosphorylated and activated upon extracellular stimuli and covalently attach phosphate to the side chain of threonine, serine or tyrosine of specific proteins inside cells. The phosphorylation of proteins by the MAPK like kinases, phosphatases, transcription factors, cytoskeletal proteins and apoptosis related proteins causes the modulation of their enzymatic activity, their interaction with other proteins and molecules, their cellular localization and their degradation by proteases. These modifications result in the control of a variety of cellular processes including cell growth, metabolism, mitosis, survival, differentiation, apoptosis, and eventually make cells capable of rapidly responding to environmental changes. MAPK interact directly or indirectly with one another and are also regulated by phosphorylation by their kinases. [66,67].

1.6.1 JNK proteins

c-Jun amino-terminal kinases (JNK), consist of 10 isoforms and three proteins: JNK1, JNK2 and JNK3. They belong to the mitogen-activated protein kinase family and are responsive to stress stimuli, such as cytokines, ultraviolet irradiation, heat shock, and osmotic shock. They were originally identified as kinases that bind and phosphorylate c-Jun on Ser-63 and Ser-73 within its transcriptional activation domain [68].

JNK-1 was found to participate also in the cell response towards oxidative stress. For example, in H_2O_2 treated normal MEF cells, JNK-1 was indicated as an upstream positive regulator of PARP-1 that promoted its activation by direct association and phosphorylation, causing cell death mediated through PARP-1 activation and PAR formation. The features of cell death mediated by JNK1, PARP-1 and PAR, were membrane leakage, an indication of necrosis and lack of apoptotic features. TNF-α caused a completely different type of cell death, with typical apoptotic features including membrane blebbing, chromatin condensation and caspase-3 activation [69].

Although JNK-1 was found to be an upstream regulator in H_2O_2 treated cells, it was indicated as a downstream molecule of PARP-1 in cells treated with the DNA alkylating agent N-methyl-N-nitro-N-nitrosoguanidine (MNNG), a potent PARP-1 activator. JNK-1 was also shown to be necessary for caspase independent necrosis through mitochondrial depolarization and AIF translocation to the nucleus [70].

JNK and p38 MAPK were activated in Jurkat cells exposed to continuously generated H_2O_2 by the glucose oxidase, in a dose- and time- dependent manner. In contrast ERK activity was decreased. Bolus addition of H_2O_2 caused a sustained activation of the three MAPK. Inhibition of these MAPK with their specific inhibitors, although it provided a small protection in cell viability it was not able to rescue cells from death [71].

1.6.2 p38 kinases

There are four p38MAPK isoforms in mammals named p38 α, β, γ and δ with overlapping substrate specificities. They are encoded by different genes and expressed in different tissues. Although p38α is ubiquitously expressed in most cell types, the others seem to be expressed in a more tissue-specific manner. p38β is expressed in brain, p38γ in skeletal muscle and p38δ in endocrine glands [72]. The p38 activity is usually upregulated as a result of external stimuli like pathogens, growth factors, cytokines and other forms of environmental stress, contributing thus in inflammation, cell growth, cell differentiation, cell cycle and cell death [73]. The p38 kinases have been reported as both

anti-apoptotic and pro-apoptotic probably depending on the cell type and the stimuli. Upon H_2O_2 insult, p38α was shown to increase the antioxidant enzymes superoxide-dismutase 1 (SOD-1), SOD-2, and catalase protecting thus MEF cells from cell death [74]. On the other hand, p38 was necessary for the induction of apoptosis in cardiomyocytes and fibroblasts upon serum deprivation or IFN-γ addition. The apoptotic effect was mediated through upregulation of pro-apoptotic proteins like Bax and FAS and down-regulation of the ERK proteins [75].

1.6.3 Extracellular signal Regulated Kinases (ERK)

Although there are eight isoforms of ERK (i.e., ERK 1, 2, 3, 4, 5, 6, 7, and 8), only ERK1 and ERK2 have been extensively studied. ERK1/2 were shown to be implicated in a variety of biological responses like cell survival, apoptosis, differentiation and migration depending on the cell type, the stimulus, and the duration of activation [76]. ERK is mainly activated upon mitogenic stimuli, whereas JNK and p38 are mainly activated upon stressful stimuli [77]. In oxidative stress, the implication of ERK remains controversial. Some authors support a protective role of ERK, while others support involvement in the apoptotic pathway.

1.7 PARP-1 protein

Poly (ADP-ribose) polymerase 1 (PARP-1) is a 113-kDa nuclear protein composed of 1014 amino acids [78] and three domains: a N-terminal DNA-binding domain (42 kDa), a central auto-modification domain (16 kDa), and a C-terminal catalytic domain (55 kDa) (Figure 3). The enzyme requires the functional DNA-binding domain to perform efficient poly (ADP)-ribosylation. The N-aminoterminal DNA binding domain binds to single or double stranded breaks with high affinity, and induces immediate activation of the catalytic centre in the C-terminal NAD+-binding domain. The automodification domain is basic and it contains the majority of the 15 glutamic acid residues that are involved in PARP automodification. This domain can not serve as an acceptor for ADP-ribose chains unless it is associated with the catalytic and DNA binding domain of the enzyme [79].

PARP-1 is the main and most studied protein of the PARP family which contains 18 members [80]. These homologues possess the PARP-1 catalytic domain, which is responsible for the poly (ADP-ribose) polymerase activity. In response to DNA damage, PARP-1 uses NAD^+ that is cleaved into ADP-ribose and nicotinamide in order to build a poly (ADP-ribose) polymer (PAR) on nuclear proteins and on itself (automodification). Poly

(ADP-ribosyl)ation has been proposed to function in genome repair by modifying proteins proximal to DNA breaks. This modification facilitates the opening of the condensed structure of chromatin, required for the recruitment of the repairing complex in order to repair DNA and thus rescue cell from death [79]. The cell attempts to restore NAD+ pools by recycling nicotinamide with 2 ATP molecules. So in cases of excessive activation of PARP-1, the pools of intracellular NAD+ and ATP are depleted and consequently the energy-dependent cellular processes are impeded, leading to necrosis (Figure 4) [81],[82].

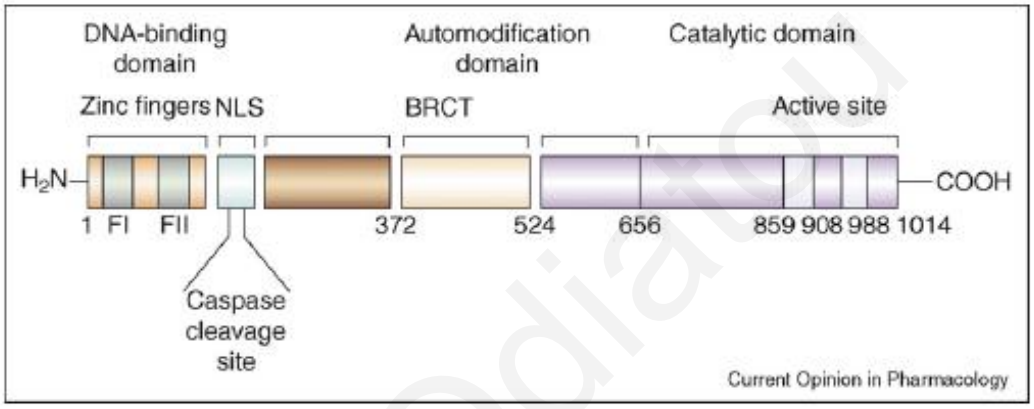

Figure 3: PARP-1 protein structure.
PARP-1 protein consists of three parts. 1) the amino(N)-terminal domain with two zinc fingers for DNA binding and a nuclear localisation signal (NLS), in the caspase cleavage site, 2) the automodification domain with a breast cancer-susceptibility protein-carboxy (C)-terminus (BRCT) motif, common in many DNA repair and cell cycle proteins for protein-protein interactions and 3) the C-terminal catalytic domain with the NAD-binding region. Taken from Jagtap et al [83]

During apoptosis, PARP-1 is cleaved into two fragments: p89 and p24 by caspase-3 and caspase-7 [84] [85]. These proteases recognize a DEVD motif in the nuclear localization signal of PARP-1 and cleavage at this site separates the DNA binding domain from the catalytic domain [86]. This event results in the inactivation of the enzyme and the prevention of the cellular energy loss, preserving in this manner the energy for the ATP sensitive steps of apoptosis [87]. The 24 kDa cleaved PARP-1 fragment binds DNA in a way that inhibits the binding of the active PARP-1 and other repair enzymes attenuating as a consequence the DNA repair [88].

During necrosis though, there is a completely different cleavage pattern of PARP-1. Apparently a 50 kDa fragment of PARP-1 is produced, that is unique and specific for the necrotic death. This cleavage product was evident in necrosis induced by cytochalasin B in HL-60 cells, whereas etoposide produced the 89 kDa apoptotic fragment. The authors

suggested that this unique necrotic degradation of PARP could be used as a sensitive indicator for necrotic cell death [89]. Necrosis induced by various stimuli like $HgCl_2$, 10% ethanol, 0.1% H_2O_2 and 55 ºC heat in Jurkat cells, indicated that PARP-1 has a predominant cleavage product of 50 kDa instead of 89 kDa that is the predominant product during apoptosis [90]. In a similar study with the same inducers, the authors detected a 55 kDa fragment that was the active C-catalytic domain and was produced by the lysosomal cathepsins [91].

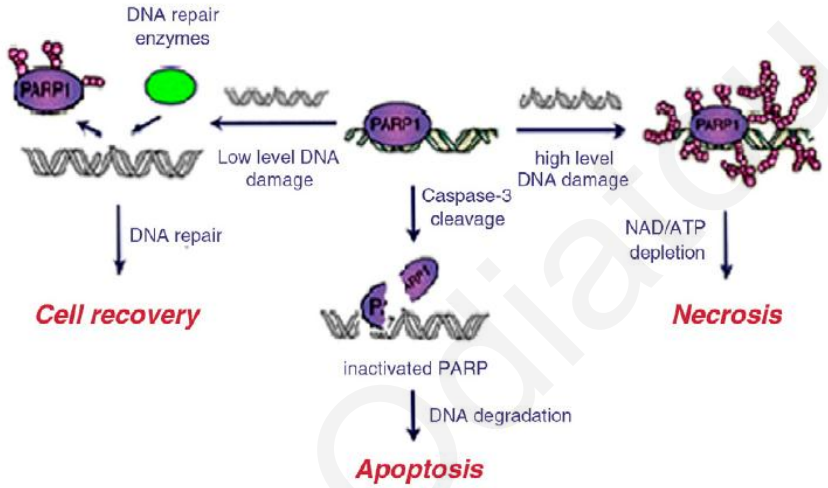

Figure 4: PARP-1 response in cell recovery and death
Upon mild DNA damage, PARP-1 rescues cells by repairing the damage. Moderate damage activates the apoptotic cleavage of PARP-1 and severe DNA damage causes excessive PARP-1 activation resulting in necrosis through NAD/ATP depletion. Taken by Sodhi R.K. et al [92].

In a study with H_2O_2-induced cell death in the murine L929 fibroblast cell line and the CAL-27 human squamous cell carcinoma, it was shown that death was dose- and time-dependent. Higher concentrations caused necrosis, while lower concentrations caused apoptosis or PARP dependent death. Calcium and magnesium were necessary for the endonucleosomal fragmentation, whereas the Bcl-2 protein, protected cells against the lowest concentrations of H_2O_2 (0.1 and 0.5 mM) [93].

1.8 Poly (ADP) Ribose Polymer - PAR

The discovery of PAR was initially demonstrated to be a homopolymer of riboadenylate units (polyA) that required NAD+ as a precursor or immediate substrate of the reaction

[94]. Poly(ADP-ribosyl)ation is a post-translational modification of proteins, catalyzed by PARP, during which, many molecules of ADP-ribose are added on to acceptor proteins to form branched polymers affecting DNA repair. PARP is the main acceptor of the poly ADP ribosylation [79]. PAR polymer was shown to be an efficient death signal in neurons. PAR alone, even in the absence of PARP-1, was sufficient to cause caspase independent death that was prevented by Poly(ADP-ribose) Glycohydrolase (PARG) [95].

PAR is a death signal downstream of PARP-1, sufficient to mediate AIF translocation from the mitochondria to the nucleus and thus nuclear condensation. When PAR polymer was introduced into normal or PARP-1 knock-out cortical neurons, it induced AIF translocation and nuclear condensation. Pretreatment of the PAR polymer with the PARG, failed to induce AIF release. Poly (A) also failed to induce AIF release, indicating that the negative charge of the polymer is not responsible for this release. Moreover cells with reduced levels of AIF were resistant to PARP-1-dependent cell death and PAR polymer cytotoxicity, indicating the crucial role of AIF in parthanatos (see section 1.10) [96].

Further investigation indicated that in parthanatos, PAR binding to AIF in mitochondria, is the decisive step for AIF release from the cytosolic mitochondrial outer membrane into the cytoplasm (Figure 5) [97]. Mutation of the PAR binding site of AIF, although it inhibited AIF release, it had no effect on the activity of AIF or its nuclear condensation ability. The implication of AIF was monitored in BJAB and Jurkat cells treated with continuously generated H_2O_2 by glucose oxidase. H_2O_2 caused energy depletion and caspase independent cell death mediated through mitochondria, by the translocation of AIF to the nucleus. Morphological characteristics of death included nuclear condensation and phosphatidyl-serine translocation [98].

1.9 Apoptosis Inducing Factor (AIF)

Apoptosis-inducing factor (AIF) is a mitochondrial intermembrane oxidoreductase, essential for oxidative phosphorylation and for the anti-oxidant defense of the cell [99], with homology with the bacterial oxidoreductase. The translocation of AIF into the nucleus causes chromatin condensation, large scale fragmentation of DNA and phosphatidylserine exposure to the plasma membrane. The induced apoptosis is independent of caspases and is inhibited by hyperexpression of the Bcl-2 protein that inhibits the release of AIF from the mitochondria [100] [101].

The translocation of AIF to the nucleus was found to be a necessary step for the PARP-1 induced cell death in immortalized mouse embryonic fibroblasts treated with H_2O_2, MNNG and N-methyl-D-aspartate (NMDA). This resulted in a caspase independent death

that was reversed when AIF or PARP-1 were inhibited or depleted. PAR polymer was shown to be produced early after treatment with these agents [102].

Although in cell-free systems AIF is cleaved by calpain to the 57 kDa fragment, in cells undergoing parthanatos caused by NMDA or MNNG, AIF is transferred to nucleus in the uncleaved form of 62 kDa. Moreover inhibition of calpain failed to inhibit the mitochondrial release of AIF, indicating that calpain is not required in parthanatos [103].

1.10 Parthanatos

Since it was shown that PAR alone was sufficient to cause cell death, this form of cell death was named Parthanatos after PAR and Thanatos, the personification of death in Greek mythology [104]. Parthanatos is a caspase independent process, different than apoptosis, necrosis and autophagy. The characteristics of parthanatos, involve loss of the mitochondrial membrane potential, chromatin condensation and loss of the membrane integrity. Unlike apoptosis, it does not cause formation of apoptotic bodies and DNA fragmentation. Although parthanatos causes loss of the membrane integrity resembling necrosis, it does not induce cell swelling.

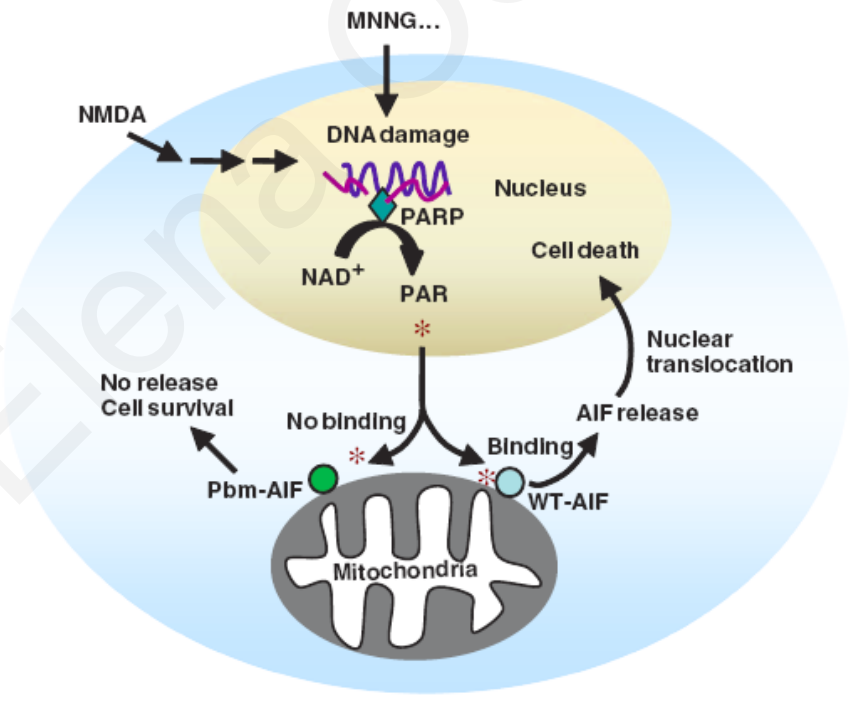

Figure 5: Molecular pathway of cell death induced by PARP activation in Parthanatos.
MNNG and NMDA-induced DNA damage causes the production of PAR by PARP. PAR translocates to the mitochondria and causes AIF release. AIF then translocates to the nucleus and causes cell death. Taken from K.N. Wang, 2011 [97].

Lastly, it differs from autophagy since no formation of autophagic vacuoles is observed. These features indicate that parthanatos differs from the other modes of cell death and has a unique morphological and biochemical identity [105].

1.11 Mitochondrial Permeability Transition-Cyclophilin D

Calcium is an important intracellular messenger in cells that controls many processes like gene transcription, cell proliferation and death. Calcium homeostasis is strictly regulated by channels on the plasma membrane and on organelles inside the cell, like the endoplasmic reticulum and mitochondria. [106].

Cyclophilin D (CypD) is a mitochondrial 40 kDa peptidyl-prolyl cis-trans isomerase that has a role in protein folding [107] [108]. Cyclophilin D was shown to be necessary for necrosis caused by reactive oxygen species and calcium overload, since CypD -deficient cells were resistant to these stimuli. Necrosis occurs due to the disruption of the mitochondrial membranes and mitochondrial dysfunction. This dysfunction starts with the mitochondrial permeability transition (mPT) which is an increase in the permeability of the mitochondrial membrane, resulting in a loss in mitochondrial membrane potential (Δψ).

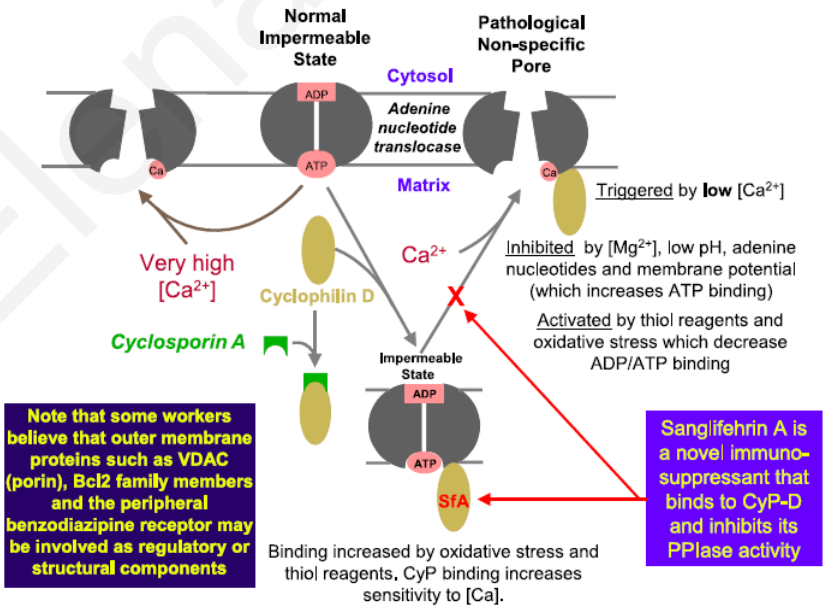

Figure 6: Effect of cyclophillin D and calcium in oxidative stress induced opening of the mitochondrial pore.

These events are absent in CypD deficient cells [109] [110]. The mPT happens through the mitochondrial permeability transition pore (MPTP), which consists of a voltage-dependent anion channel, an adenine nucleotide translocator (ANT), CypD and other molecules. MPTP is a non-specific pore, permitted by molecules up to 1.5 kDa, which opens in the inner mitochondrial membrane under conditions of elevated matrix calcium [111], especially when this is accompanied by oxidative stress and depleted adenine nucleotides [112]. The permeability pore is inhibited by cyclosporine A (Figure 6) [113]. Calcium and oxidative stress promote the opening of the pore through cyclophilin D binding. Cyclosporin A inhibitis cyclophilin D [114].

1.12 Lysosomes

Lysosomes are dynamic organelles that receive and degrade macromolecules in the cell. These macromolecules can be intracellular (autophagy) or extracellular (endocytosis) [115]. Lysosomes were discovered in 1955 as cytoplasmic organelles that contained hydrolytic enzymes active at acidic pH [116]. These enzymes include proteases, lipases, nucleases, glycosidases, phospholipases, phosphatases and sulfatases [117]. Depending on the extent of the lysosomal disruption, cell death can be mediated through apoptosis (partial) or necrosis (complete) [118]. The continuous digestion of iron-containing metalloproteins, makes the lysosomes a pool of redox-active iron, and consequently vulnerable to oxidative stress, causing lysosomal destabilization that is prevented by the iron chelator deferoxamine. Lysosomal destabilization causes the leakage of the destructive hydrolases and reactive iron in the cytoplasm with lethal consequences [119].

Apparently, once significant lysosomal rupture has occurred, the cells are irreversibly committed to death. Some authors support that lysosomal rupture is an upstream event of mitochondrial injury and cell death, induced by H_2O_2 [120]. It is well known that H_2O_2 reacts with ferrous ions to produce hydroxyl radicals. This reaction is called the Fenton reaction [121] [122] [123]. Incubation of DNA with H_2O_2 in the presence of ferric ions, indicates the presence of DNA modifications, typical of hydroxyl radical production [124]. Jurkat cells exposed to continuously generated H_2O_2 by the glucose oxidase in the presence of deferoxamine mesylate (DFO), were protected from DNA damage, as seen with the comet assay. This illustrates the crucial role of the redox active lysosomal iron ions in H_2O_2 induced DNA damage [125].

The lysosomal iron ions were shown to translocate to the nucleus upon H_2O_2 insult and lysosomal rupture, causing hydroxyl radical production in the proximity of DNA and thus DNA damage (Figure 7). No DNA damage was evident upon lysosomal rupture with the

detergent O-methyl-serine dodecylamine hydrochloride (MSDH) excluding the contribution of the hydrolases in the DNA damage observed [126].

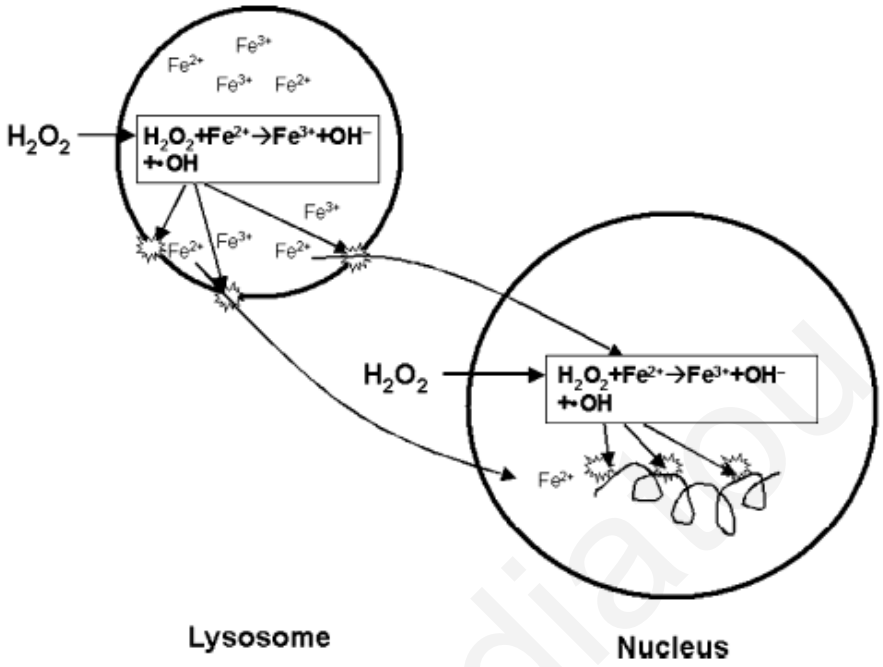

Figure 7: Effect of the lysosomal iron on H_2O_2-induced DNA damage.
Under H_2O_2 induced oxidative stress, lysosomal iron produces hydroxyl radicals that cause lysosomal rupture. The iron ions then translocate to the nucleus where they cause DNA damage. Taken from Kurz et al [127].

1.13 Necrosis

Although necrosis was previously reported as an uncontrolled and accidental procedure, recent publications have shown that it is rather an organized and programmed form of cell death, as essential for cells as apoptosis [128]. The main events of necrosis are considered to be the plasma membrane rupture and the energetic failure i.e. the ATP consumption. The caspases, although important for apoptosis, do not possess a crucial role for the completion of the process of necrosis.

1.14 Apoptosis

The term apoptosis was first introduced by Kerr et al to describe a specific form of cell death. The main morphological features of apoptosis are plasma membrane blebbing

without impairment of its integrity until the final stage, rounding of cells, reduction of cellular volume, chromatin condensation, and nuclear fragmentation [129]. The main biochemical features of apoptosis are the activation of caspases and DNA fragmentation although apoptosis independent of these features are well documented.

Caspases, cysteinyl aspartate proteinases, are a family of evolutionary conserved enzymes that cleave their substrates following an aspartate residue. During apoptosis, caspases are responsible for the cleavage of specific substrates that give specific morphological and biochemical features to cells. Therefore, the detection of activated caspases is considered to be a significant marker for this mode of cell death. Caspases are synthesized as inactive precursors (zymogens, procaspases) that are cleaved during activation. There are two groups of caspases, the intrinsic caspases initiate apoptosis and are activated by autoactivation and the effector caspases are activated by the initiator caspases and are responsible for the execution of apoptosis [130]. The differences between Necrosis, Apoptosis and Parthanatos are summarized in Table 1.

Table 1: Differences between apoptosis, necrosis and parthanatos

	Apoptosis	**Necrosis**	**Parthanatos**
Energy	Dependent	Not dependent	Dependent
Plasma membrane integrity	Yes	No	No
Apoptotic bodies	Yes	No	No
DNA degradation	Ordered	Random	Random
Phosphatidyl serine on the outer membrane	Yes	No	Yes

1.15 Topoisomerases

During replication or transcription, DNA is negatively or positively supercoiled. Topoisomerases are enzymes used for the unwinding of DNA and depending on the strands of DNA broken; they are classified as type I and type II. Type I topoisomerases cleave only one strand of the DNA, while type II cleave both strands [131]. Known topoisomerase I inhibitors used for the treatment of cancer, are camptothecin, its derivatives topotecan and irinotecan and the indenoisoquinolines. The iridoids aucubin and geniposide also act as topo I poisons, explaining their reported antitumor activity [132]. Cell death occurs due to the trapping of the covalent complexes and the subsequent DNA damage caused by the replication and transcription, rather than the inhibition of the catalytic activity of the topoisomerase [133].

There are two categories of drugs that target Topoisomerase II. The first one includes most of the clinically used agents like etoposide, doxorubicin, and mitoxantrone. These agents called Topo II poisons, increase the levels of Topo II: DNA covalent complexes generating a “lesion” that includes DNA strand breaks and protein covalently bound to DNA. The second category, inhibits the Topo II catalytic activity and these agents are therefore termed catalytic inhibitors [134].

1.16 Glucose transporters

Six sodium dependent glucose transporters (SGLT1–SGLT6) and thirteen members of the family of facilitative sugar transporters (GLUT1–GLUT12 and HMIT) have been identified so far [135]. The levels of the glucose transporters were studied in three breast cancer lines: in the poorly invasive MCF-7, the moderately invasive MDA-MB-435 and the highly invasive MDA-MB-231 cells. The levels of the Glut-1 transporters were related to cell invasiveness with higher expression in the most invasive MDA-MB-231 cells. To the contrary, the levels of the Glut-2 and Glut-5 transporters were inversely related to cell invasion. Glut-3 levels did not correlate with invasiveness and Glut-4 transporters were undetectable in the three cell lines [136]. Phloretin and Phlorizin are competitive inhibitors of glucose transport and compete with glucose for binding to the glucose carrier. This causes the inhibition of glucose transmembrane transport [137]. Studies with cancer cell lines indicated that phloretin inhibits glucose uptake by cancer cells. In fact, the glucose uptake by the GLUT-1 transporter was inhibited by more than 80%, when cells were treated with phloretin [138] [139].

2 HYPOTHESIS AND SPECIFIC AIMS

The anticancer effect of oleuropein reported so far in many studies against a variety of cancer cell lines and the lack of toxicity in normal cell lines, gave the impression of a promising plant agent that could be used in the fight against cancer. Recent reports though, gave a contradicting perspective of the behavior of oleuropein and its metabolite hydroxytyrosol in the *in vitro* cell culture conditions. It was shown that oleuropein produced significant levels of H_2O_2 in the commonly used culture medium RPMI 1640. It was not however very clear if the produced H_2O_2 caused cell death, since apoptosis detected in cells was low. It was therefore intriguing to answer to a series of questions that aroused. Does oleuropein produce H_2O_2 in other commonly used culture media, like MEM, DMEM, and DMEM/F12? Is the produced H_2O_2 capable of causing cell death? Why are normal cells resistant to oleuropein? Is cell death cancer-specific? Does oleuropein react with a medium constituent to produce H_2O_2? What are the conditions that favor or inhibit its production? What is the molecular mechanism of death activated in cells? For answering all these questions we made the following hypothesis and postulated specific aims that we tried to answer in the present study.

Our **hypothesis** was that oleuropein and hydroxytyrosol produce high levels of H_2O_2 in the *in vitro* culturing conditions that are responsible for the reported anti-cancer activity in cancer cell lines. We hypothesized that this production of H_2O_2 is the result of the reaction with a culture medium component, or the result of the culturing conditions like the pH. We hypothesized that the produced levels of H_2O_2 have the potential to cause direct or indirect DNA damage and cell death in normal and cancer cells through molecular mechanisms characteristic for H_2O_2-induced death. In order to evaluate our hypothesis, we set the following four specific aims for investigation:

(1) to determine if oleuropein and its metabolite hydroxytyrosol produce H_2O_2 in the commonly used culture media and the mechanism behind this production
(2) to determine if oleuropein through the H_2O_2 production causes oxidative DNA damage in cells
(3) to determine if oleuropein causes cell death in both cancer and normal cells through the H_2O_2 production
(4) to determine the molecular mechanism of cell death

For our first aim, oleuropein and its metabolite hydroxytyrosol were incubated for different time intervals in the culture media MEM, DMEM and DMEM/F12 under standard culture conditions and the produced levels of H_2O_2 were measured by the FOX assay and the amplex red kit. In order to discover how oleuropein and hydroxytyrosol produce H_2O_2 in

the culture medium, the constituents of the culture medium MEM, were cultured with oleuropein or hydroxytyrosol and the produced levels of H_2O_2 were measured. The effect of oleuropein or hydroxytyrosol on the H_2O_2 production was studied in the presence of sodium pyruvate, a known H_2O_2 scavenger.

For our second aim, soon after oleuropein addition in cells, the DNA damage was assessed by the comet assay and the 8 oxo DG method. With these methods, the oxidative damage was evaluated. The effect of the H_2O_2 scavenger, sodium pyruvate on DNA damage was also evaluated. To exclude the possibility that the observed DNA damage was indirect through topoisomerase cleavage, we evaluated the catalytic activities of the topoisomerase enzymes. Nuclear extracts were used for the decatenation assay to study the effect on the topoisomerase II. Nuclear extracts and pure topoisomerase I enzyme were used for the relaxation assay to study the effect on the topoisomerase I. The effect of the reducing agent DTT and the antioxidant cysteine was also studied.

For our third aim, cell death caused by oleuropein and hydroxytyrosol was studied in cancer MDA-MB-231 and normal MCF-10A and STO cells. The effect of different concentrations of oleuropein, hydroxytyrosol and H_2O_2 was assessed on the viability of normal and cancer cells. The viability was measured with the crystal violet assay. Also the effect of the antioxidants NAC and sodium pyruvate on cell death induced by oleuropein, hydroxytyrosol and H_2O_2 was assessed by crystal violet.

For our last aim, we evaluated many molecular pathways of cell death that could have been activated by oleuropein and also pathways that are involved in the H_2O_2-induced cell death. At first we excluded the possibility that oleuropein induces cell death through the glucose transporters entrance in cells or protects cells through implication of the estrogen receptors. The mode of cell death caused by oleuropein i.e. apoptosis or necrosis was studied by staining cells with annexin V and propidium iodide with the Apoptosis Tali kit. The sub G1 apoptotic fractions were assessed by flow cytometry analysis and necrosis was assessed by the trypan blue assay. The morphology of the cells was also evaluated by DAPI staining. The biochemical characteristics of cell death were also examined. The implication of the caspases was evaluated by assessing the caspase 3 enzymatic activity, the cleavage of caspase 3 by western blot analysis, and also by assessing the effect of the caspase inhibitor z-VAD-fmk on cell viability. The implication of mitochondria was studied in two ways. Firstly the mitochondrial membrane potential was measured in order to indicate if there is a decrease and secondly the mitochondrial protein AIF was studied by immunofluorescence analysis to examine if there is nuclear translocation. The role of the lysosomes was studied by the acridine orange staining to show lysosomal membrane permeabilization and by iron chelation with DFO to study the implication of the lysosomal

iron. The proteins implicated in apoptosis and paraptosis like BAX, p53, caspase 3, PARP-1, PAR, JNK, p38, ERK, were studied by western blot.

3 MATERIALS AND METHODS

3.1 Materials and cell cultures

Human breast cancer MDA-MB-231 cells, MCF-10A "normal" immortalized breast cells and mouse embryonic fibroblasts STO cells were obtained from American Type Culture Collection (Rockville, MD, USA). MDA-MB-231 and STO cells were cultured in DMEM (Invitrogen, Carlsbad, California, USA) containing 4500 mg/l glucose and supplemented with 10% (v/v) FBS and 1% antibiotic/antimycotic (100x) (Invitrogen, Carlsbad, California, USA) and incubated under standard conditions (37ºC, 5% CO_2), in a humidified atmosphere. MCF-10A cells were cultured in DMEM/F12 (Invitrogen, Carlsbad, California, USA) or DMEM medium supplemented with 100 ng/mL cholera toxin (Biomol, Hamburg, Germany), 0.5 μg/mL hydrocortisone (LKT Laboratories, Minnesota, USA), 10 μg/mL insulin (Roche Applied Science, Penzberg, Germany), 20 ng/mL EGF, 5% (v/v) horse serum and 1% antibiotic/antimycotic solution (100x) (Invitrogen, Carlsbad, California, USA). S30 and ER β41 cells were cultured in DMEM with G418.

3.2 Isolation of oleuropein and hydroxytyrosol

Oleuropein was isolated from *Olea europaea* leaves. Air dried and pulverized leaves (1 Kg) were extracted by mechanical stirring for 12 h with acetone (2 x 2.5 L). The solvent was evaporated completely and washed with 1 L of a mixture of dicloromethane: methanol 98/2. The insoluble material (50 g) was separated, dried and subjected to medium pressure chromatography with normal silica gel 60 Merck (15-40 mm), using the dichloromethane methanol gradient as the eluent to extract pure oleuropein (2.5 g). The purity of oleuropein was 99% using analytical RP-HPLC with a Thermo Finnigan Spectra system (column: LiChrosob RP-18, 250 x 4.0 mm, 5 μm, elution solvent water acetonitrile gradient, flow: 1mL/min, UV-detection: 254nm). The purified oleuropein was entirely in the glucoside form and was free of any aglycone. Hydroxytyrosol was isolated from olive oil mill waste water, according to a previous described methodology [140]. Oleuropein and hydroxytyrosol were dissolved in dH_2O (Invitrogen, Carlsbad, California, USA), sterilized by filtration with 0.22 μm filters (Sartorius Stedim Biotech, GmbH, Goettingen, Germany) and kept at -20 ºC in the dark. Dilution into culture medium was made just before use.

3.3 Cell viability assay

Cells ($5x10^3$/well) were seeded overnight in 96 well microtiter plates. Oleuropein or hydroxytyrosol were added at concentrations ranging from 5 to 100 μg/mL for oleuropein and 3-100 μM for hydroxytyrosol in new DMEM medium and incubated at 37 ºC, 5% CO_2 for 24 h. After treatment, the medium was removed and cells were washed with phosphate buffer solution (PBS) (Invitrogen, Carlsbad, California, USA), and fixed with 10% formalin (Sigma Aldrich, Steinheim, Germany). Crystal violet (Sigma Aldrich, Steinheim, Germany), was added for 15 min followed by washing with dH_2O. Plates were dried overnight. The stain was dissolved by 10% acetic acid (Fisher Scientific, Loughborough, UK) and measured spectrophotometrically at 570 nm using a Perkin-Elmer LS50 spectrofluorimeter. Sodium pyruvate (Invitrogen, Carlsbad, California, USA) and NAC (Sigma Aldrich, Steinheim, Germany) were added 1h before treatment at final concentration of 1 mM. Experiments were performed in the continuous presence of these reagents.

3.4 Measurement of the H_2O_2 production

The production of H_2O_2 in MEM, DMEM, DMEM/F12 with and without supplements and MEM components (Invitrogen, Carlsbad, California, USA), was assessed by the ferrous oxidation-xylenol orange (FOX) assay and by the Amplex® Red Hydrogen Peroxide/Peroxidase Assay Kit (Invitrogen, Carlsbad, California, USA). For the FOX assay, oleuropein and hydroxytyrosol were incubated in phenol-red free culture media or components for different time points at 37ºC, 5% CO_2 or 37 ºC, atmospheric CO_2. 20 μL of sample was added to 200 μL of FOX reagent containing 125 μM xylenol orange, 100 mM sorbitol, 250 μM ammonium iron sulphate in 25 mM H_2SO_4 (Sigma Aldrich, Steinheim, Germany). For the Amplex Red kit, phenol-red free culture media or medium components were incubated with oleuropein at 37ºC, 5% CO_2. 50 μL of sample was added to 50 μL of Amplex red reagent with HPR enzyme diluted in PBS. For both of the methods, H_2O_2 was used as positive control and media or components without oleuropein or hydroxytyrosol, as negative controls. The H_2O_2 production was measured spectrophotometrically at 570 nm after 30 min incubation at room temperature. The concentration of H_2O_2 was derived from a standard curve obtained by adding different concentrations of H_2O_2 in dH_2O.

3.5 Detection of 8-oxo-DG by Immunocytochemistry

DNA oxidation was assessed by staining the cells with the monoclonal antibody Anti-8-oxo-dG (Clone 2E2) (Trevigen, Gaithersburg, USA) which detects the oxidized derivatives of deoxyguanosine. Cells were plated on cover slips in 6 well plates and the next day, were incubated with 100 μg/mL oleuropein in the presence or absence of 1 mM sodium pyruvate for 1h. Untreated cells were used as negative control and H_2O_2 (50 μM) as positive control. The staining of the oxidized guanines (8-oxo-2'-deoxyguanosine) was performed according to the manufacturer's protocol. Fluorescence was visualised and photographed under the fluorescence microscope (Leica DM IL, Wetzlar, Germany). Cells with DNA oxidative damage had intense green colour. DAPI staining was used as control.

3.6 Alkaline single-cell gel electrophoresis (Comet) assay

DNA damage was assessed by the single cell gel electrophoresis assay under alkaline conditions, with the CometAssay kit from Trevigen (Gaithersburg, USA). Cells were treated with oleuropein (100 μg/ml) for 2h. Untreated cells were used as negative control and H_2O_2 treated cells (100 μM, 20 min at 4 ºC) as positive control. The cells were harvested by trypsinisation, resuspended in PBS, mixed with low melting agarose and transferred on comet slides. Cell lysis, electrophoresis and staining were performed as described in the Trevigen instruction manual. Cells were stained with Sybr Green and examined under the fluorescence microscope (Leica DM IL, Wetzlar, Germany). Scoring was performed with the TriTek CometScore Freeware using the tail moment.

3.7 Topoisomerase I and II assays

The effect of oleuropein on the activity of the topoisomerase I and II enzymes was examined with the topoisomerase I and II assays respectively. Either purified topoisomerase I enzyme or nuclear extracts of treated with oleuropein and untreated cells were serially diluted and used for the relaxation of supercoiled DNA with incubation at 37 ºC for 30 min.

Relaxation assay

The Topo I assay kit (Topogen) was used. The topoisomerase I activity was assessed by the relaxation of the supercoiled DNA (SC) in the presence or absence of oleuropein. Supercoiled DNA was incubated with purified Topo I enzyme and dilutions of oleuropein

or nuclear extracts of treated and untreated cells and incubated at 37 ºC for 30 min. The reaction was ended by addition of the stop buffer followed by electrophoresis (1% agar gel/50V) in TBE solution, staining with SyBr green and washing. Relaxed DNA is observed as higher bands. In case of any inhibition on the activity of the enzyme, supercoiled DNA remains unrelaxed and is seen as a lower band.

Decatenation assay

Topoisomerase II activity was assessed in nuclear extracts for the decatenation of catenated DNA. The extracts were incubated with catenated DNA and ATP and incubated at 37 ºC for 30 min. Electrophoresis was performed in the presence of SyBr green. In case of topoisomerase II inhibition by oleuropein, the levels of decatenated DNA are decreased.

3.8 Treatment with inhibitors

All the inhibitors were added to cells 1h before treatment with oleuropein, except for the deferoxamine mesylate DFO that was preincubated for 3h. Experiments were then performed in the continuous presence of these reagents.

Table 2: Inhibitors used

Inhibitor	Target	Diluted in	Stock	Used	Company
3-ABA	PARP-1	dH_2O	1M	10 mM	Sigma Aldrich
Cocl2	Calcium channels	dH_2O	1 M	100 μM	Sigma Aldrich,
CSA	Cyclophilin D	DMSO	100 mM	1 μM	SantaCruz Biotechnology
DFO	Lysosomal Iron	dH_2O	100 mM	1 mM	Sigma Aldrich,
DPQ	PARP-1	DMSO	25 mM	100 μM	SantaCruz Biotechnology
EB-47	PARP-1	dH_2O	10 mM	50-200 μM	SantaCruz Biotechnology
NAC	Antioxidant	dH_2O	1 M	1 mM	Sigma Aldrich,
PD98059	ERKs	DMSO	100 mM	25 μM	Cayman Chemicals
Phloretin	Glucose transporters	DMSO	1 M	100 μM	Sigma Aldrich,
SB202190	p38	DMSO	100 mM	25 μM`	Sigma Aldrich,
Sodium pyruvate	Antioxidant	dH_2O	100 mM	1 mM	Invitrogen,
SP600125	JNKs	DMSO	100 mM	25 μM	Sigma Aldrich,
z-vad-fmk	Caspases	DMSO	10 mM	20 μM	Calbiochem

3.9 BCA assay

The total protein concentration of the cell lysates were measured with the BCA assay kit, Thermo Scientific Pierce, (Rockford, IL USA). The BCA assay is based on the reduction of Cu+2 to Cu+1 by proteins in an alkaline solution and the subsequent complexing of the Cu+1 to BCA reagent, yielding a purple color detectable at 562nm. Treated cells were harvested with trypsinization and centrifugation, washed with PBS and then lysis buffer was added on ice. 1 μl of the lysate was added to 199 μl of the BCA reagent: bicinchoninic acid+ Copper(II) Sulfate Pentahydrate (50:1), incubated at 37 ºC for 30 min and measured at 570 nm with the Perkin-Elmer spectrophotometer (Multilabel counter 3.00 software). A standard curve was made each time with different concentrations of the protein bovine serum albumin. The concentrations were automatically calculated with the GraphPad Prism 5 software (San Diego, CA, USA).

3.10 Caspase activation assay

The caspase activation assay was conducted according to the Caspase-3/CPP32 Colorimetric Protease Assay kit instructions, Invitrogen, (Camarillo, CA). Treated and untreated cells were harvested by trypsinization, washed with PBS and lysis buffer was added. They were then left on ice for 10 min and the protein concentration was quantified by the BCA assay. 100 μg of lysate was used for the assay. The substrate was added in reaction assay buffer with DTT and incubated for 2h at 37 ºC. Upon cleavage of the substrate DEVD-pNA (Asp-Glu-Val-Asp-p-nitroanilide) by caspase-3, free p-nitroanilide chromophore (pNA) is released with resulting increase in absorbance at 400-405 nm. Comparison of the absorbance of lysates made from treated cells with lysates made from untreated cells, allows determination of the increase in caspase-3 activity.

3.11 Whole cell extraction

After treatment with oleuropein for different time intervals, whole cell extracts were obtained using 3 different lysis buffers depending on the method - RIPA buffer with protease cocktail and phosphatase inhibitors (sodium orthovanadate 1 mM and sodium fluoride 5 mM) for western blot analysis, ready to use caspase lysis buffer (Biosource) for the caspase assay and ready to use lysis buffer for the comet assay (Trevigen). The concentrations of the lysates were measured by the BCA method using bovine serum albumin as a standard. 50 μg of protein per sample was analysed by Western blot.

3.12 Nuclear extraction

Nuclear extracts for the topoisomerase assays were prepared according to Raffo et al with a minor modification at the speed of the last centrifugation (25,000 g instead of low speed centrifugation) [141]. Briefly, cells were harvested, washed with PBS and lysed with douncing in hypotonic lysis buffer (10 mM HEPES, pH 7.9, 1.5 mM MgCl2, 10mM KCl and 0.5 mM dithio- threitol (DTT), protease inhibitors). Then the crude nuclei were harvested by low speed centrifugation, homogenized again by douncing and centrifuged. The pellet was diluted in nuclear lysis buffer (20 mM HEPES, pH 7.9, 25% (v/v) glycerol, 0.42 M NaCl, 0.2 mM EDTA, 0.5 mM DTT, protease inhibitors) and stirred on ice for 30 min followed by centrifugation to obtain the supernatant protein lysate. The concentration of the nuclear extracts was measured by the BCA assay. The nuclear extracts were tested for cytoplasmic cross-contamination by western blot.

.

3.13 Western-blot analysis

Briefly, sample buffer (0.5 M Tris-HCl pH 6.8, 10% glycerol, 2% (w/v) SDS, 5% (v/v) 2-b-mercaptoethanol, 0.05% bromophenol blue) was added to the samples and denatured by boiling at 99 ºC for 5 min. They were then separated by electrophoresis on 10% acrylamide gels and proteins were subsequently transferred to nitrocellulose or polyvinylidene fluoride sheets (ImmobilonTM- P, Millipore Corp., Bedford, MA) using a transblot apparatus (BioRad). The membranes were blocked for 1h with 5% skim milk dissolved in TBS-T buffer (Tris 50 mM; NaCl 1.5%; Tween 20, 0.05%, pH 7.5). They were then incubated overnight with primary monoclonal antibodies against GAPDH, p-p38, p-JNK, p-ERK, Bax, p53, PARP1/2 (Santa Cruz Biotechnology), p38, caspase 3, AIF (Cell Signaling), tubulin and actin (Sigma). After incubation, blots were washed thoroughly in TBS-T buffer and incubated for 1 h with a peroxidase-conjugated secondary antibody (SantaCruz Biotechnology). Bands were visualized using a chemiluminescence-based detection system.

3.14 Decrease in the mitochondrial transmembrane potential

ψΔm was measured using the mitochondria-specific fluorescence probe JC-1 (Molecular Probes, Eugene, OR). Stock solution of JC-1 was prepared at 5 mM in dimethylsulfoxide. This dye is incorporated into the mitochondria and forms aggregates that fluorescence orange-red with blue light excitation (485 nm). When there is a decrease in the mitochondrial membrane potential, JC-1 is diffused in the cytoplasm as monomers giving

cells a green colour. Cells were seeded on coverslips and treated with oleuropein for 4h and 24h. JC-1 dye (5 μM) was then added and cells were incubated for 30 min at 37 ºC. Untreated cells were used as negative and cells treated with H_2O_2 (100 μM) as positive control. Cells were observed under fluorescence microscope and photographed.

3.15 Immunofluorescence analysis

MDA-MB-231 and STO cells were incubated with oleuropein (100 μg/ml) or H_2O_2 (50 μM) for 8h and then stained with the AIF (Cell signaling) antibody to observe if there is translocation from the mitochondria to the nucleus. Untreated cells were used as negative control. In brief the immunofluorescence protocol was as follow: the cells were washed with PBS and fixed in 4% paraformaldehyde in PBS. Glycine 50mM, pH 8 was added for 10 min, washed in PBS, followed by addition of 0.2% Triton X in PBS for 10 min, washed and blocked with 10% Goat serum in PBS for 10 min (serum from the same host species as the labeled secondary antibody). After washing, primary antibody in 0.1 % BSA (1:500 for Rabbit AIF) was added for 1.5 h at RT and then washed. The secondary antibody was added in 0.1 % BSA (1:100 for Cy3-conjugated anti Rabbit) for 40min at RT and then washed. For nuclear staining Hoechst dye (1:5000) was added for 10 min followed by washing and mounting in Prolong Gold mounting medium. Imaging was done under the fluorescence microscope.

3.16 Lysosomal permeabilization assay

Cells were preloaded with 2 μg/ml acridine orange (Invitrogen, Carlsbad, California, USA)) for 30 min, then treated with 100 μg/ml oleuropein or 50 μM H_2O_2 for the indicated time intervals and viewed under the fluorescence microscope with blue light (485 nm).

3.17 Tali™ Annexin V labeling

The expression of phosphatidylserine (PS) in the outer membrane of oleuropein treated cells and control untreated cells was monitored by labeling with the Tali apoptosis kit with Annexin V Alexa Fluor 488/ Propidium iodide staining. Annexin V specifically stains the cells green with phosphatidyl serine transferred on the outside part of the plasma membrane upon apoptosis. Propidium iodide stains red the DNA of cells with damaged membranes. Tali automatically measures cells as live, apoptotic and dead (late apoptotic, necrotic) depending on the staining. Live cells do not fluorescence, apoptotic have green

fluorescence and dead cells have red fluorescence. Cells were seeded in plates, treated with oleuropein (100 μg/ml) and then the labelling was performed according to the instructions of the kit. Specifically, the floating and attached cells were harvested by trypsinization and centrifugation and resuspended in Annexin binding buffer. Annexin V was added for 20 min in the dark. Centrifugation followed and resuspension in binding buffer with propidium iodide for 1-5 min. Samples were placed in the Tali cellular analysis slides and counted by the Tali image based cytometer as live, dead and apoptotic.

3.18 Trypan blue assay

Cell death was measured by the insertion of the trypan blue dye. Since the dye enters cells only when the membrane is damaged, trypan blue staining detects dead cells i.e necrotic or late apoptotic. MDA-MB-231 cells were treated with different concentrations of oleuropein for 24h, the floating cells were collected and the attached cells were trypsinized and then measured under the microscope with a neuebauer haemocytometer.

3.19 DAPI staining

MDA-MB-231 cells were seeded overnight in 6 well plates and then treated for the indicated time intervals with oleuropein (100 μg/ml) alone or in combination with the pan-caspase inhibitor z-VAD-fmk (20 μM). Attached and floating cells were collected by trypsinization, washed with PBS, stained in the dark with 1 μg/ml DAPI for 10 min, washed with PBS and visualized with 350 nm wavelength under the fluorescence microscope (Zeiss, Axio Observer, A1, HB100 Microscope Illuminating System).

3.20 Sub-G1 FACS analysis

MDA-MB-231 cells were treated for 24h with oleuropein (100 μg/ml) or H_2O_2 (100 μM). Floating and attached cells were harvested and fixed in ice-cold ethanol 70 % overnight. They were then incubated with Propidium iodide (10 μg/ml) and 0.2 mg/ml RNase A at 37 ºC for 45 min and analysed with the flow cytometer (Beckton Dickinson). The Cell Quest 3.3 software was used for the estimation of the cell percentage in the phases Sub-G1, G0/G1, S, G2/M. Untreated cells were used as negative control.

3.21 Data analysis

The graphs were designed with the GraphPad Prism 5 software (San Diego, CA, USA). The data are the Mean + SD of two or three independent experiments. Statistical analysis was performed by the Student´s two-tailed t-test. Differences were considered significant at $p < 0.05$.

4 RESULTS

4.1 Oleuropein produces H_2O_2 in common culture media

When oleuropein was incubated in DMEM or MEM media at a concentration of 100 μg/ml, under standard cell culture conditions (37ºC, 5% CO_2), substantial amounts of H_2O_2 were produced as shown in Table 3. The levels were time dependently increased in both media indicating that there is a continuous production of H_2O_2. In contrast, only minor amounts of H_2O_2 (<10 μM for up to 5 h) were produced when oleuropein was added in DMEM/F12 medium and under the same culture conditions. DMEM/F12 contains sodium pyruvate, a scavenger of H_2O_2 [142,143]. The supplementation of the MEM or DMEM media with FBS and antibiotic/antimycotic solution to mimic the cell culture conditions produced lower levels of H_2O_2 (Table 3).

The addition of 100 μM H_2O_2 in DMEM, followed by the determination of its levels at different time intervals, resulted in a decrease in the concentration of H_2O_2, which was more prevalent in the FBS supplemented medium. However, no significant decay was evident when H_2O_2 was incubated in distilled water (data not shown). These observations indicate that DMEM has the capacity to decrease H_2O_2, even in the absence of sodium pyruvate, probably due to reducing agents like glutamine that are present in the medium, or those included in the FBS. Indeed, the addition of H_2O_2 in FBS (100%) diminished the H_2O_2 levels within 1 h (see Figure 9).

4.2 Sodium pyruvate abrogates H_2O_2 produced by oleuropein

The addition of sodium pyruvate for 24 h in MEM or DMEM media diminished the H_2O_2 levels produced by oleuropein under normal culture conditions (Figure 8). Furthermore, when 100 μM H_2O_2 were added in DMEM/F12, a medium that already includes sodium pyruvate and is used for culturing normal MCF-10A cells, the H_2O_2 levels were diminished, indicating that indeed this medium has the capacity to rapidly eliminate H_2O_2 (Figure 9). These data show that sodium pyruvate, either when added in the media (MEM and DMEM) or when it is included in the original composition of the medium (DMEM/F12), abrogates H_2O_2 produced by oleuropein.

Table 3: Production of H_2O_2 (μM) in the culture media

Time (h)	DMEM (μM) Supplements		MEM (μM)		DMEM/F12 (μM)	
	-	+	-	+	-	+
0	<10	<10	<10	<10	<10	<10
1	38.6 ± 6.7	30.3 ± 1.3	25.3 ± 1.7	7.6 ± 1.2	<10	<10
2	52.6 ± 4.2	44.2 ± 9.8	36.9 ± 5.6	19.3 ± 3.2	<10	<10
3	67.9 ± 1.6	60.4 ± 5.5	53.9 ± 0.8	31.3 ± 2.6	<10	<10
4	74.5 ± 5.0	63.2 ± 1.5	53.6 ± 0.6	31.1 ± 1.7	<10	<10
5	78.7 ± 4.6	61.9 ± 2.2	64.1 ± 3.7	32.7 ± 5.2	<10	<10
24	72.5 ± 12.3	59.7 ± 4.4	82.5 ± 5.8	47.8 ± 13	26.2 ± 9.3	<10

Oleuropein (100 μg/ml) was added in DMEM, MEM or DMEM/F12 and following incubation for 24 h at 37°C, 5% CO_2 atmosphere the levels of H_2O_2 were determined by the FOX assay as described in the methods with (+) or without (-) supplements. The supplementation of MEM and DMEM was with 10 % (v/v) FBS, plus antibiotics. The supplementation of DMEM/F12 was with 5 % (v/v) horse serum plus 1% antibiotics, 100 ng/ml cholera toxin, 0.5 μg/ml hydrocortisone, 10 μg/ml insulin and 20 ng/ml EGF. Data represent the mean ± SD of three independent experiments

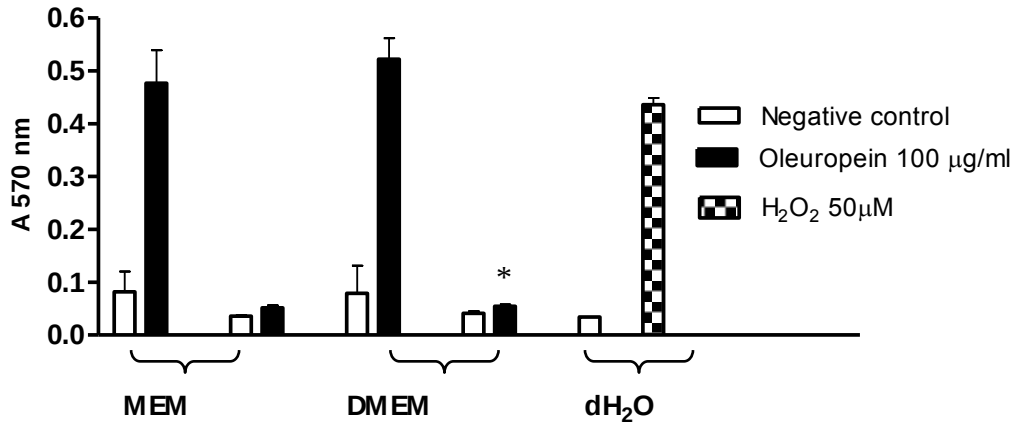

Figure 8: **Effect of sodium pyruvate on the levels of H_2O_2 produced by oleuropein**. Oleuropein was added in DMEM or MEM as indicated at 100 µg/ml for 24 h, in the presence (+) or absence (-) of 1 mM sodium pyruvate under standard cell culture conditions (37°C, 5% CO_2) and the levels of H_2O_2 were measured by the Amplex Red kit spectrophotometrically at 570 nm. H_2O_2 (50 µM) in dH_2O was used as a positive control. The data represent the mean ± SD of three independent experiments. **, indicates significant difference ($p<0.01$) between the values with (+) and without (-) sodium pyruvate.

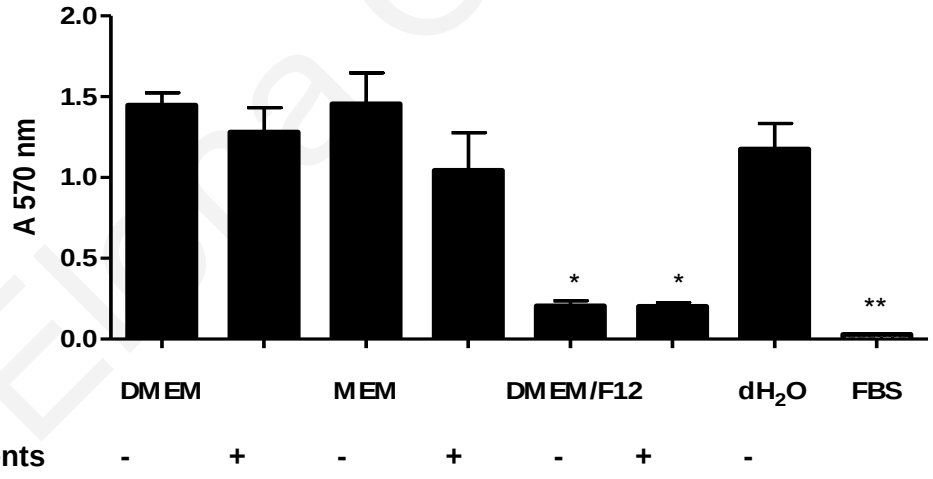

Figure 9: Effect of the media supplementation on the levels of H_2O_2.
H_2O_2 (100 µM) was added in FBS (100%) and in the media DMEM, MEM, DMEM/F12 with (+) and without (-) supplements. The H_2O_2 levels were measured after 1 h incubation at 37°C, 5% CO_2 by the FOX assay. In DMEM and MEM, the supplements were 10% (v/v) FBS and 1% antibiotic/antimycotic solution. In DMEM/F12 medium the supplements were 5% (v/v) horse serum, cholera toxin, hydrocortisone, insulin, and antibiotic/antimycotic solution. DMEM/F12 included sodium pyruvate. Positive control was H_2O_2 in dH_2O. The data represent the mean ± SD. Statistical differences between the treated samples and positive control are represented as follows: *$p<0.05$, **$p<0.01$.

4.3 Sodium bicarbonate is the responsible component for the production of H_2O_2

To identify whether any components of the medium are responsible for the H_2O_2 production, the main constituents of MEM i.e. vitamins, aminoacids, Earle's balanced salt solution (EBSS) and salts, were tested for H_2O_2 production in combination with 100 μg/ml oleuropein or 100 μM hydroxytyrosol. EBSS was found to produce H_2O_2 at comparable levels to those of the complete medium (Figure 10). Vitamins, aminoacids (AA) and salts of calcium and magnesium produced only minor levels of H_2O_2.

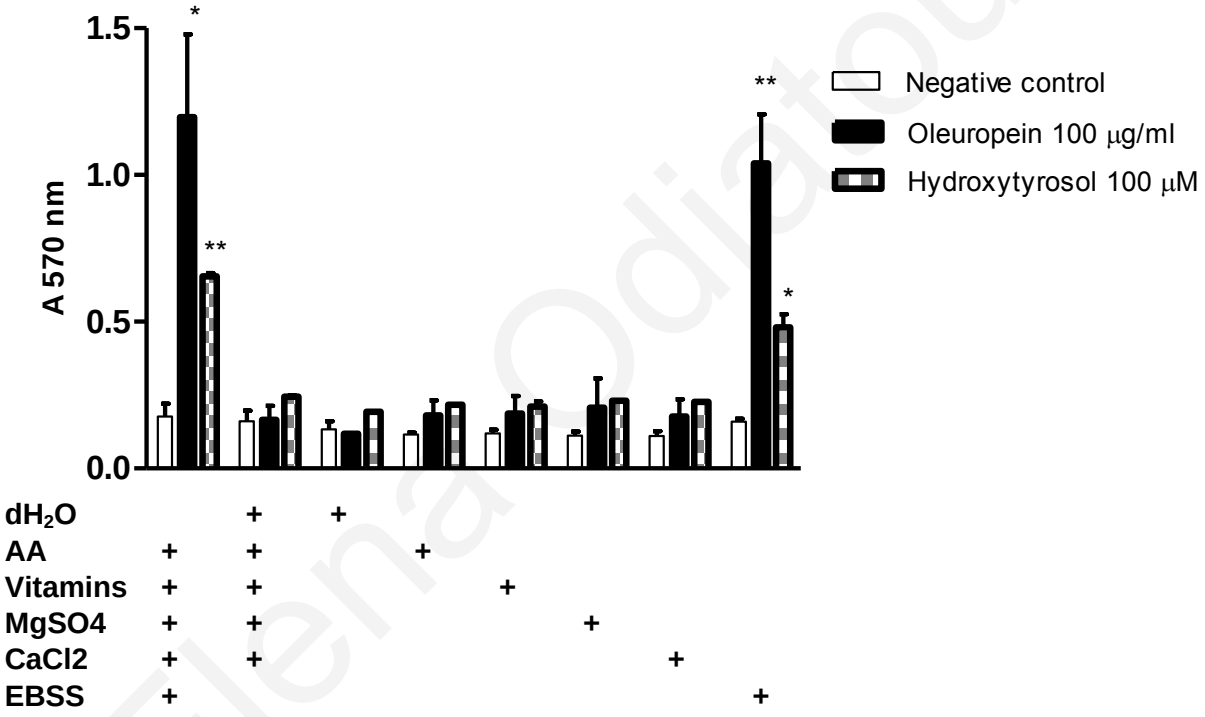

Figure 10: Effect of the medium components on the H_2O_2 production.
The components of the MEM medium i.e. vitamins, aminoacids, salts and EBSS were incubated with and without oleuropein (100 μg/m) or hydroxytyrosol (100 μM) for 24 h at 37°, 5% CO_2 and the produced levels of H_2O_2 were measured by the FOX assay spectrophotometrically at 570 nm. The data represent the mean ± SD of three independent experiments. Statistical differences between the treated samples and vehicle control are represented as follows: *p<0.05, **p<0.01, ***p<0.001.

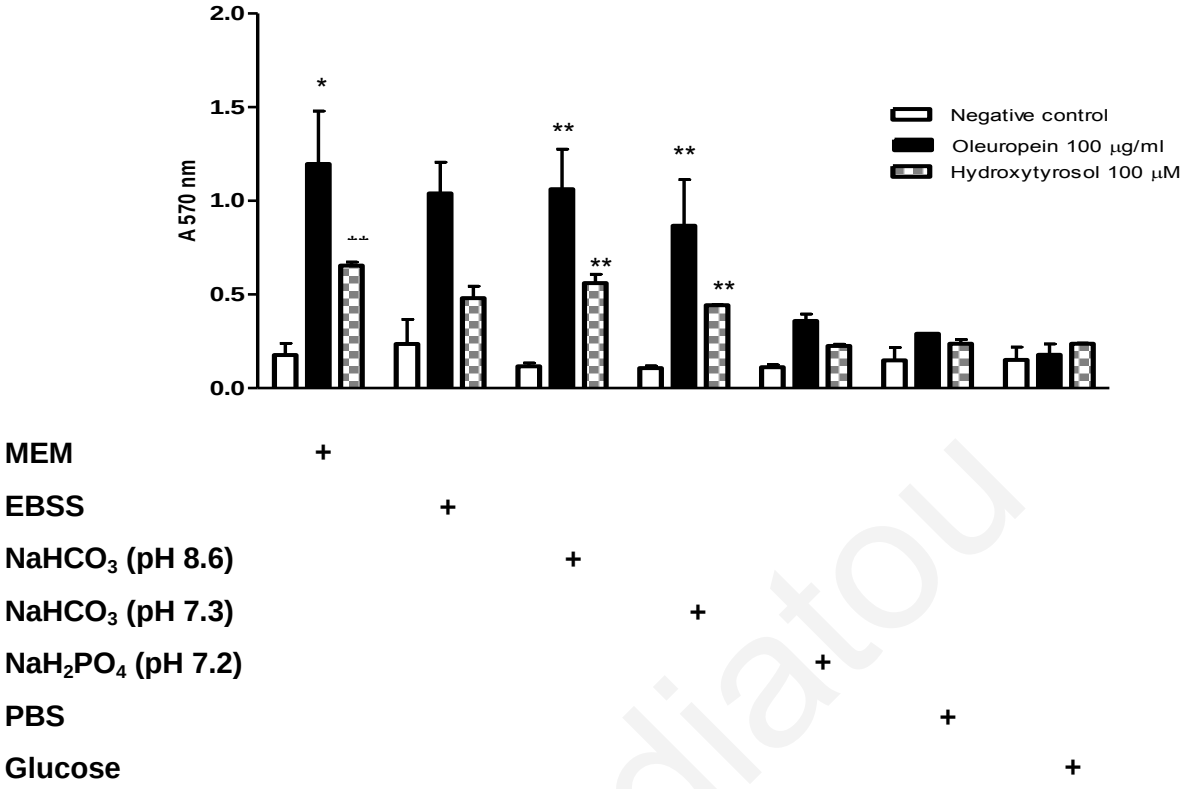

Figure 11: Effect of the EBSS constituents on the H_2O_2 production.
The constituents of the EBSS were individually evaluated under the same conditions. The data represent the mean ± SD of three independent experiments. Statistical differences between the treated samples and vehicle control are represented as follows: *p<0.05, **p<0.01, ***p<0.001.

EBSS contains potassium chloride, sodium chloride, sodium bicarbonate ($NaHCO_3$), monobasic sodium phosphate ($Na_2H_2PO_4$) and D-glucose. By adding these individually, it was determined that sodium bicarbonate (26 mM) was responsible for the H_2O_2 production (Figure 11). To exclude the possibility that the alkaline pH of sodium bicarbonate alone (pH 8.6) was responsible for the H_2O_2 production (in the presence of oleuropein or hydroxytyrosol), we evaluated the effect of neutralized (pH 7.3) sodium bicarbonate and observed that there was significant production of H_2O_2 at this neutral pH as well (Figure 11).

To further investigate the role of sodium bicarbonate in the production of H_2O_2, in conjunction with the cell culture conditions, we prepared three MEM solutions that were incubated for 24 h with oleuropein or hydroxytyrosol at 5% CO_2 (Figure 12). These were as follows: (a) MEM with sodium bicarbonate at pH 7.1, (b) MEM without sodium bicarbonate at pH 7.1 and (c) MEM without sodium bicarbonate at pH=8.0. The first

solution, that included sodium bicarbonate, produced significant levels of H_2O_2 when incubated at 5% CO_2. The exclusion of sodium bicarbonate from the second and third solutions caused almost the complete absence of H_2O_2 production. It is interesting that at a starting pH 8.0, there was no H_2O_2 production (Figure 12), although it has been reported that polyphenols produce high levels of H_2O_2 in alkaline pH [144]. This apparent discrepancy is due to a drop in the pH to 6.0, due to the lack of a buffering system (sodium bicarbonate) in the incubation conditions (5% CO_2).

In a study, incubation of hydroxytyrosol in MEM, in the absence of oxygen, failed to produce any significant levels of H_2O_2 [65]. Our data show that although oxygen is necessary, it is not sufficient to cause alone H_2O_2 production, since all samples were incubated at the same levels of oxygen, but H_2O_2 was produced only in the presence of sodium bicarbonate (Figure 12). As expected, in the MEM medium that contained sodium bicarbonate, the pH increased from pH 7.1 to pH 7.4 where it stabilized. These results demonstrate that, under standard cell culture conditions (37°C, 5% CO_2) sodium bicarbonate is the defining component being responsible for the production of H_2O_2 by oleuropein and hydroxytyrosol.

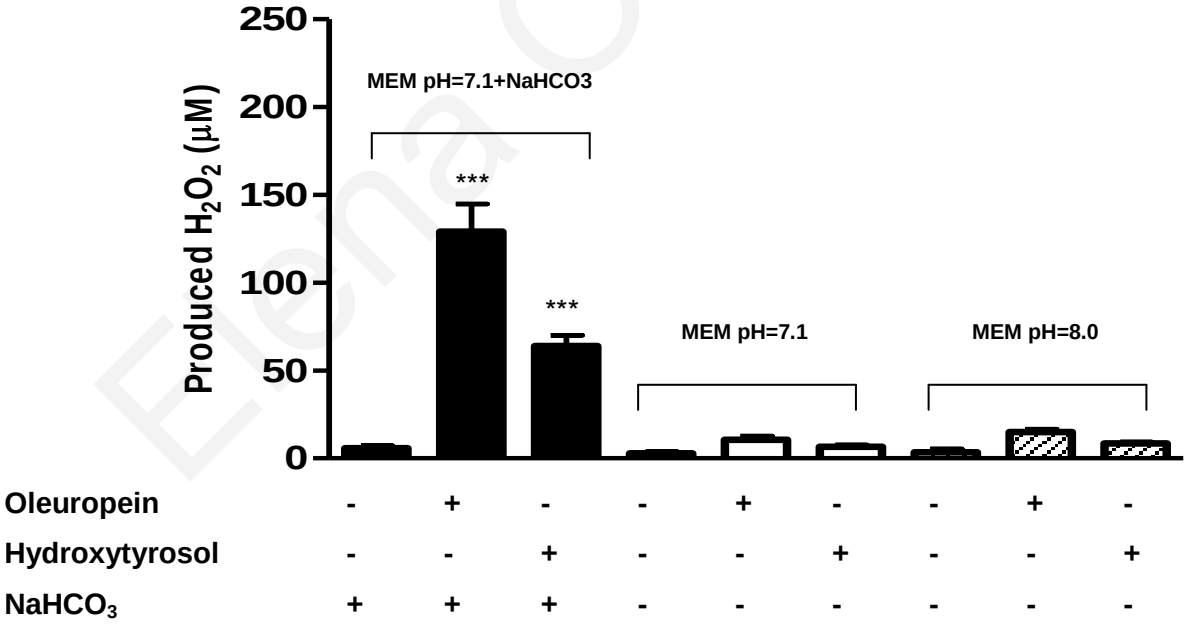

Figure 12: Effect of the sodium bicarbonate-pH on the H_2O_2 production.
The role of sodium bicarbonate was determined under the same conditions by incubating the polyphenols in MEM, in the absence (at either pH=7.1 or pH=8.0) or presence of sodium bicarbonate (pH=7.1) as shown. The data represent the mean ± SD of three independent experiments. Statistical differences between the treated samples and vehicle control are represented as follows: ***p<0.001.

4.4 Hydrogen peroxide produced by oleuropein causes oxidative DNA damage to cells

The H_2O_2 levels produced by oleuropein after 1 h incubation in MDA-MB-231 cells were able to cause extensive DNA oxidation of deoxyguanosines (8-oxo-dG), as visualized by immunocytochemistry using the anti-8-oxo-dG antibody (Figure 13). This clearly indicates that H_2O_2 enters cells causing adverse effects. A result that further supported this indication was that sodium pyruvate prevented completely DNA oxidation, showing that H_2O_2 causes the DNA damage and not the molecule of oleuropein or its oxidized product. Extensive DNA damage was evident by the comet assay at 2 h incubation with oleuropein in MDA-MB-231 cells (Figure 14) and MCF-10A cells (Figure 15, Figure 16). Oleuropein thus, has a pro-oxidant activity under standard culture conditions that is entirely attributed to the produced H_2O_2, which enters cells and causes oxidative DNA damage.

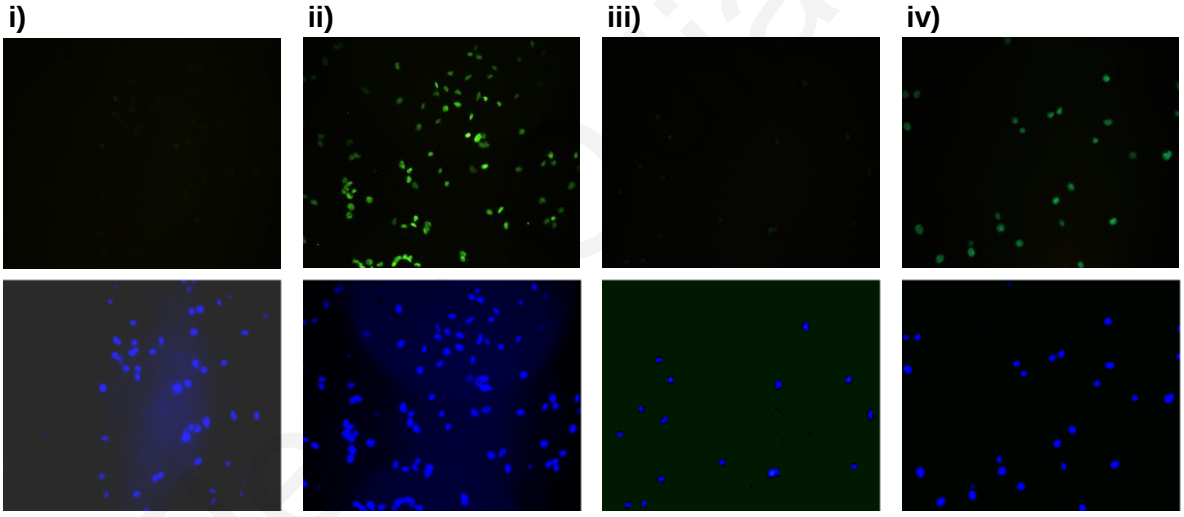

Figure 13: Oleuropein causes DNA oxidation in cells that is prevented by sodium pyruvate.
Immunocytochemistry of MDA-MB-231 cells treated with oleuropein for 1 h and stained with anti-8-oxo-dG antibody or DAPI (blue), visualized under the fluorescence microscope. Treatments were as follows: i) untreated, ii) oleuropein (100 μg/ml), iii) oleuropein (100 μg/ml) in the presence of 1 mM sodium pyruvate, iv) H_2O_2 (50 μM). The results are representative of two independent experiments.

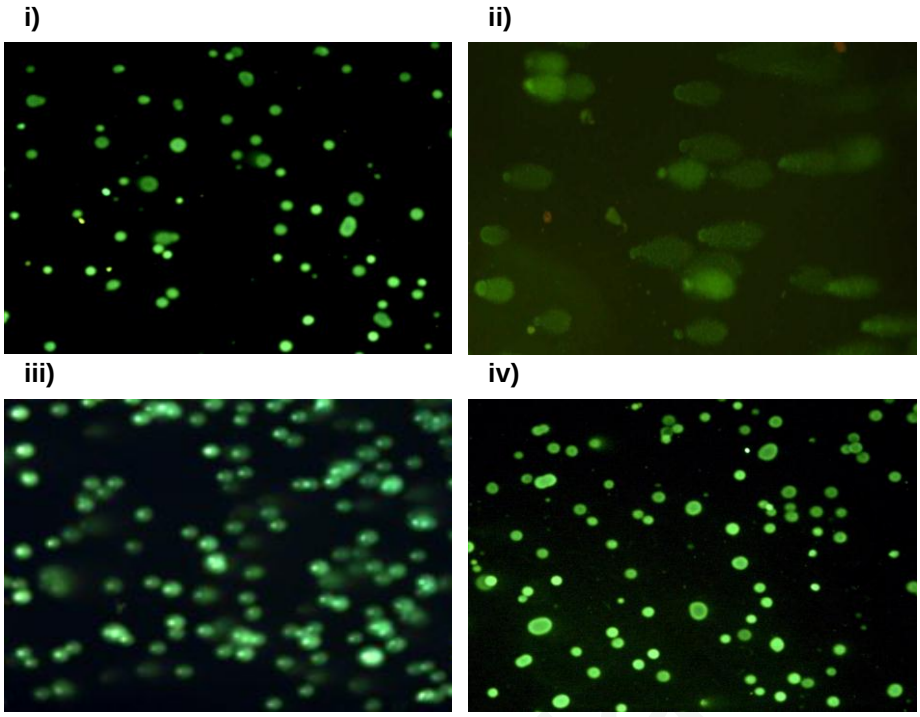

Figure 14: DNA damage in oleuropein treated MCF-10A cells and protection by sodium pyruvate.
MCF-10A cells (i) were treated with oleuropein (100 µg/ml) for 2h (ii) and DNA damage was assessed by the comet assay. Cells were cultured in DMEM. H_2O_2 (100 µM) was added in PBS for 15 min and used as positive control (iii). Cells were also treated with oleuropein in medium with sodium pyruvate (iv).

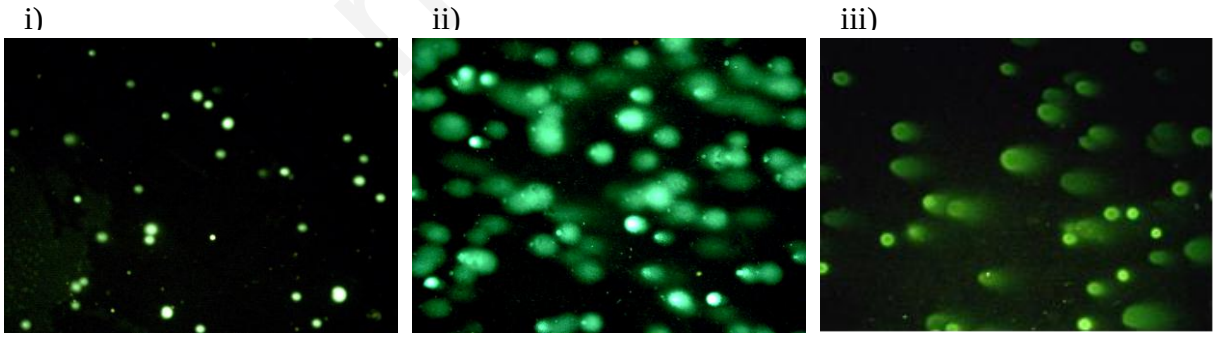

Figure 15: DNA damage in oleuropein treated MDA-MB-231 cells
MDA-MB-231 cells (i) were treated with oleuropein (100 µg/ml) for 2h (ii) and DNA damage was assessed by the comet assay. MDA-MB-231 cells were cultured in DMEM. H_2O_2 (100 µM) was added in PBS for 15 min (iii).

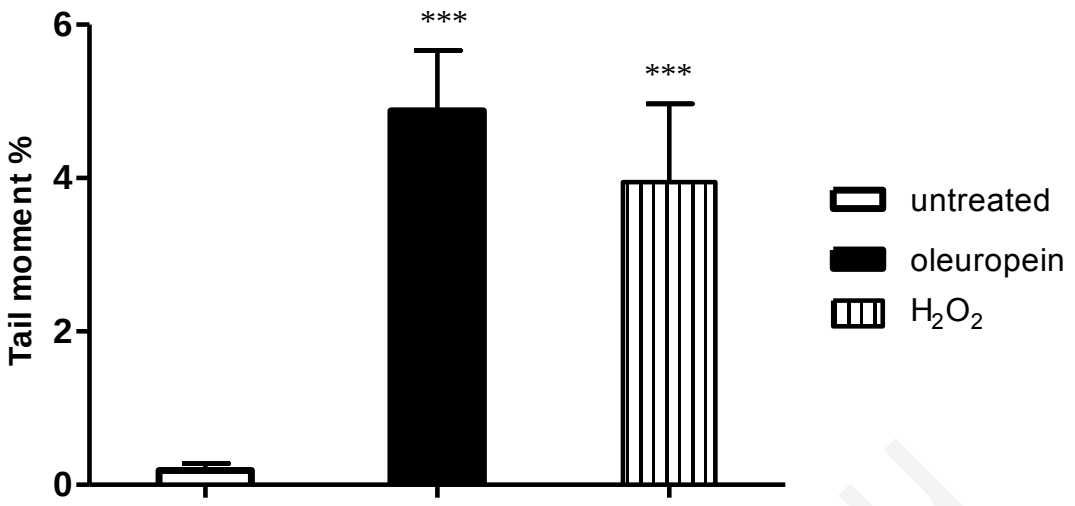

Figure 16: DNA damage of MDA-MB-231 cells.
Alkaline comet assay of MDA-MB-231 cells treated with oleuropein (100 μg/ml) for 2 h and tail moment (%) scored with the TriTek CometScore Freeware. H_2O_2 (75 μM) treated cells were used as positive control and untreated cells as negative. The data represent the mean ± SD of three independent experiments. Statistical difference between the treated and untreated samples: ***p<0.001.

4.5 DNA damage is not mediated through Topoisomerase inhibition

We have also investigated the possibility that the observed DNA damage is indirect and is mediated through the inhibition of the DNA topoisomerases. For this, we performed topo I and II assays as described in the methods section. No inhibition was observed in the activities of the Topoisomerases in nuclear extracts of treated cells compared to untreated (Figure 17). However, when pure Topoisomerase I enzyme was incubated with different concentrations of oleuropein, there was a significant inhibition of activity (Figure 18). Further investigation indicated that this inhibition was reversed in the presence of the anti-oxidant DTT (Figure 19). Cysteine a known antioxidant, in contrast to glycine restored the inhibitory effect of oleuropein (Figure 20). These data show that the observed inhibition by oleuropein is probably the result of a pro-oxidant activity that caused damage to the enzyme rather than a specific inhibition to the enzyme activity.

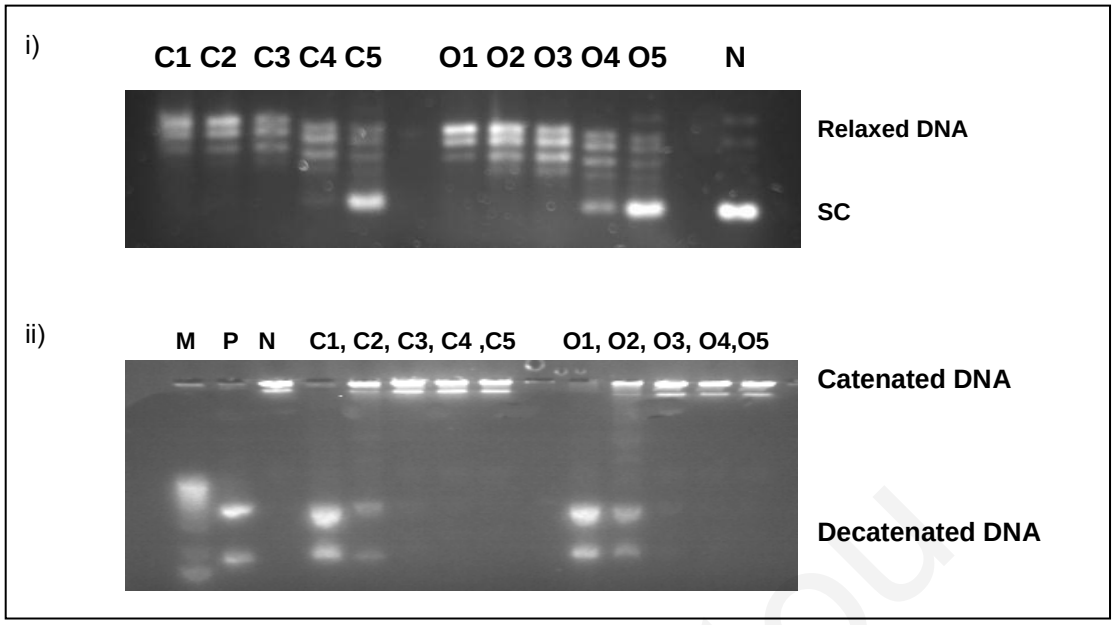

Figure 17: Oleuropein has no effect on Topo I and II activities in nuclear extracts: i) Topo I relaxation assay after treatment with 100 μg/ml oleuropein for 1h in MDA-MB-231 cells. Nuclear extracts of treated (O1-5) and untreated cells (C1-5) were serial diluted and used for the Topo I relaxation of supercoiled DNA (SC). Relaxed DNA is observed as higher bands. ii) Topo II assay in nuclear extracts of MDA MB 231 cells. Extracts were used for the decatenation of catenated DNA. Electrophoresis was performed with EtBr. In case of TOPO II inhibition by oleuropein, the levels of decatenated DNA should have been decreased. M: Marker, P: Positive control- Decatenated DNA, N: Negative control: Reaction Buffer.

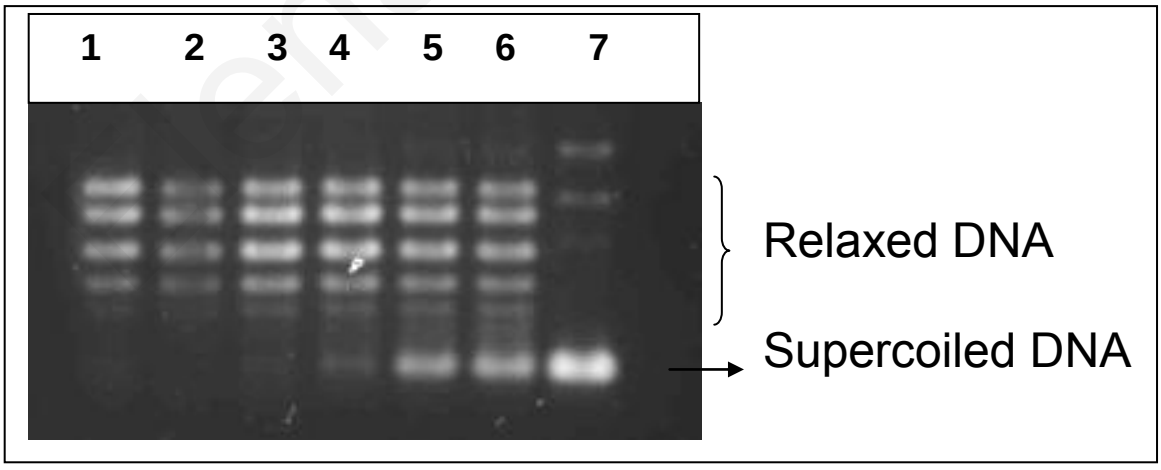

Figure 18: Oleuropein inhibits the Topoisomerase I activity.
Topo I relaxation assay with isolated Topo I enzyme, in the presence of increasing concentrations of oleuropein. 1:Positive control, 2-6: Oleuropein at 12.5, 25, 50, 100, 200 μg/ml, 7: Negative control

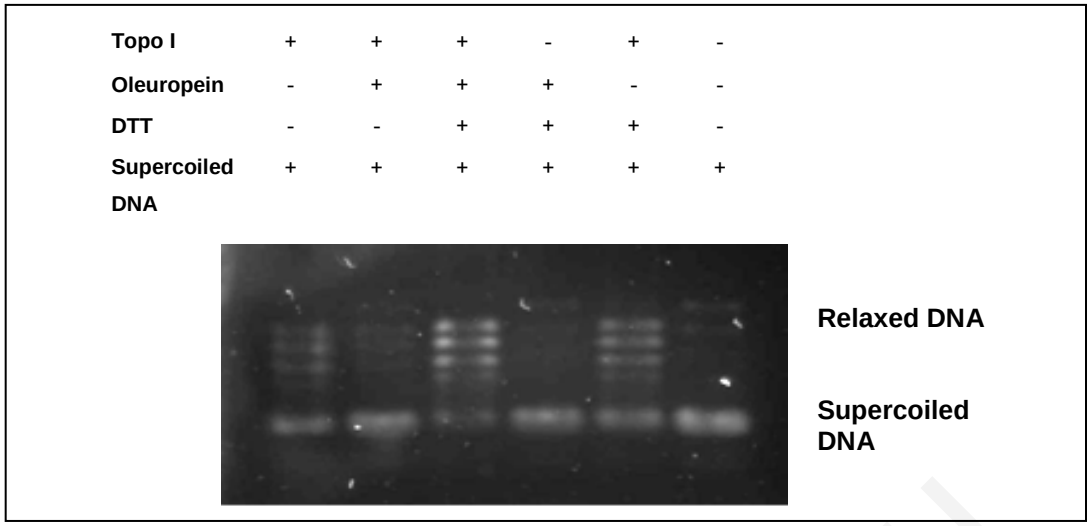

Figure 19: DTT restores Topo I inhibition by oleuropein.
Topo I relaxation assay, for the evaluation of the reducing agent's DTT effect on the activity of the Topo I enzyme, in the presence of oleuropein. Topo I enzyme and supercoiled DNA were incubated with oleuropein (50 μg/ml) alone or in combination with DTT followed by electrophoresis and staining with SyBr green. Supercoiled DNA runs faster than the relaxed DNA.

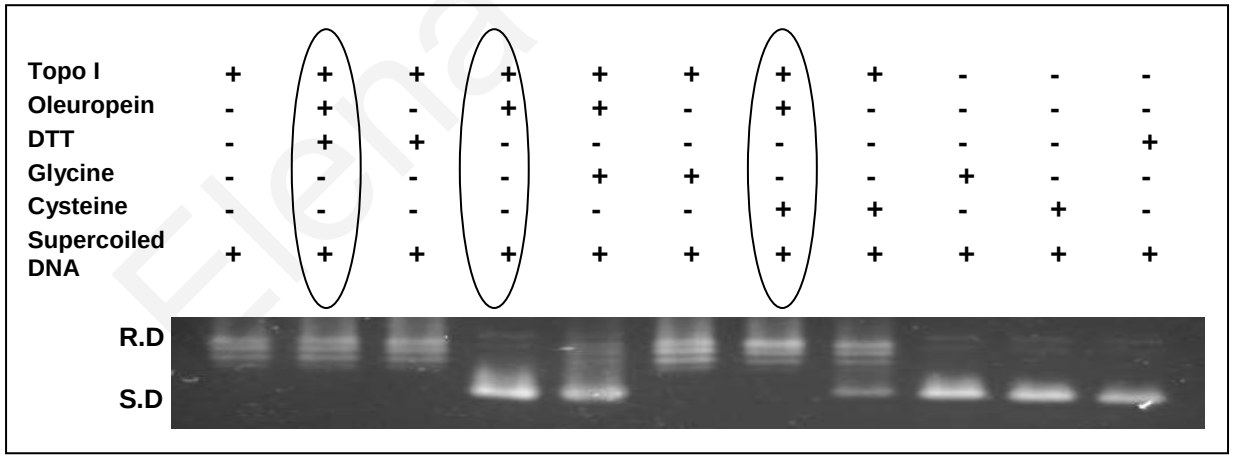

Figure 20: Inhibition of the Topo I activity by oleuropein is restored by antioxidants.
Topo I relaxation assay of the Topo I enzyme incubated with oleuropein in the presence of DTT, cysteine or glycine.. Topo I enzyme and supercoiled DNA were incubated with oleuropein (50 μg/ml) alone or in combination with DTT, cysteine or glycine followed by electrophoresis and staining with SyBr green. Supercoiled DNA runs faster than the relaxed DNA.

4.6 Inhibitory effect of oleuropein and hydroxytyrosol on the viability of cancer and normal cells and prevention by sodium pyruvate

As presented in our previous data, oleuropein and hydroxytyrosol produced increasing concentrations of H_2O_2 in the culture media MEM and DMEM with almost undetectable levels in DMEM/F12. This H_2O_2 production caused oxidative DNA damage at 1h of treatment. It is well known, that cells have molecules that eliminate the oxidative stress like catalase and glutathione and also repair mechanisms for repairing the DNA damage. Taking into account these, we were interested to see if the levels of H_2O_2 produced by oleuropein and hydroxytyrosol were sufficient to override the cell defenses and cause cell death. We were also curious if the effect would be cancer specific or similar in normal and cancer cells. In addition, we were interested to see if scavenging of the H_2O_2 levels, would promote cell survival.

To answer these questions, we incubated MDA-MB-231 breast cancer cells, "normal" immortalized MCF-10A cells or STO normal mouse embryonic fibroblasts with oleuropein at concentrations ranging from 5-100 μg/ml in DMEM. Cell viability was assessed after 24h of treatment. Oleuropein caused a dose-dependent decrease in the viability of all the cell lines. When 1 mM sodium pyruvate was added into the DMEM medium for culturing MDA-MB-231, MCF-10A and STO cells, or when DMEM/F12 (that contains 1 mM of sodium pyruvate) was used for culturing MCF-10A cells, the cytotoxic effects of oleuropein were completely reversed in all cell lines (Figure 21). Hydroxytyrosol also at concentrations ranging from 3-100 μM produced a similar response and was shown to inhibit the viability of MDA-MB-231, MCF-10A and STO cells.

These data demonstrate that H_2O_2 produced by oleuropein and hydroxytyrosol in the culture medium overcomes the cell defences of cancer, normal and immortalized "normal" cells, causing oxidative stress. This has as a result the cytotoxicity that is prevented by the H_2O_2 removal, through the H_2O_2 scavenger sodium pyruvate. Treatment of these cell lines with exogenously added H_2O_2 at the concentrations produced by oleuropein and hydroxytyrosol induced a comparable inhibitory effect on cell viability. These results indicate that the levels of H_2O_2 produced by oleuropein and hydroxytyrosol are sufficient to diminish cell viability. Sodium pyruvate completely reversed this effect, indicating that H_2O_2 is the cause of cell death.

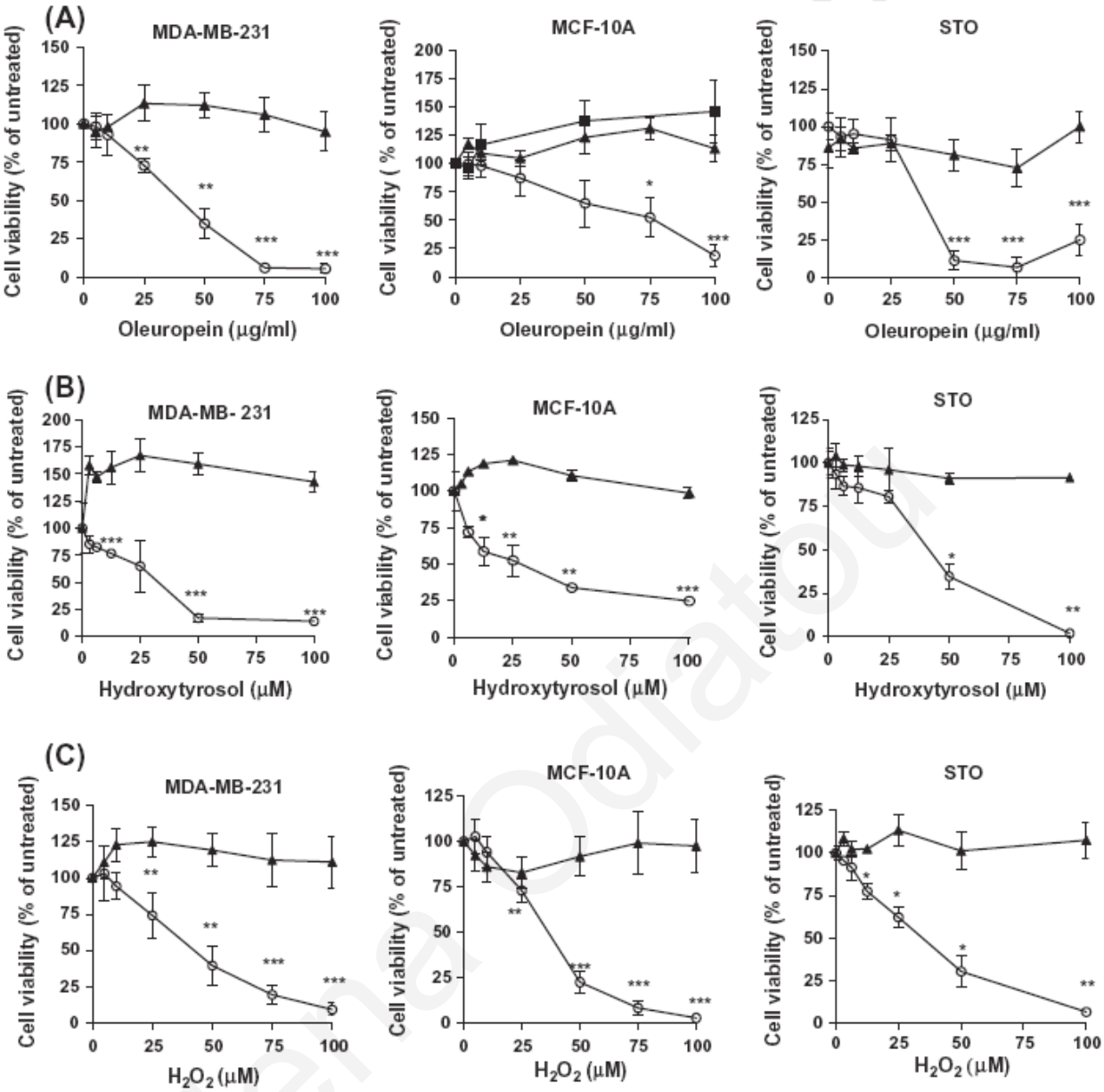

Figure 21: Anti-proliferative effect of oleuropein, hydroxytyrosol and H_2O_2 on cancer and normal cells and restoration by sodium pyruvate.

Cell viability assays of breast cancer MDA-MB-231 cells, immortalized "normal" breast MCF-10A cells and normal mouse embryonic fibroblasts STO cells cultured for 24 h in DMEM with different concentrations of A) oleuropein, B) hydroxytyrosol and C) H_2O_2 in the presence (▲) or absence (○) of 1 mM sodium pyruvate. MCF-10A cells treated with oleuropein were also cultured in DMEM/F12 (■) (A). After staining with crystal violet, absorbance was measured at 570 nm. Sodium pyruvate was added 1 h before treatment. The data represent the mean ± SD of three independent experiments with triplicates. Statistical differences between the treated samples and vehicle control are represented as follows: *p<0.05, **p<0.01, ***p<0.001.

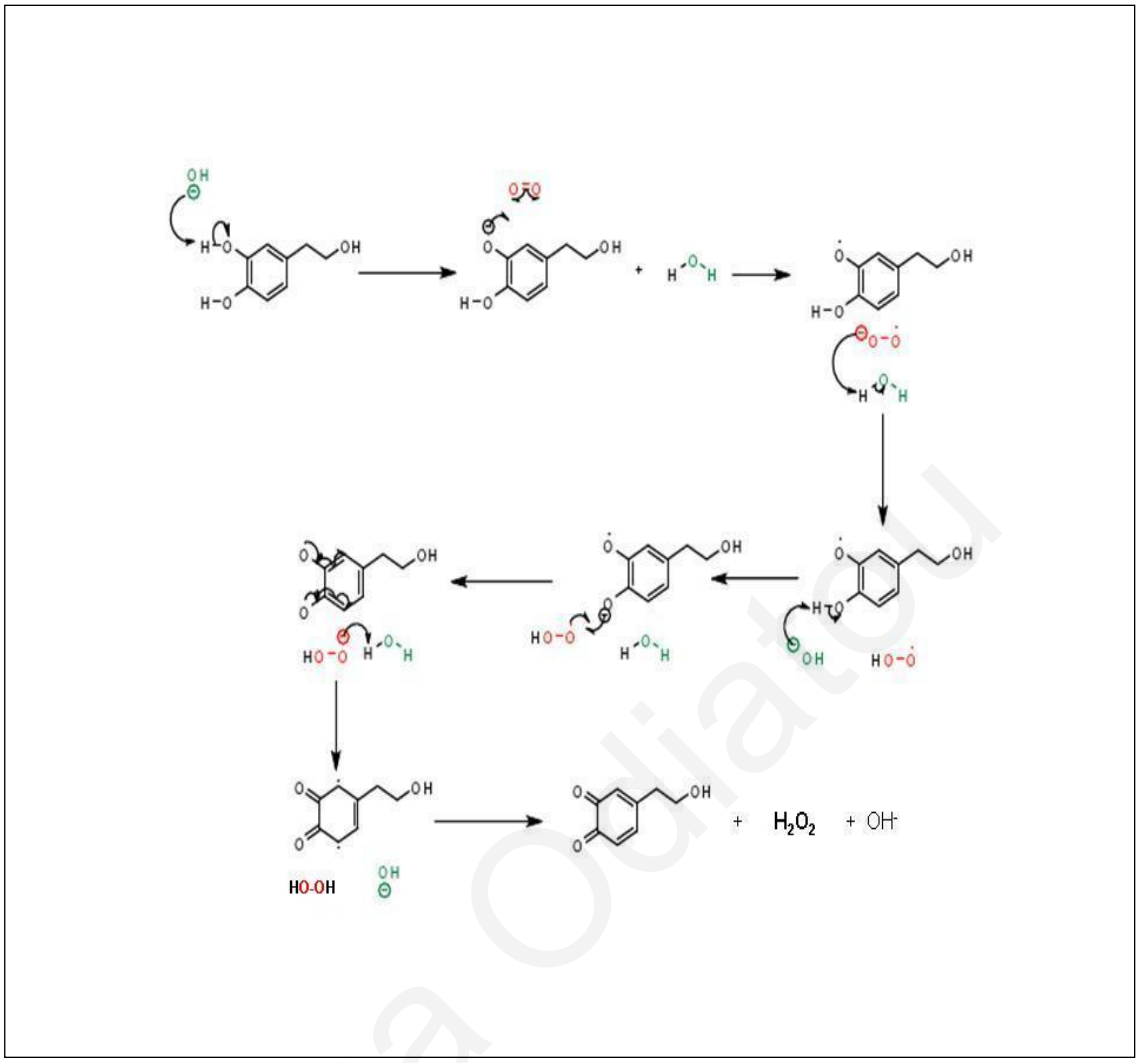

Figure 22: Suggested mechanism for H_2O_2 production.
The catechol molecule of hydroxytyrosol reacts with the hydroxide ions and oxygen to produce o-benzoquinone and H_2O_2. At first, the hydroxide anion abstracts the phenolic hydrogen to form the phenoxide anion. Subsequently, the phenoxide ion reacts with oxygen to produce the corresponding phenoxyl radical that eventually leads to the formation of the o-benzoquinone product and H_2O_2. The structures were designed by the ChemDraw program.

4.7 Continuous PARP activation in cells by oleuropein

The observation of the DNA damage in oleuropein treated cells led us to investigate whether the DNA repair protein PARP-1 is activated upon oleuropein addition. Indeed, treatment of cells with oleuropein (100 μg/ml), for time intervals ranging from 1h to 24h, revealed a substantial increase in the PAR formation which was evident at all-time points of treatment (Figure 23). This indicates that in oleuropein treated cells, DNA damage is severe and not repairable. PARP is activated early and remains continuously activated until cell death occurs. Since PARP-1 is activated upon oxidative DNA damage, this complies with our finding that treated cells are oxidatively damaged at 1h of treatment. The 55 kDa necrotic form of PARP1 increased substantially after 12h and 24h of treatment (Figure 23). Since the antibody we used is specific for the C-terminus of PARP-1, the fragment could be the catalytic domain of PARP-1 (55 kDa) responsible for the PAR production. This 55 kDa fragment was previously shown by others to be the result of cathepsin cleavage and remains active even after the PARP-1 cleavage by necrotic inducers like H_2O_2 [91]. Interestingly, treatment of cells with the PARP-1 inhibitors DPQ, EB-47 and 3-ABA, failed to rescue cells from oleuropein- induced cell death, while 3-ABA failed to rescue cells from H_2O_2 induced cell death.

These results comply with the previous results where DNA damage was evident and indicate that in oleuropein treated cells the severe and continuous DNA damage causes the continuous activation of PARP-1. The lack of protection by the PARP-1 inhibitors indicates that PARP-1 activation is not the decisive step for cell death.

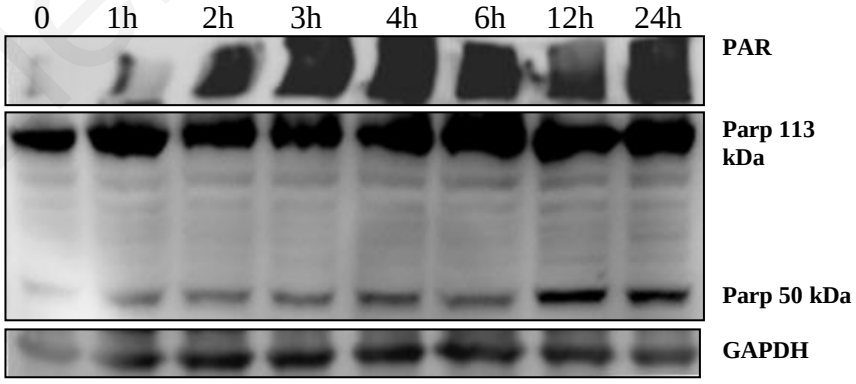

Figure 23 : PARP activation by oleuropein.
Western blot analysis of whole cell lysates (50 μg) treated with oleuropein for different time points up to 24h. GAPDH was used as a loading control. PARP-1 antibody is specific for the C-terminus of PARP-1.

A)

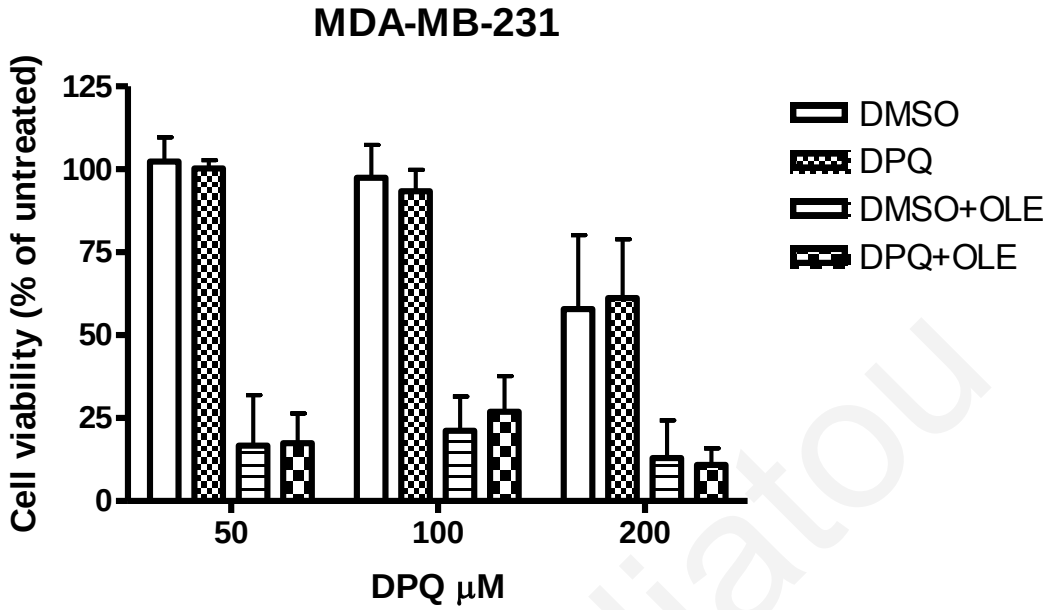

B)

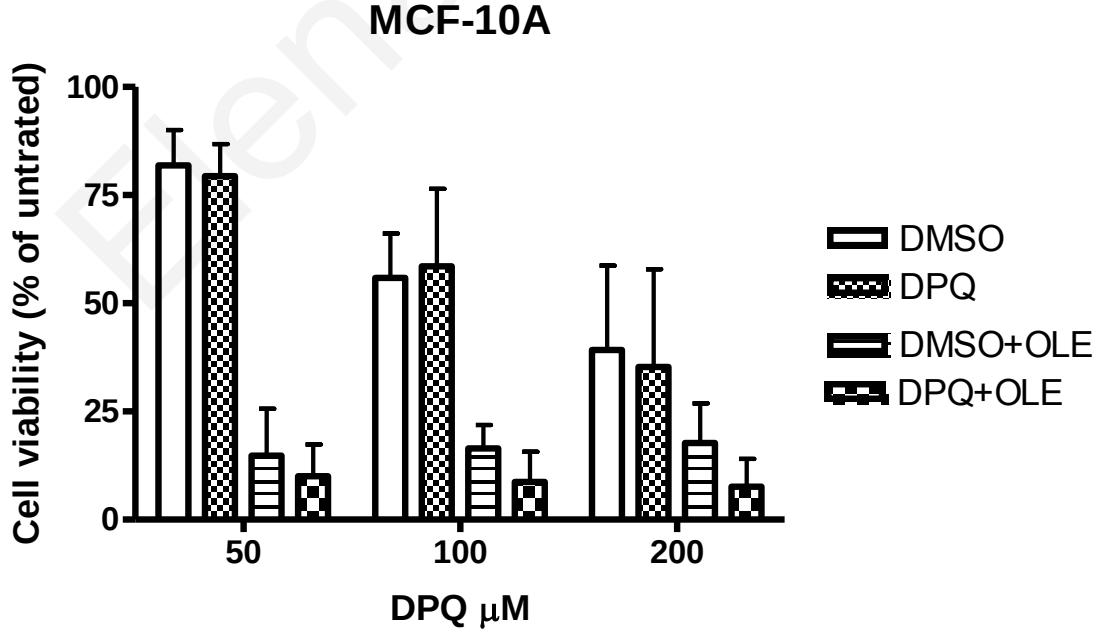

C)

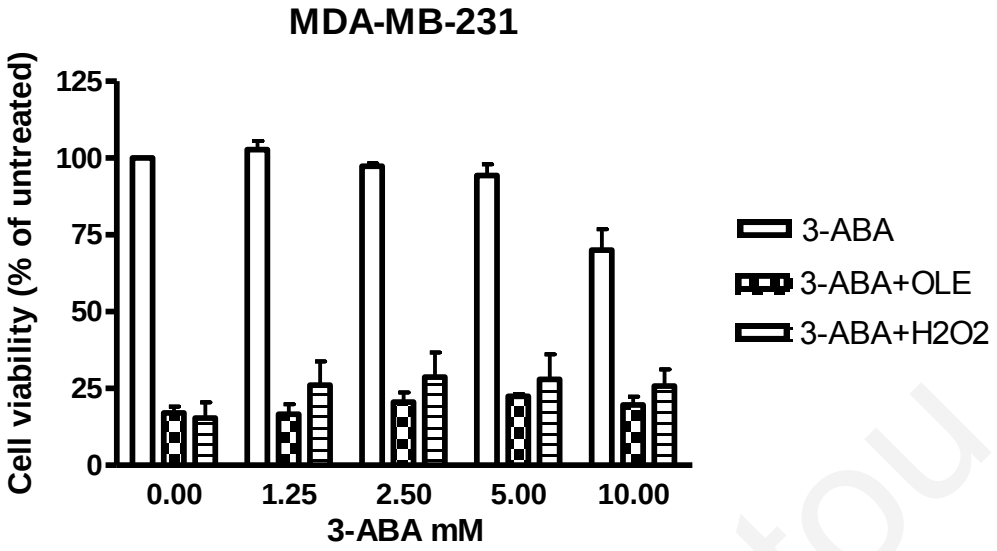

D)

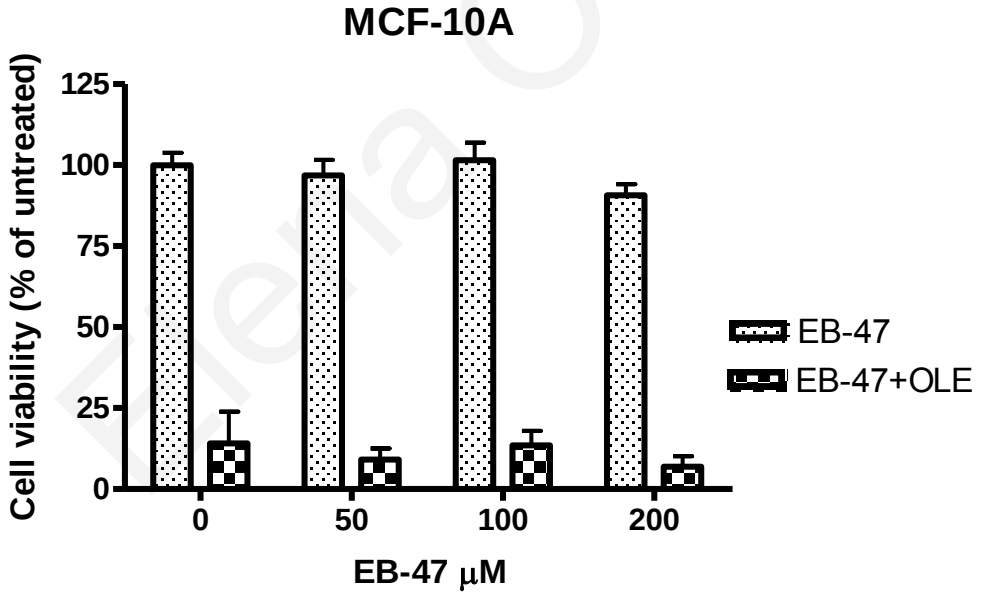

Figure 24: PARP-1 inhibition fails to reverse cell death in normal and cancer cells. MDA-MB-231 cells were pretreated with different concentrations of DPQ (A, B) 3-ABA (C) EB-47 (D) for 1h and then co-treated with 100 μg/ml oleuropein or 100 μM H_2O_2 for 24h. Cell viability was measured by crystal violet. No significant statistical differences between cells treated with oleuropein in the presence and absence of the PARP-1 inhibitors.

4.8 Activation of the MAP kinases

It is well known that the MAPKs are activated through phophorylation by their kinases as a response to environmental changes with oxidative stress among them. Since our results indicated H_2O_2 production by oleuropein and oxidative DNA damage, we assumed that JNK1/2, ERK1/2 and p38 may have a role in the response of cells towards the extracellular production of H_2O_2 by oleuropein. For this, we examined their phosphorylation after 1h of treatment with oleuropein (100 μg/ml) by western blot analysis (Figure 25). An increase in the phosphorylation state of the three MAPKs was observed, an indication that they are activated and implicated in the cell response to the H_2O_2 produced by oleuropein.

The activation of the MAPKs supports our hypothesis that the cells are affected by the produced levels of H_2O_2 in the culture medium during oleuropein treatment. Inhibition of the three MAPKs though, with the inhibitors SP600125, SB202190 and PD98059 was not able to inhibit cell death (Figure 26). Although these kinases are clearly activated, it seems that their inhibition is not sufficient to reverse cell death. It is also interesting to note that increasing concentrations of the p38 inhibitor SB202190 caused a dose dependent decrease in cell viability. This was not observed with the inhibitors of the other two MAPKs indicating the possibility that p38 is important for cell survival (Figure 26).

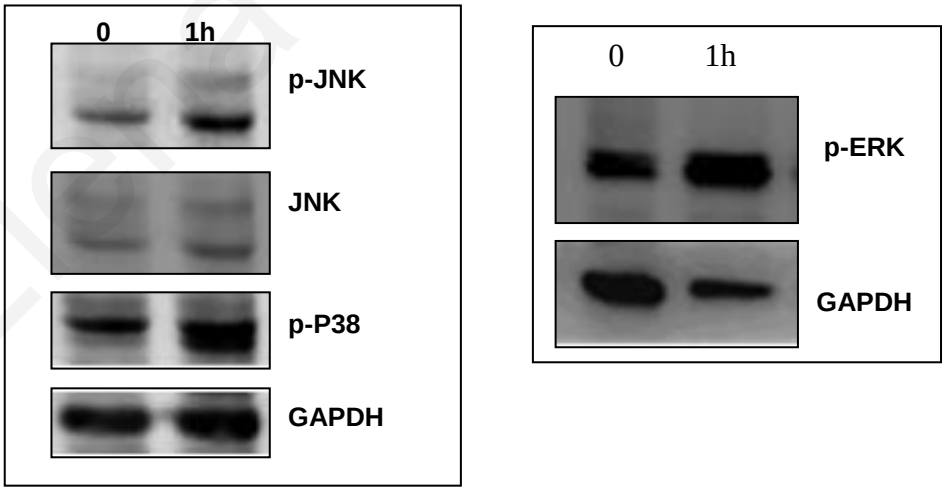

Figure 25: Oleuropein increases JNK, p38 and ERK phosphorylation.
Western blot analysis of MDA-MB-231 whole lysates treated with oleuropein (100 μg/ml) for 1h. GAPDH was used as loading control.

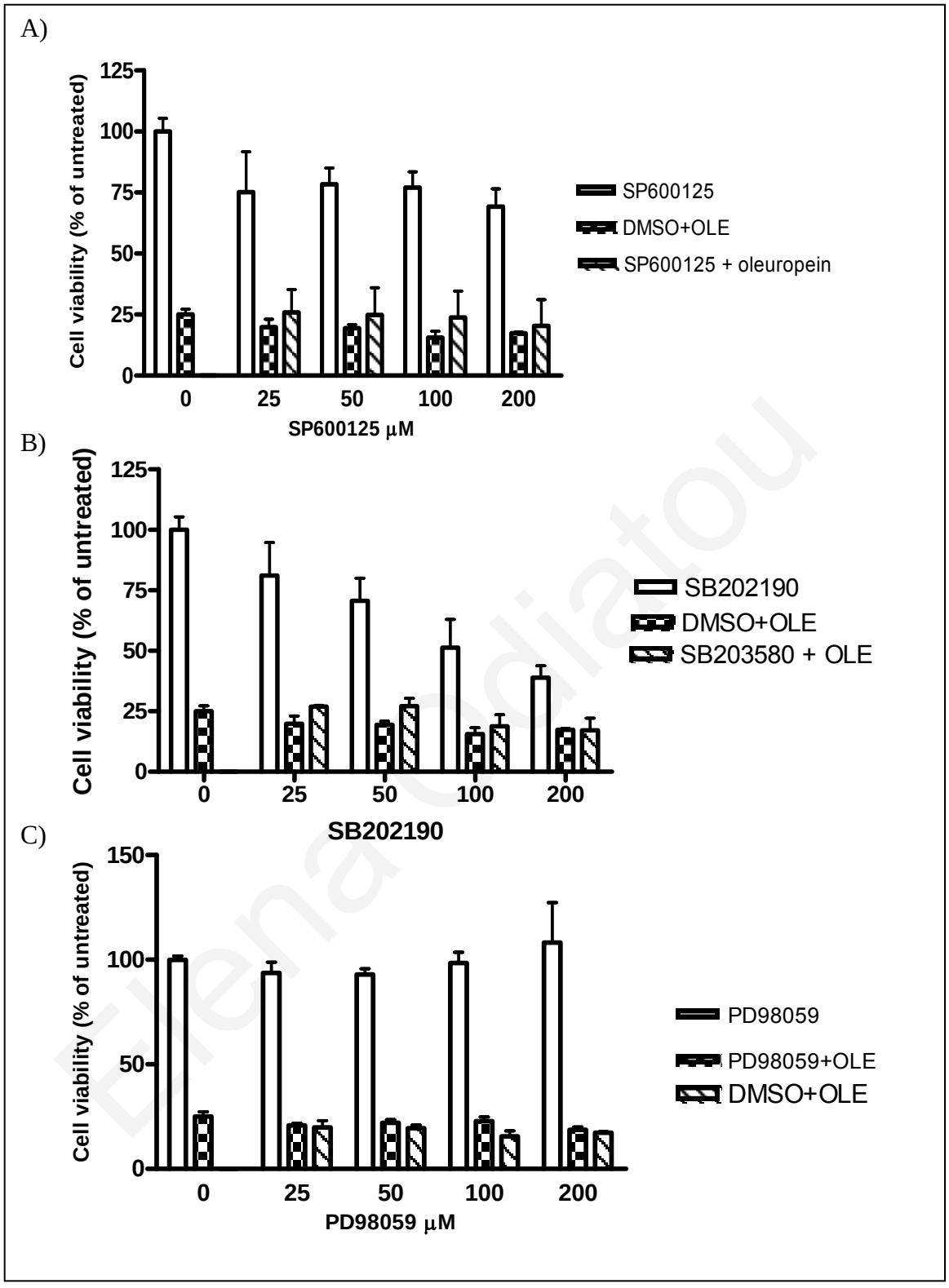

Figure 26: Inhibition of JNK, p38 or ERK, fails to prevent cell death caused by oleuropein.

Cell viability assay of MDA-MB-231 cells treated with oleuropein (100 μg/ml) in the presence of different concentrations of the JNK inhibitor SP600125 A), the p38 inhibitor SB202190 B) and the ERK inhibitor PD98059 C). After staining with crystal violet, absorbance was measured at 570 nm. No statistical significance between treated cells with oleuropein in the presence and absence of the inhibitors.

4.9 The PARP inhibitors DPQ and 3-ABA act differently on the MAP kinases in oleuropein treated cells

As presented earlier, PARP inhibition was not sufficient to reverse cell death (Figure 24). We therefore tried to elucidate if there is any effect of these inhibitors on molecules that were found to be activated upon oleuropein treatment i.e. the MAP kinases p38 and JNK. To our surprise the PARP inhibitor 3-ABA had the opposite effects of that expected. 3-ABA in combination with oleuropein activated p38 and JNK as determined by the increase in their phosphorylated forms that were evident after 17h of treatment (Figure 27, Figure 28). Oleuropein alone caused a small increase in the phosphorylated levels of JNK and p38. This indicates that MAPK activation by oleuropein is not only at the beginning of the treatment as presented earlier, but is also sustained for many hours. In contrast, treatment of cells with the PARP inhibitor DPQ (100 μM), either alone or in combination with oleuropein, caused a complete decrease in the total levels of the JNK protein (Figure 28). As a result there is no production of JNK either in the presence or absence of oleuropein.

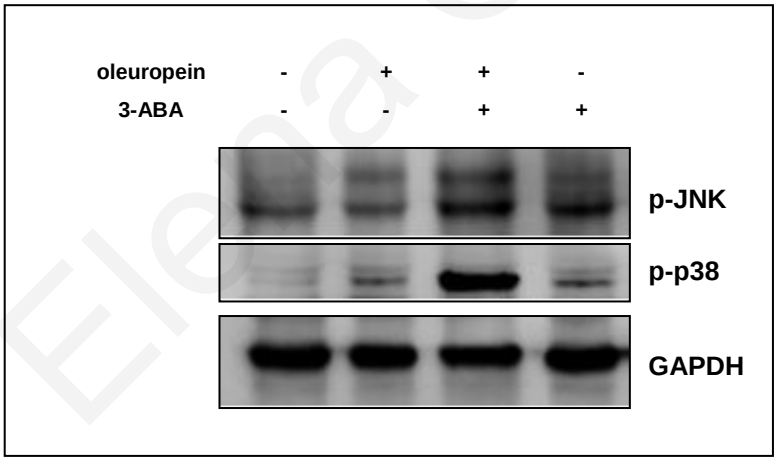

Figure 27: PARP inhibitor 3-ABA increases the phosphorylation of JNK and p38 when incubated with oleuropein.
Western blot of whole MDA-MB-231 lysates treated for 17h. Although oleuropein (100 μg/ml) caused a small increase in the phosphorylation of the two MAPK, the inhibitor strongly enhanced their phosphorylation.

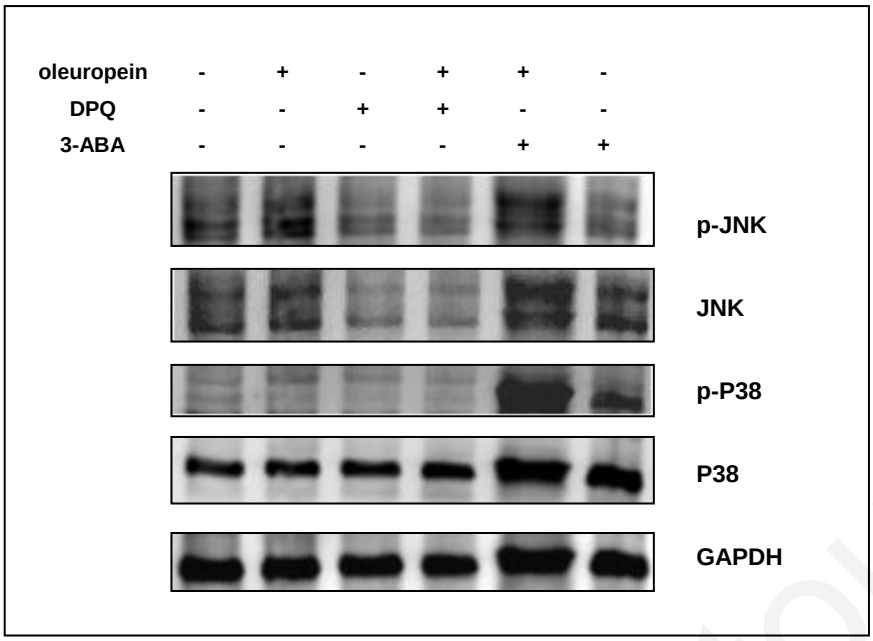

Figure 28: The PARP inhibitors 3-ABA and DPQ have opposite effects on the p38 and JNK MAPK.
Western blot analysis of MDA-MB-231 whole lysates treated for 24h. The PARP inhibitor DPQ(100 μM), diminished the levels of JNK while 3-ABA (10 mM) strongly increased the levels of both the MAPK, in combination with oleuropein (100 μg/ml).

4.10 Oleuropein causes mitochondrial damage

In an attempt to elucidate the molecular pathway of death and the molecules involved, we tried to elucidate the implication of the mitochondria. The mitochondrial membrane was stained with the JC-1 dye to detect any modifications in the mitochondrial potential. Normal mitochondria are stained orange and damaged mitochondria are stained green. Oleuropein was found to cause extensive mitochondrial damage, time dependently, starting early during treatment and continuing for 24h of treatment (Figure 29). This was also evident with hydrogen peroxide treated cells.

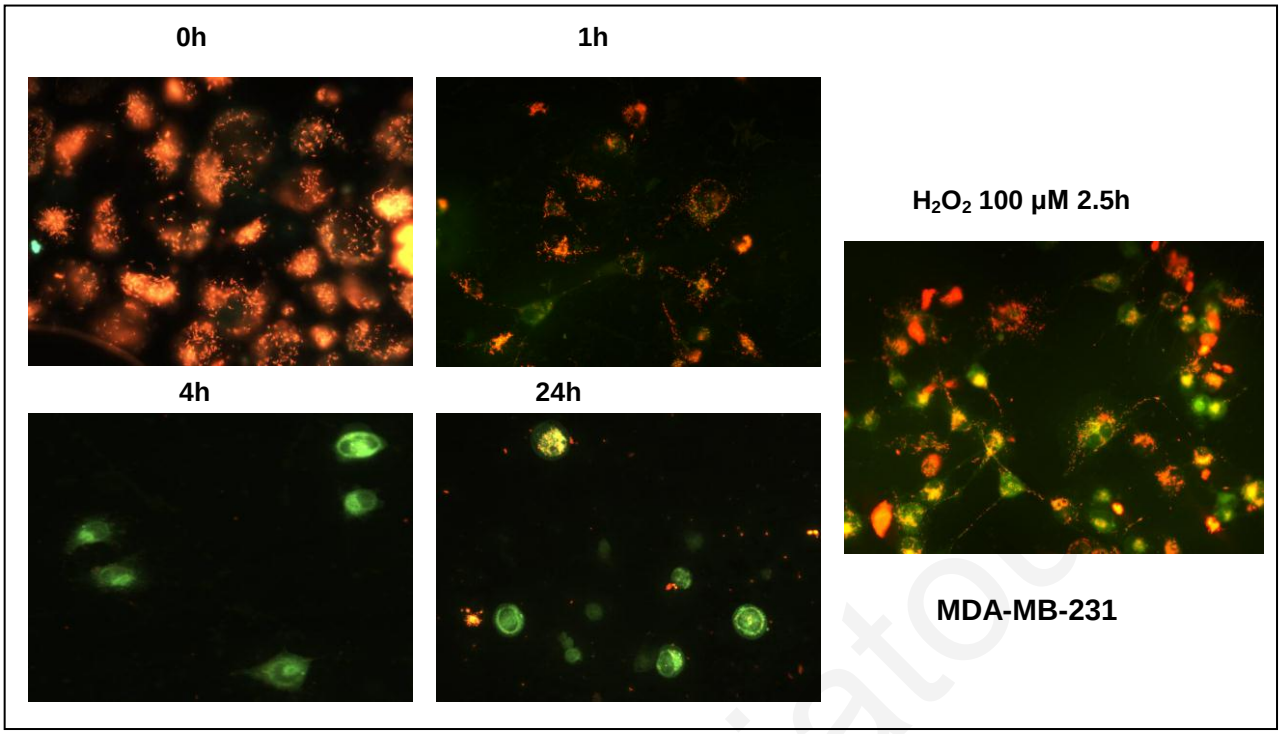

(B)

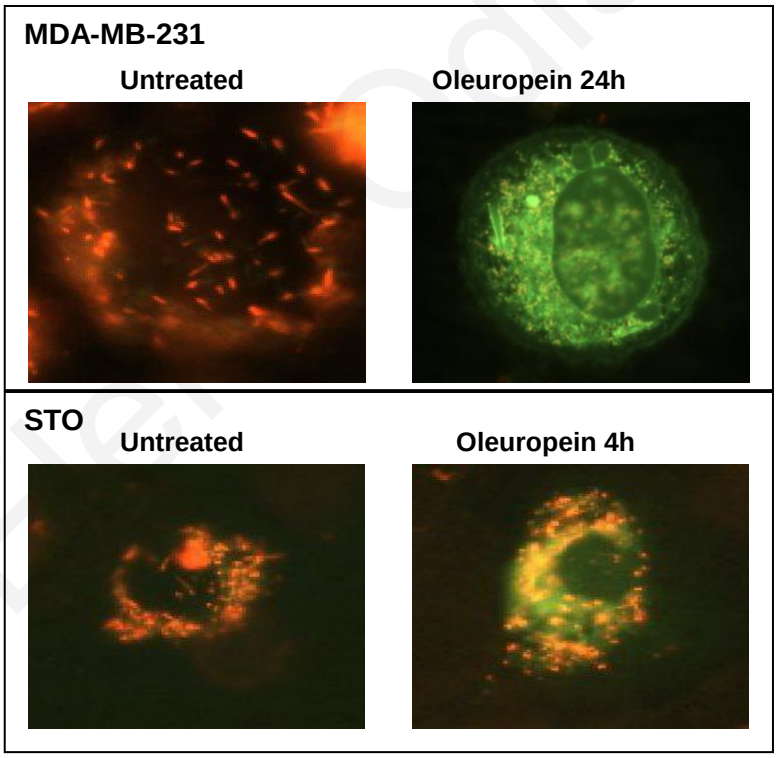

Figure 29: Oleuropein causes mitochondrial membrane potential decrease.
(A) Breast cancer MDA-MB-231 cells were treated with 100 µg/ml oleuropein for 4h and then labeled with the dye JC-1 and visualized under the microscope. Undamaged mitochondria are stained orange and damaged are stained green. (B). MDA-MB-231 cells untreated and treated with 100 µg/ml oleuropein for 24h and STO normal cells untreated and treated with 100 µg/ml oleuropein for 4h stained with JC-1.

4.11 AIF is not transferred to the nucleus

Since we observed mitochondrial damage, activation of PARP-1 and continuous production of PAR we were interested to see if there is a cross talk between the mitochondria and the nuclei upon oleuropein treatment. It has been reported that PAR reacts with AIF leading to its mitochondrial release and nuclear translocation. We therefore investigated this possibility by immunofluorescence detection of AIF in the normal STO cells and cancer MDA-MB-231 cells. As seen in Figure 30, treatment of cells with oleuropein (100 μg/ml) for 8h or 11h indicated that AIF protein was not transferred into the nucleus but it was instead clustered outside the nucleus along with the rest of the cytoplasm. Treated cells were rounded and the cytoplasm was condensed. The same was evident in cells treated with H_2O_2 (50 μM). Although we did not observe translocation during the first 11h we can not exclude the possibility that translocation may happen at later incubation time points.

A)

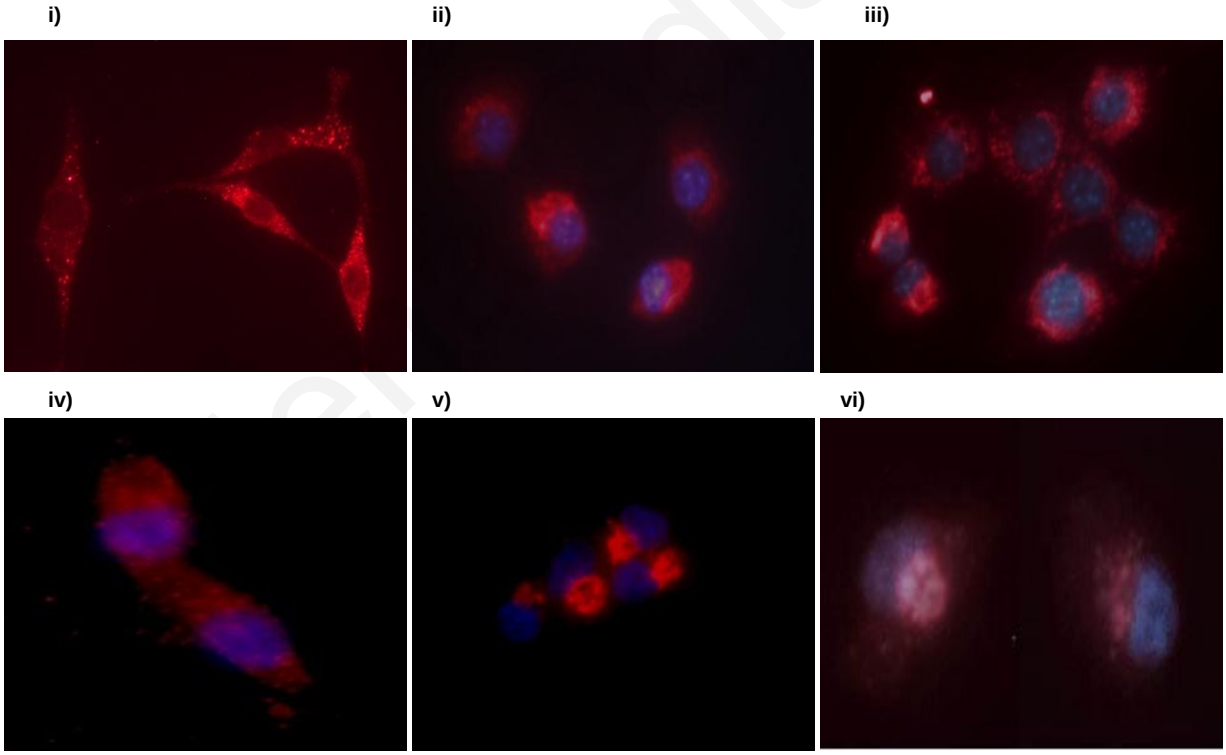

B)

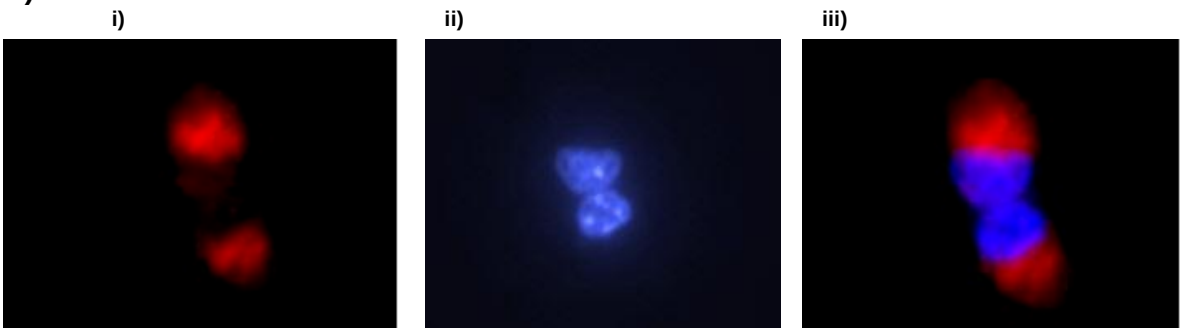

Figure 30: The mitochondrial protein AIF does not translocate to the nucleus upon oleuropein treatment.
A) Immunofluorescence analysis of STO (i) and MDA-MB-231 cells (iv) treated with 100 μg/ml oleuropein (ii and v) or 50 μM H_2O_2 (iii and vi) for 8h. The mitochondrial protein (red) was detected with anti-AIF antibody produced in rabbit (Cell Signaling, 1/100). The nuclei (blue) were stained with Hoechst. B) MDA-MB-231 cells treated for 11h and detection of AIF with immunofluorescence i) untreated cells, ii) oleuropein treated cells (100 μg/ml), iii) H_2O_2 treated cells (50 μM). Cells were visualized under the fluorescence microscope (x400).

4.12 Calcium is not implicated in cell death

Calcium overload is a mechanism of cell death through mitochondrial damage. In an attempt to determine the possible role of calcium ions in the mitochondrial damage, caused by oleuropein and subsequently cell death, we treated cells with cobalt chloride in the presence of oleuropein and measured cell viability by crystal violet staining. In previous studies cobalt chloride was found to be a calcium channel blocker that inhibits calcium ions from entering cells and causing death after H_2O_2 treatment. Cobalt was able to rescue normal cells from death caused by oleuropein (Figure 31). Further investigation though, indicated that this was not the result of calcium inhibition, but rather the elimination of the produced levels of H_2O_2 by cobalt chloride. No levels of H_2O_2 were detected when oleuropein was incubated with cobalt chloride in culture medium and measured by the fox assay (Figure 32). This shows that cobalt chloride either scavenges H_2O_2, or inhibits its production, and the observed protection towards oleuropein is not through the inhibition of calcium overload in cells.

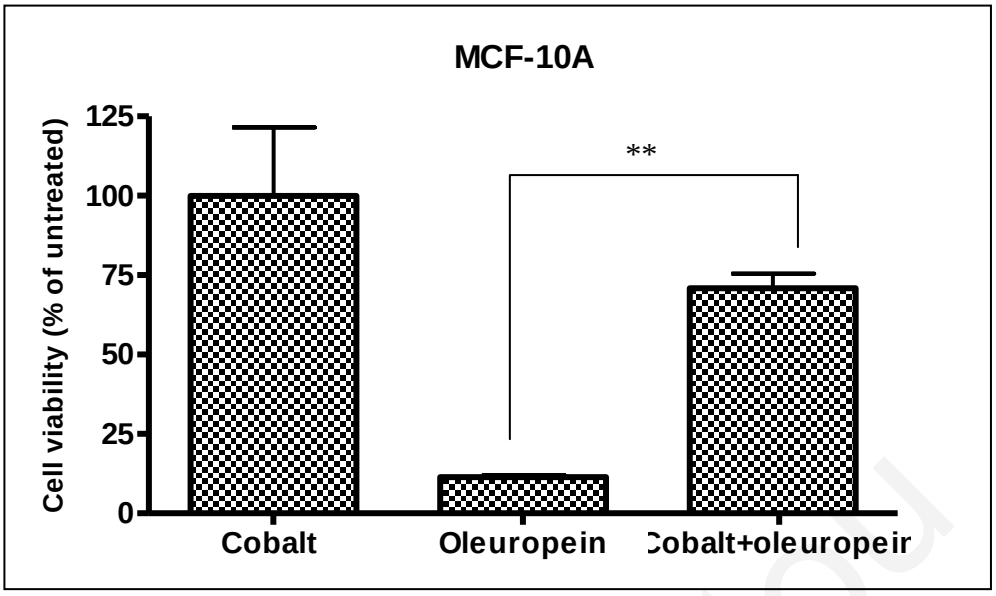

Figure 31: Restoration of viability with cobalt chloride.
Cell viability of MCF-10A cells treated with oleuropein and cobalt chloride (100 μM). No statistical difference between untreated cells and cobalt-oleuropein treated cells was recorded. Statistical differences between oleuropein treated and cobalt-oleuropein treated cells: **p<0.01.

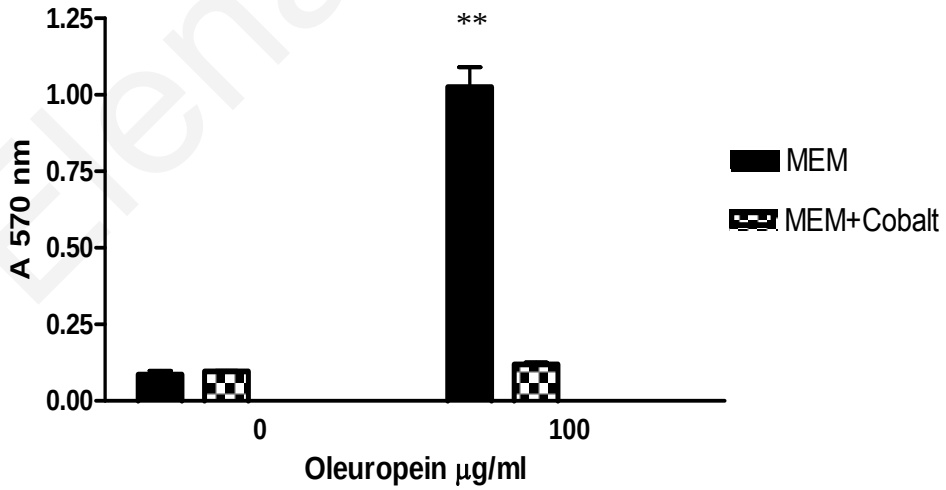

Figure 32: H_2O_2 is not detected in the presence of cobalt chloride.
Oleuropein (100 μg/ml) was incubated for 24h with MEM in the presence and absence of cobalt chloride (100 μM). The produced levels of H_2O_2 were measured by the fox assay with the spectrophotometer.

To further elucidate the implication of calcium, we investigated the possibility that cell death was due to the mitochondrial permeability pore opening, triggered by calcium ions overload. To evaluate this, MDA-MB-231 cells were cultured in home-made MEM, where all the components were added except calcium. In this way, upon oleuropein (100 μg/ml) treatment, the calcium ions could not enter and overload cells causing mitochondrial damage. Even in the absence of calcium, oleuropein killed MDA-MB-231 cells (Figure 33).

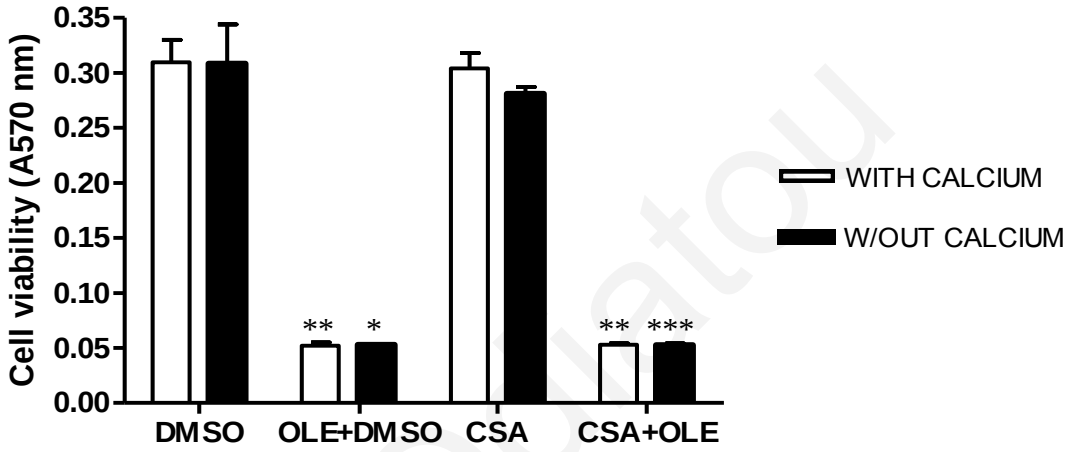

Figure 33: CSA does not inhibit cell death.
MDA-MB-231 cells were cultured in home-made MEM with or without calcium. Cells were treated with oleuropein (100 μg/ml) in the presence of the mitochondrial permeability pore inhibitor Cyclosporine A (CSA). Cell viability was measured with crystal violet. Statistical differences between the treated samples and vehicle control are represented as follows: *p<0.05, **p<0.01, ***p<0.001.

Cells cultured with and without calcium, were also treated with oleuropein in the presence of the mitochondrial permeability pore inhibitor cyclosporine A (CSA). CSA failed to rescue cells even when calcium was absent. These results indicate that calcium ions are not implicated in cell death caused by oleuropein.

4.13 Cell death by oleuropein is caspase independent and mediated through necrosis

Investigation of the mode of cell death caused by oleuropein in MDA-MB-231 cells showed that death was due to necrosis rather than apoptosis. This can be seen from the staining of cells with annexin V and propidium iodide showing a time-dependent increase in necrotic cells without increase in apoptotic cells (Figure 34). The cells that have phosphatidylserine on the outer membrane as a marker of apoptosis, fluorescence green, while cells with damaged plasma membranes fluorescence red. Etoposide an apoptotic inducer was used as a positive control (50 μM) and caused both apoptotic and dead cells. The dead cells in the case of etoposide were most probably late apoptotic cells since the assay was performed after 48h of treatment. The plasma integrity of cells treated with oleuropein was also examined by the trypan blue assay. Trypan blue is impermeable to cells with intact membranes. Oleuropein after 24h of treatment caused a massive increase on the trypan blue permeable membranes (Figure 36). Flow cytometry analysis did not indicate a vast increase in sub-G1 fraction representations in oleuropein treated cells (Figure 35) compared to death seen with the crystal violet assay, the annexin V/propidium iodide staining and the trypan blue assay. Cell death caused by oleuropein was caspase 3 independent, since i) the caspase 3 activity was decreased instead of increased in oleuropein treated cells compared to untreated cells (Figure 37), ii) there was no caspase 3 cleavage to the active form as shown by western blot (Figure 38), iii) the pan-caspase inhibitor z-VAD-fmk failed to reverse cell death (Figure 40, Figure 42), iv) no apoptotic bodies were evident with DAPI staining (Figure 41), and v) the absence of the 89 kDa form of PARP-1, cleaved by caspase 3 (Figure 23). Moreover the levels of the apoptotic proteins p53 and bax were not altered in treated cells (Figure 39). On the contrary, the 55 kDa fragment of PARP-1 representative of necrosis was increased time dependently.

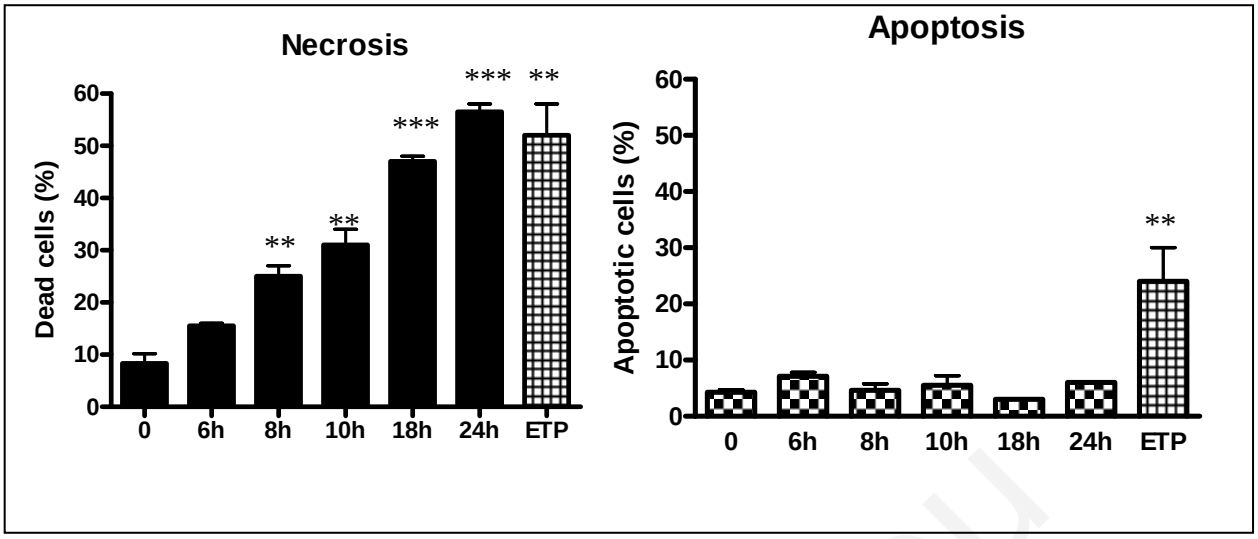

Figure 34: Cell death by oleuropein in MDA-MB-231 cells is through necrosis.
Annexin V/propidium iodide staining measured by the Tali instrument. Cells were incubated with 100 µg/ml of oleuropein for the indicated time points. Etoposide (ETP, 50 µM) for 48h was used as a positive control. Statistical differences between the treated samples and vehicle control are represented as follows: *p<0.05, **p<0.01, ***p<0.001.

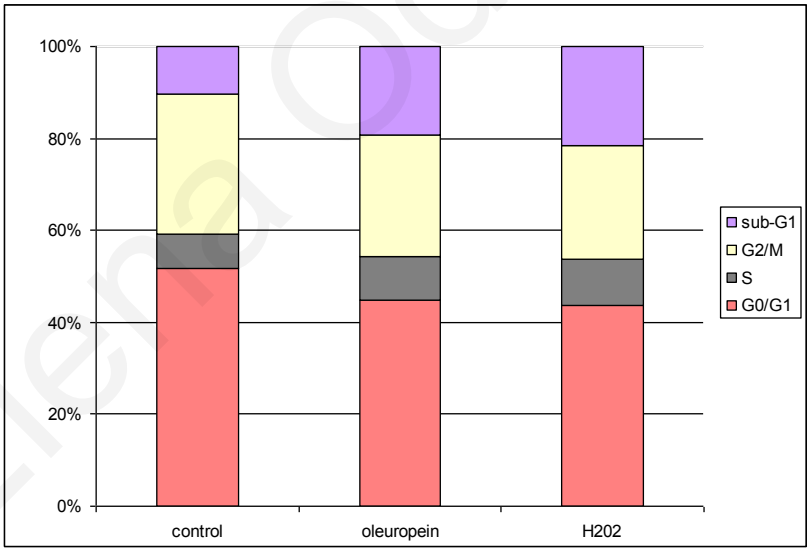

Figure 35: Small increase of sub-G1 phase in oleuropein (100 µg/ml) or H_2O_2 (100 µM) treated MDA-MB-231 cells.
Cells were treated for 24h in DMEM, fixed, stained with propidium iodide and analysed by Flow cytometry.

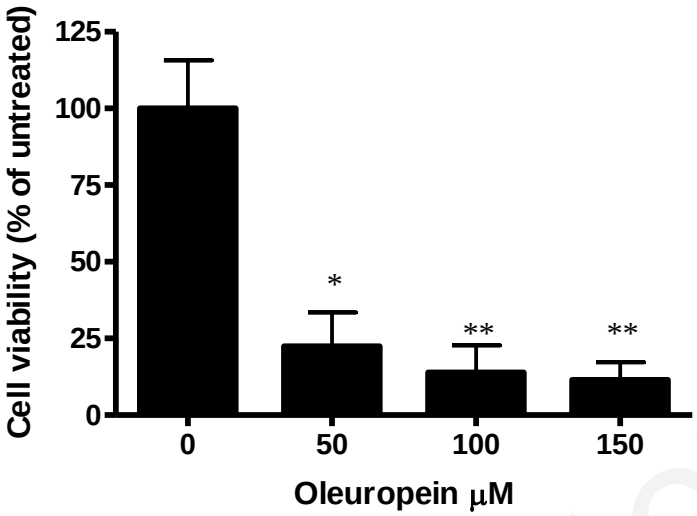

Figure 36: Oleuropein causes cell death.
Cell death of MDA-MB-231 cells treated with different concentrations of oleuropein for 24h and measured by the trypan blue assay under the microscope. Dead cells were stained blue.

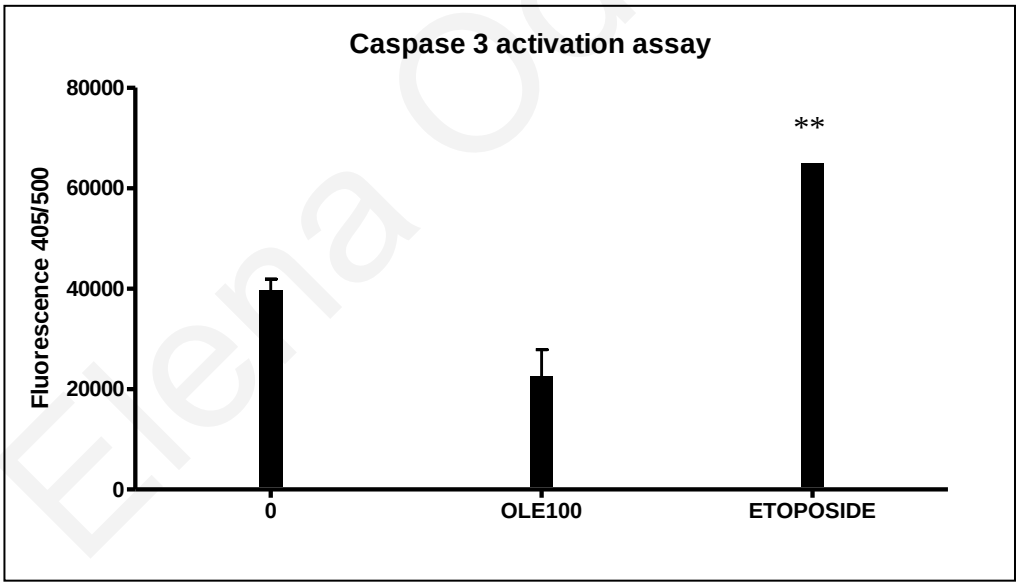

Figure 37: Caspase 3 activity is decreased in oleuropein treated cells.
Caspase 3 activity assay in whole cell lysates (100 μg) of MDA-MB-231 cells incubated with the caspase 3 substrate DEVD-pNA. Cells were untreated, treated with oleuropein (100 μg/ml) for 24h, or treated with etoposide (50 μM) for 48h. The cleaved product was measured spectrophotometrically at 405/500 nm. Extract from etoposide treated cells was used as positive control and extract from untreated cells as negative control.

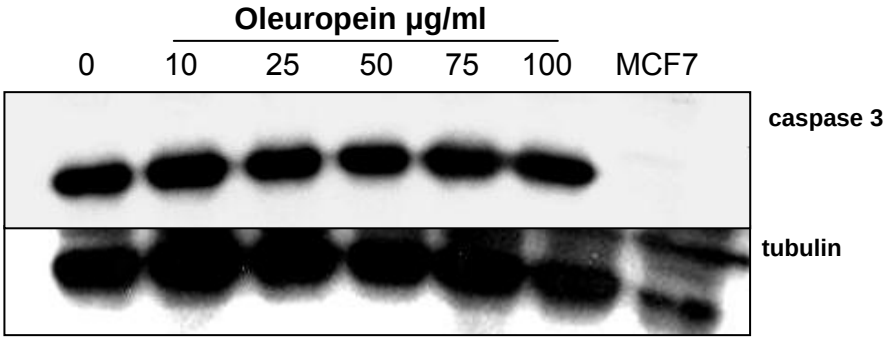

Figure 38: Caspase 3 is not activated by oleuropein.
Western blot analysis of caspase 3 in MDA-MB-231 whole cell lysates treated with different concentrations of oleuropein for 24h. Tubulin was used as a loading control.

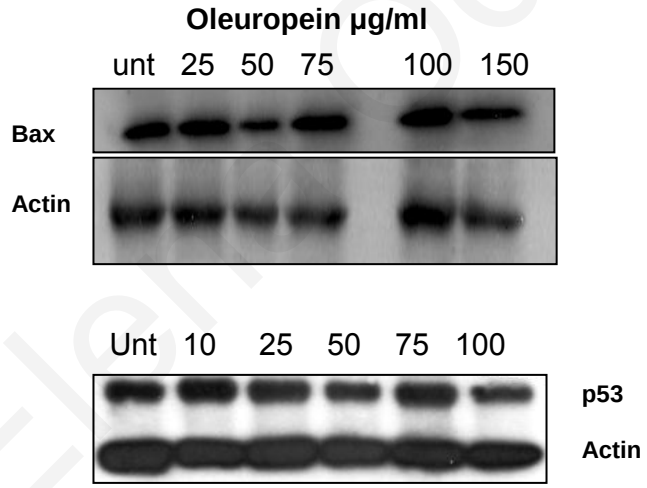

Figure 39: Apoptotic proteins are not implicated in oleuropein cell death.
Western blot analysis of whole cell extracts of MDA-MB-231 cells treated with different concentrations of oleuropein for 24h. p53 and bax levels were not altered by oleuropein.

A.

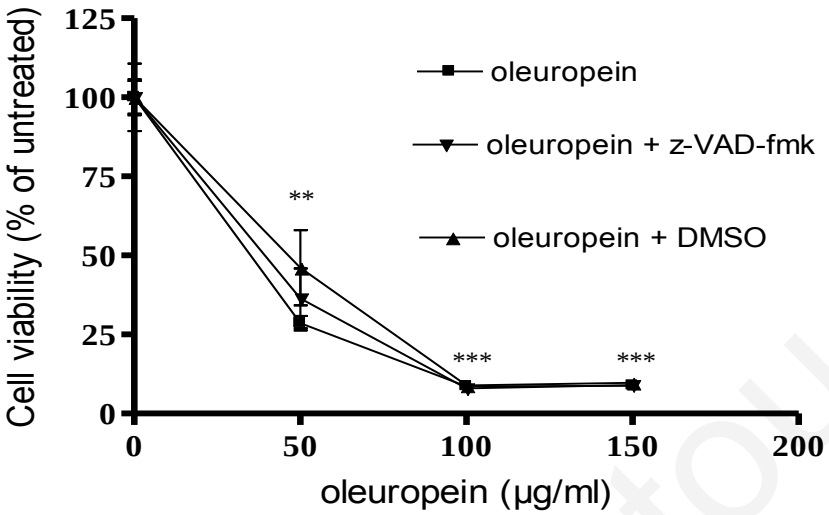

B.

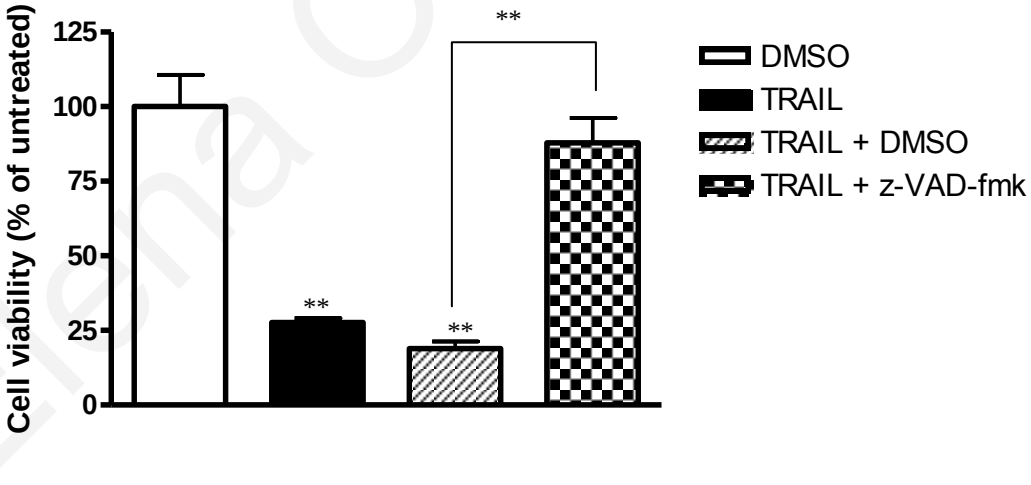

Figure 40: Cell death is independent of caspase 3.
A) Cell viability assay in MDA-MB-231 cells. Cells were treated with different concentrations of oleuropein alone or in the presence of the pancaspase inhibitor z-VAD-fmk (20 µm). DMSO was used as a control for the inhibitor. No statistical differences were observed at the 3 concentrations of oleuropein in the presence and absence of z-VAD-fmk. B) The activity of z-VAD-fmk was tested with the apoptotic agent TRAIL in MDA-MB-231 cells. z-VAD-fmk (20 µM) restored cell death caused by TRAIL. Statistical differences between the treated samples and vehicle control are represented as follows: *p<0.05, **p<0.01, ***p<0.001.

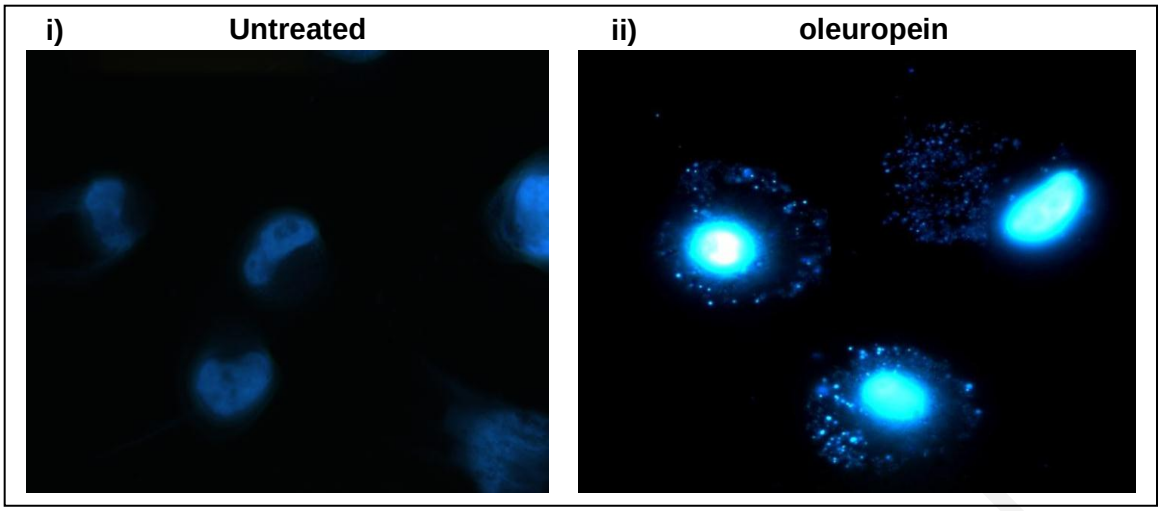

Figure 41: Absence of apoptotic bodies.
MDA-MB-231 untreated cells and (ii) oleuropein treated cells (100 µg/ml for 24h) were stained with DAPI and visualized under the fluorescence microscope after ultra violet excitement (350 nm). The nuclei of dead cells were stained with intense blue colour compared to the untreated cells.

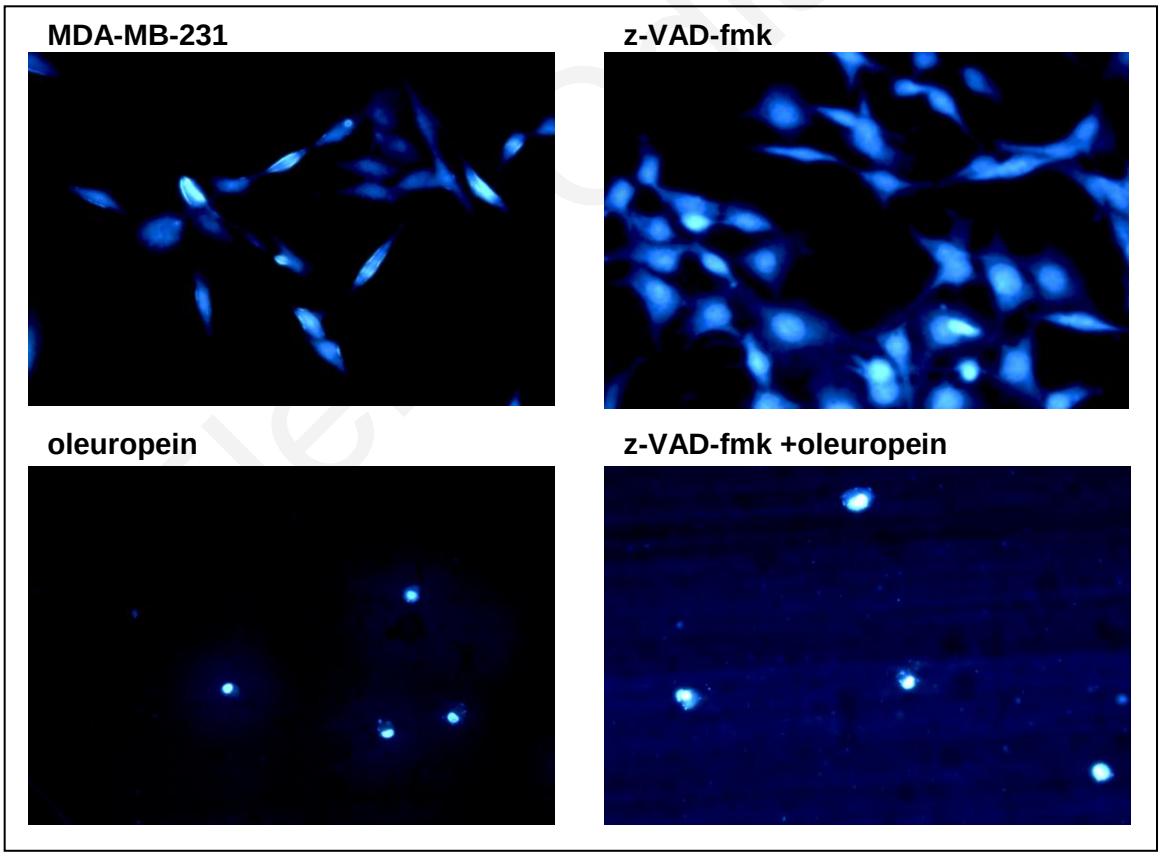

Figure 42: Cellular shrinkage by oleuropein is not prevented by the pancaspase inhibitor z-VAD-fmk.
MDA-MB-231 cells were treated for 24h and then stained with DAPI. Oleuropein (100 µg/ml) treated cells caused nuclear condensation that was not prevented when coincubated with the pan caspase inhibitor z-VAD-fmk (20 µM) added 1h before oleuropein treatment.

4.14 The lysosomal iron is implicated in cell death by oleuropein

The implication of the lysosomal iron in cell death caused by oleuropein was assessed by the co-incubation of cells with the iron chelator deferoxamine mesylate (DFO). As expected, oleuropein and H_2O_2 reduced substantially cell viability. However, DFO protected cells from death caused by oleuropein (Figure 43). Similarly, H_2O_2 caused cell death reversed by DFO pretreatment. Implication of lysosomes in cell death was further assessed by the acridine orange staining of treated and untreated cells. Normal lysosomes are stained orange and cells with permeabilized lysosomes are stained green. As seen in Figure 44, treatment of cells with oleuropein (100 μg/ml) or H_2O_2 (50 μM), caused a time-dependent lysosomal permeabilization which was evident at some lysosomes 1h after treatment. All the lysosomes became entirely damaged at 20h of oleuropein treatment (Figure 44).

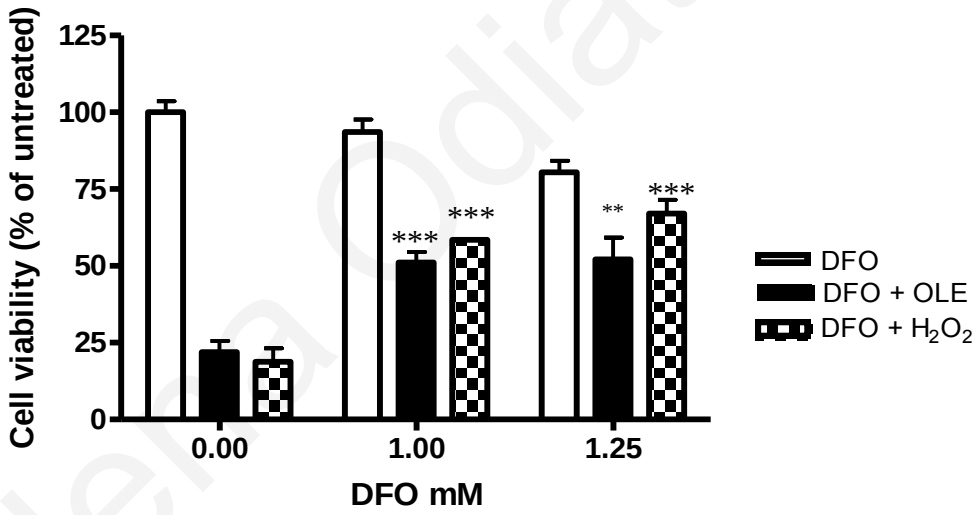

Figure 43: Cell protection by iron chelation.
MDA-MB-231 cells were preincubated with desferrioxamine (DFO) for 3h and then treated with 100 μg/ml oleuropein or 100 μM H_2O_2. Statistical differences between oleuropein or H_2O_2 treated samples compared to oleuropein-DFO and H2O2-DFO treated samples are represented as follows: **p<0.01, ***p<0.001.

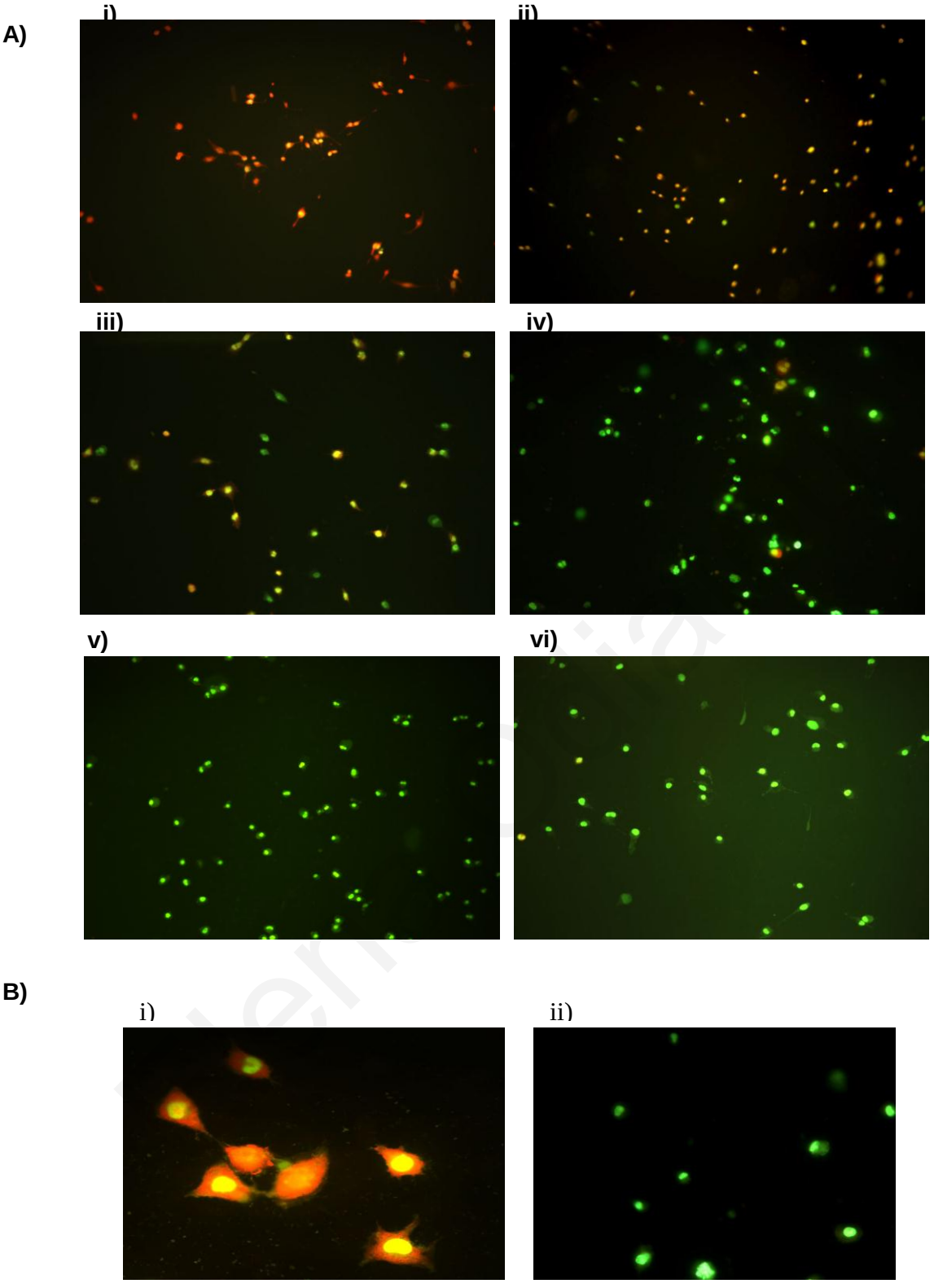

Figure 44: Lysosomal membrane permeabilization by oleuropein.
A) MDA-MB-231 cells were preloaded with acridine orange and then treated with 100 µg/ml oleuropein for 1h (ii), 5h (iii), 12h (iv), 20h (v). Untreated cells (i) were used as negative control and cells treated with 50 µM H_2O_2 for 5h as positive control (vi). B) Magnification of untreated (i) and oleuropein treated MDA-MB-231 cells for 20h (ii) stained with acridine orange and visualized under the fluorescence microscope (x400).

NAC, a known anti-oxidant, with higher selectivity towards hydroxyl radicals, totally reversed the observed decrease in cell viability of MDA-MB-231 cells caused by oleuropein (Figure 45). This is a further indication that death caused by oleuropein is mediated through the lysosomes.

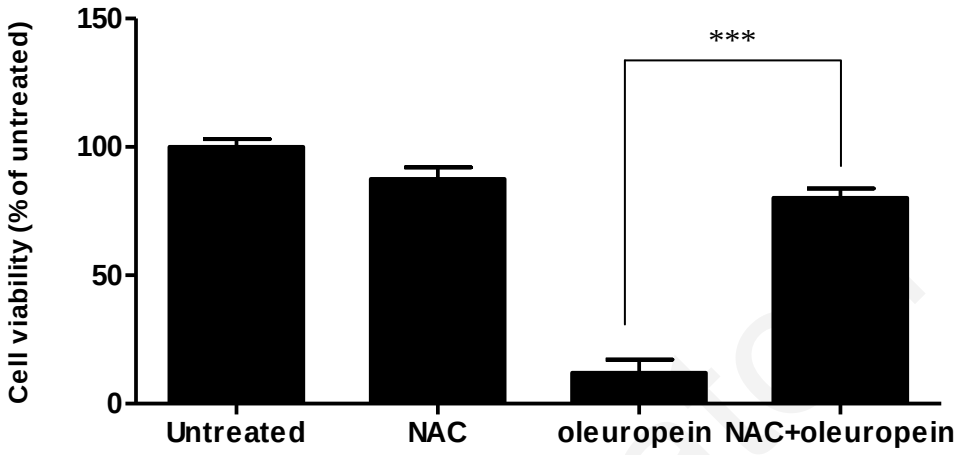

Figure 45: Prevention of MDA-MB-231 cell death by NAC.
Cell viability assay of breast cancer MDA-MB-231 cells cultured for 24 h in DMEM with oleuropein (100 µg/ml) in the presence and absence of 1 mM NAC. Cells were stained with crystal violet and absorbance was measured at 570 nm. NAC was added 1 h before treatment. The data represent the mean ± SD. ***, indicates statistically significant difference ($p<0.001$) between the oleuropein treated cells in the presence and absence of NAC.

4.15 Cell death is not inhibited by the glucose transporter inhibitor phloretin

Since every molecule of oleuropein includes a molecule of glucose, there is a possibility that oleuropein enters the cell through the glucose transporters. To investigate this possibility, cells were pre-treated with the glucose transporter inhibitor phloretin and then treated with oleuropein for 24h prior to determining cell viability. As seen in Figure 46, phloretin was unable to rescue cells from death. This indicates that cell death caused by oleuropein is not through the entrance of oleuropein through the glucose transporters.

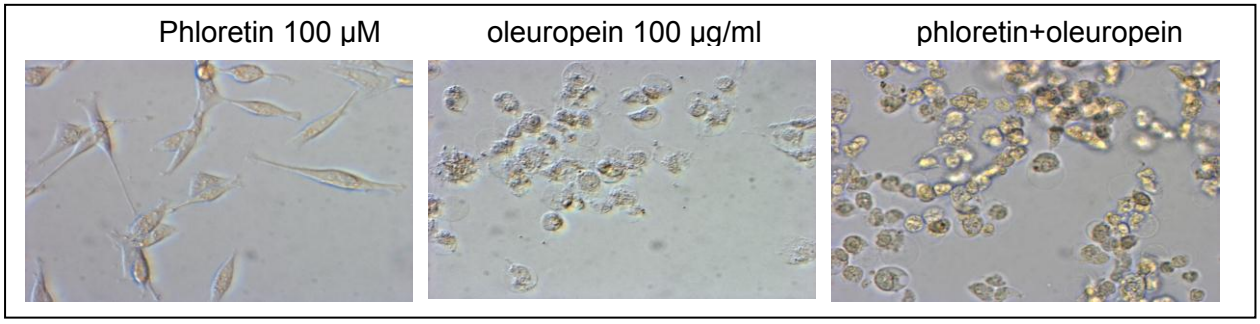

Figure 46: Blockage of glucose transporters does not prevent cell death by oleuropein.
Light microscopy of cells treated with oleuropein for 24h in the presence and absence of the glucose transporter inhibitor phloretin. Treated cells are detached with condensed chromatin.

4.16 Cell death is independent of Estrogen Receptors

Since MDA-MB-231 cells do not express estrogen receptors, we wanted to exclude the possibility that ERs have any implication in the protection of cell death. We used MDA-MB-231 cells overexpressing ER-alpha (S30 cells) or ER-beta (ER-beta 41 cells) and treated them with increasing concentrations of oleuropein. Cell viability was measured after 24h. As seen in

Figure **47**, ERs, did not offer any protection towards cell death caused by oleuropein. This indicates that cell death caused by oleuropein is independent of Estrogen Receptors.

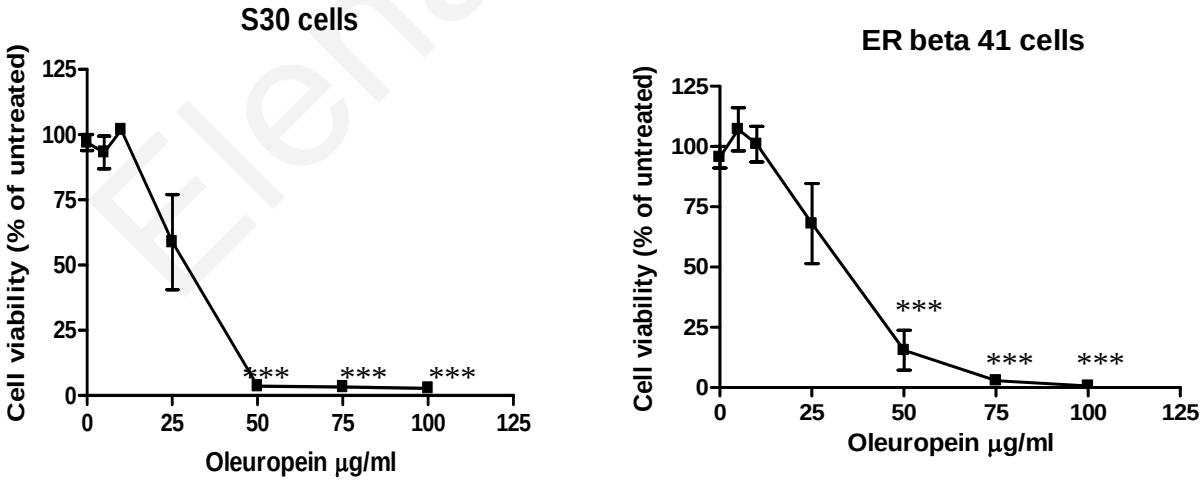

Figure 47: Effect of oleuropein on MDA-MB-231 cells overexpressing the Estrogen Receptors.
Cell viability assay of MDA-MB-231 cells transfected with ER-α (S30 cells) and ER-β (ER-β41 cells) and treated with different concentrations of oleuropein for 24h. The data represent the mean ± SD. ***, indicates statistically significant difference ($p<0.001$) between the oleuropein treated cells compared to untreated cells.

5 DISCUSSION

In this study we aimed to elucidate the *in vitro* production of H_2O_2 by the olive secoiridoid oleuropein and its metabolite hydroxytyrosol, under standard culture conditions, the effect on normal and cancer cells and the molecular mechanism of cell death.

In their pioneering studies, Long et al [3,59] have speculated that an unknown culture medium component reacts with compounds such as hydroxytyrosol, delphinidin chloride, rosmarinic acid, EGCG, catechin and quercetin, producing H_2O_2, and that this is responsible for the *in vitro* artifacts of these phenols. In the present study we have identified this "unknown compound" as well as the exact conditions that lead to H_2O_2 production when the phenolic compounds hydroxytyrosol and oleuropein are introduced to culture media. Furthermore, we have shown how H_2O_2 can be quenched or avoided.

We have shown, for the first time, that H_2O_2 production by the olive phenols oleuropein and hydroxytyrosol under standard cell culture conditions (37 ºC, 5% CO_2) is due to sodium bicarbonate, which is a component of most media formulations. Sodium bicarbonate in the presence of CO_2 stabilizes the pH of the medium to 7.4 by producing hydroxide ions. In the absence of sodium bicarbonate, the pH decreases due to H^+ production, a condition that does not promote H_2O_2 production. We propose that oleuropein produces H_2O_2 through oxidation of the hydroxytyrosol molecule as shown in Figure 22. In the proposed scheme, under standard cell culture conditions, oxygen and hydroxide ions react with the catechol molecule to produce o-benzoquinone and H_2O_2.

Our results have immediate applications in the interpretation of the *in vitro* data, since we have identified that sodium bicarbonate in the culture media, in the presence of oleuropein, hydroxytyrosol and possibly other polyphenols, produce sufficient quantities of H_2O_2 to possibly override any other effects attributed to these compounds (such as antioxidant, estrogenic, signal transduction etc.), and lead to reduced cell survival due to H_2O_2 -induced necrosis, apoptosis or cell cycle arrest. Also, quite often, comparisons are being made in the response of different cell lines to the treatment with polyphenols that are cultured in different media. Media containing sodium pyruvate in their formulations, such as DMEM/F12, apparently will produce little or no H_2O_2 in comparison to media like MEM and DMEM that do not contain it. Since DMEM/F12, is used for culturing "normal" immortalized MCF-10A breast cells and MEM and DMEM for culturing cancer cells, one can be lead to the erroneous conclusion that the polyphenols kill selectively cancer cells [145,146]. Similarly to oleuropein and hydroxytyrosol, resveratrol and EGCG were shown

to be degraded in the presence of sodium bicarbonate producing H_2O_2 in the culture medium BMEM [147].

To understand how the produced levels of H_2O_2 affect cells, we studied the oxidative DNA damage and the cell viability of MDA-MB-231 breast cancer cells, "normal" immortalized MCF-10A breast cells and normal mouse embryonic STO fibroblasts, in the presence and absence of sodium pyruvate. A time dependent decrease of proliferation was observed in all cell lines with a complete recovery in the presence of sodium pyruvate. Also, an extensive DNA oxidative damage was evident in cells treated with oleuropein which was completely prevented by sodium pyruvate. These findings demonstrate that the observed decrease in cell viability is due to H_2O_2.

In order to elucidate the molecular mechanism of cell death, we exclusively studied many possible pathways of cell death. Firstly, we studied the mode of cell death (i.e. apoptosis, necrosis, and parthanatos) and then the possible implication of glucose transporters, topoisomerases, Estrogen Receptors, calcium, mitochondria, lysosomes and apoptotic proteins.

In our study we have evaluated many possible pathways through which oleuropein could cause cell death. Based on our results we have excluded the involvement of apoptosis; since no morphological nor biochemical features of apoptosis were evident, glucose transporters for the entrance of oleuropein; since blocking them fail to restore cell viability, Estrogen Receptors; since ER-α or ER-β transfected MDA-MB-231 cells responded similarly to MDA-MB-231 cells, topoisomerases; since no effect was observed in the catalytic activities of these enzymes, calcium; since cell death was also evident in cells cultured in calcium free medium and also cyclosporine A failed to rescue cells.

The involvement of the mitochondria in cell death caused by oleuropein was indicated by visualizing the decrease in the mitochondrilal transmembrane potential ($\Psi\Delta$m), by monitoring the location of AIF and by investigating the role of calcium and the mitochondrial permeabilization pore. Indeed, there was a clear decrease in the membrane potential early after treatment with oleuropein and still evident at 24h. No increase in the nuclear AIF levels was evident after 8h or 11h of incubation, excluding the implication of AIF as the executioner of the death pathway. Although the mitochondrial damage and the nuclear translocation of AIF has been reported in H_2O_2 induced cell death [148] we only observed the mitochondrial damage in our experiments without the AIF translocation in either cancer or normal cells. Cyclosporine A, an inhibitor of cyclophilin D, a mitochondrial protein activated by calcium and involved in the opening of the mitochondrial permeabilization pore, failed to inhibit cell death. In addition, removal of the calcium from the culture medium did not manage to rescue cells. These data indicate that the decrease

in the mitochondrial potential was not caused by high levels of calcium entering the cytosol upon oleuropein treatment.

Although PARP-1 protein was clearly shown to be activated, its inhibitors could not restore cell viability. This is something that has been observed also by others [149] and could mean that either these indicators are ineffective under these conditions, that other pathways are activated when PARP-1 is inhibited or that PARP-1 is activated for cell protection and is not the executioner of necrosis. Our data showed that treatment of cells with oleuropein in the presence of the PARP inhibitor 3-ABA caused an increase in the phosphorylated levels of JNK and p38 while treatment with the PARP inhibitor DPQ caused a reduction in the levels of JNK. These data show that inhibition of PARP disturbs the levels and activity of the MAPK and probably activates other pathways. It is not however clear if these proteins are activated for cell protection or for the execution of death.

Inhibition of PARP in oxidatively stressed cells has been shown to prevent necrosis but not apoptosis. Specifically, in intestinal epithelial cells HT-29-18-C1 treated with 1 mM of H_2O_2 the PARP inhibitors 3-aminobenzamide and nicotinamide decreased cell death mediated by necrosis and ATP loss was prevented. These treatments however did not prevent detachment of cells mediated through apoptosis. Similar results were observed in renal epithelial LLC-PK1 cells exposed to 1 mM of H_2O_2 where although necrosis, NAD and ATP depletion were prevented by the PARP inhibitor 3-aminobenzamide, apoptosis was not prevented. The authors did not indicate however, if apoptosis was the result of the oxidative stress or the result of the PARP inhibition [150] [151]. In the study of Yu et al [102] H_2O_2 treated fibroblasts were rescued after PARP-1 inhibition by DPQ at 4h and 8h of treatment. No data were shown for 24h treatment. So it is possible that PARP inhibition by the chemical inhibitors is successful only at the first stages of cell death and not at the final stages. It could also denote that inhibitors are effective only against early necrosis and not late apoptosis. Since the viability assay we performed with the PARP-1 inhibitors did not separate necrotic from apoptotic cells, we can not exclude the possibility that the observed death after PARP-1 inhibition, is caused by apoptosis or even by side effects of the PARP-1 inhibitors in the presence of oxidative stress. It is worth to mention that the concentration of the PARP-1 inhibitor 3-ABA used, based on the bibliography, was 10 mM, which is undoubtly an extremely high concentration that could activate other pathways. Indeed, western blot of cells treated with 3-ABA demonstrated an increase in the phosphorylated levels of the p38 protein that was very intense in oleuropein treated cells. This was not observed when DPQ was used. The inability of the inhibitors to rescue oleuropein treated cells could also be attributed to the loss of activity during increasing production of H_2O_2 under our experimental conditions.

Inhibition of the MAPKs failed to rescue cells indicating that although they are clearly activated upon oxidative stress, they are not crucial for cell death. Indeed, in a study with bovine aortic epithelial cells treated with 300 μM H_2O_2 for 24h, although p38 was phosphorylated, its inhibitor SB203580 (10 μM) exhibited no effect on the H_2O_2 induced decrease in cell viability [152]. This was also shown in human lung adenocarcinoma CL3 cell line treated with 50-500 μM H_2O_2 for 30 min. Although p38 and JNK were clearly dose dependently activated by phosphorylation, the cytotoxicity could not be attenuated by the specific p38 inhibitor SB202190 or by the suppression of the upstream JNK activators [153]. It is well known that the role of the three MAPKs is to respond to various external environmental stimuli such as the oxidative stress. Our results showed that the three MAPKs are activated in oleuropein treated cells early during treatment. Whether this activation contributes to further activate other proteins and contribute to cell death or as a protective mechanism for the survival of cells is not clear. Conflicting studies support both of the mechanisms so far.

Our data clearly show that cells treated with oleuropein, have a profound production of PAR that is continuously present up to 24h of treatment. PARP-1 was not inactivated by caspase 3, since the 89 kDa cleaved part was missing. On the contrary, the 55 kDa cleaved part of PARP-1, was time dependently increased, a further indication that death was not through apoptosis, but rather necrosis. How PARP-1 is cleaved to the 55 kDa fragment is not very clear but it could be through the lysosomal cathepsins. This was shown in a study, where PARP-1 was digested *in vitro* with lysosomal extract and the cathepsins B, D and G. Indeed the cathepsins and the lysosomal extract produced similar fragments with the lysates of cells treated with H_2O_2 but instead of a 50 kDa fragment, a 55 kDa was evident [91]. Since our data show the implication of the lysosomes, it could be possible that the observed cleaved PARP-1 fragment is produced by the lysosomal cathepsins.

In the study of Dawson et al [154], it was shown beyond any doubt, that PAR alone is capable and sufficient to cause cell death *in vitro* and *in vivo*. PAR has been described as a signal from the nucleus to the mitochondia which causes the release of AIF, the translocation to the nucleus and finally chromatin condensation and death.

There are countless studies describing apoptotic, caspase independent or necrotic pathways through which H_2O_2 causes cell death. In our study we did not observe any activation of the apoptotic machinery. We observed a decrease instead of an increase, in the activation of the caspase 3, the most important executioner of apoptosis. This is in agreement with the bibliography, since H_2O_2 has been reported to directly and reversibly inactivate the caspases *in vitro* either as recombinant enzymes or as cell lysates inhibiting thus the pathway of apoptosis [155]. The choice between apoptosis and necrosis is highly

dependent on the H_2O_2 concentration due to the caspases' sensitivity to the oxidative inactivation. Higher amounts switch cell death from apoptosis to necrosis most likely through oxidation of the active cysteine group [156].

Due to the Fenton reaction, H_2O_2 becomes lethal in the cells with the iron found in the lysosomes. This reaction causes the production of highly destructive hydroxyl radicals that react with the DNA to cause damage. Our results demonstrate the involvement of the lysosomes in cell death induced by oleuropein, starting soon after treatment. Lysosomes were damaged as shown with acridine orange staining and cell death was inhibited by scavenging the lysosomal iron by DFO. The same characteristics were observed in cells treated with H_2O_2, an indication that death by oleuropein is highly dependent on the H_2O_2 production. Although the chelation of the lysosomal iron did not protect completely from cell death, it gave a considerable protection. This discrepancy could be attributed to the fact that the cytosolic iron, that is released from ferritin and other proteins during oxidative stress, in the cells is not inactivated by DFO which enters cells through endocytosis and is restrained in the lysosomes [119]. NAC, a known antioxidant that scavenges hydroxyl radicals more effectively than H_2O_2, rescued cells from death, further indicating that lysosomes are implicated in cell death [157].

Oxidative DNA damage in oleuropein treated cells was evident early on after treatment. This observation, in combination with the early defects in the lysosomes and the inhibition of death by the iron chelator DFO, strongly suggest that lysosomal iron has an important role in the DNA damage and the subsequent death caused by oleuropein. Additionally, the continuous activation of the PARP-1 protein, which is responsible for the repair of DNA, indicates a severe and not repairable DNA damage that ultimately leads to cell death. Although the involvement of both the mitochondria and the lysosomes is obvious, it is difficult to specify which organelle was damaged first.

During massive lysosomal membrane permeabilization (LMP), the cathepsins and the hydrolases that reside in the lysosomes are released in the cytosol causing digestion of proteins, and activation of other hydrolases leading cells to necrosis [118]. This seems to happen also with oleuropein, since the observed cell death was necrotic and PARP-1 was cleaved to a 55 kDa fragment similar to the one cleaved by the cathepsins. H_2O_2 has been shown to induce iron dependent necrosis through LMP in MEFs, supporting our data that the produced levels of H_2O_2 by oleuropein, cause cell death through extensive damage of the lysosomes [158].

Our results demonstrate that death caused by oleuropein in MDA-MB-231 cells is caspase independent, with evident oxidative DNA damage and MAPK activation, damage in the mitochondria and the lysosomes, necrotic cleavage of PARP-1 and PAR overproduction and permeability of the cell membrane. Only inhibition of the lysosomal

damage by iron chelation managed to rescue cells. These results strongly suggest that the mode of cell death is necrosis mediated through lysosomal membrane permeabilization.

Although the findings of the present work can provide explanations to oleuropein´s effect in the various *in vitro* studies, it cannot explain recent reports where oleuropein aglycone was found to reverse acquired autoresistance to herceptin [159,160]. In these interesting reports, where the aglycone form of oleuropein was used, sodium pyruvate was included in the culture medium. This suggests that at least the aglycone form of oleuropein may exert its anticancer effect in a manner that is independent of H_2O_2 production. Regardless, caution should be exercised when using oleuropein and the possibility that the observed effects might be due to the production of H_2O_2 or the oxidized form of oleuropein should also be considered.

The Mediterranean diet, rich in virgin olive oil and olive fruit, containing hydroxytyrosol and oleuropein, besides the documented cancer preventive effects, has shown a variety of other health promoting properties. These include cardioprotective, anti-inflammatory, antimicrobial, antiviral, anti-oxidant and anti-ageing effects. The results of our studies were not intended to challenge any of the above results that are strongly supported by *in vivo* or human intervention studies. Our goal was rather to point-out that the differences between the *in vitro* and *in vivo* results could be due to the culture conditions that favor the pro-oxidant effects of the polyphenols. It is well documented that olive polyphenols exert antioxidant effects and prevent DNA-damage at concentrations ranging from 1-10 μM [161], but have opposite effects at concentrations higher than 100 μM [32,65]. Also, the metabolism of the polyphenols in living systems is different and the serum levels are much lower from those used routinely in the *in vitro* systems [162,163]. At these low plasma/serum concentrations achieved by the consumption of olive oil or olive fruit, the antioxidant effects may override the pro-oxidant effects.

In the present report we show conclusively that although oleuropein and hydroxytyrosol have been characterized as anti-oxidants [161], in the commonly used media containing sodium bicarbonate, under standard culture conditions and at high concentrations they are transformed to pro-oxidants by producing significant amounts of H_2O_2. The adverse effects on cell viability are not observed only in cancer cells but also in normal cells. Our results, that provide the exact mechanism of H_2O_2 production by the two main olive polyphenols in the culture media and their effect on normal and cancer cells, together with the exact molecular mechanism of death, raise serious questions regarding data interpretation of previous *in vitro* studies with these polyphenols.

6 CONCLUSIONS

In the present work, we thoroughly evaluated the *in vitro* reported anticancer property of the main secoiridoid of the olive plant, oleuropein. We have shown that the observed selective anticancer activity is misleading and the result of the extracellular production of H_2O_2 through its metabolite hydroxytyrosol. Specifically, we have determined the responsible components that promote or retard the H_2O_2 production by oleuropein and hydroxytyrosol under standard culture conditions and the mechanism of cell death.

Our results indicate that a lot of *in vitro* studies concerning the anticancer effect of these and probably other similar phytochemical agents need thorough evaluation in order for one to be completely sure for their validity. The culture medium is highly crucial for the interpretation of the results and often leads to misleading conclusions.

For the first time, we have explained the observed anticancer activity of oleuropein and associated it with the production of H_2O_2 in the culture medium. We have also rejected previous statement that normal cells are resistant to oleuropein.

We suggest that when studying potent anti cancer agents, one has to be cautious with the interpretation of results, due to artifacts caused by the instability of the agents in the standard culture conditions.

Our study was conducted for evaluation of the reported *in vitro* anticancer activity of oleuropein and by no means intents to dispute the protective effects of oleuropein in cells and *in vivo*.

REFERENCES

[1] R.F. R. Fabiani, F. Pieravanti, A. De Bartolomeo, G. Morozzi,, Production of hydrogen peroxide is responsible for the induction of apoptosis by hydroxytyrosol on HL60 cells, Mol Nutr Food Res, 53 (2009) 887-896.

[2] R. Fabiani, P. Rosignoli, A. De Bartolomeo, R. Fuccelli, M. Servili, G. Morozzi, The production of hydrogen peroxide is not a common mechanism by which olive oil phenols induce apoptosis on HL60 cells., Food Chemistry 125 (2011) 1249-1255.

[3] L.H. Long, A. Hoi, B. Halliwell, Instability of, and generation of hydrogen peroxide by, phenolic compounds in cell culture media, Arch Biochem Biophys 501 (2010) 162-169.

[4] J. Ferlay, H.R. Shin, F. Bray, D. Forman, C. Mathers, D.M. Parkin, Estimates of worldwide burden of cancer in 2008: GLOBOCAN 2008, Int J Cancer 127 (2010) 2893-2917.

[5] A. Hadjisavvas, M.A. Loizidou, N. Middleton, T. Michael, R. Papachristoforou, E. Kakouri, M. Daniel, P. Papadopoulos, S. Malas, Y. Marcou, K. Kyriacou, An investigation of breast cancer risk factors in Cyprus: a case control study, BMC Cancer 10 (2010) 447.

[6] C.A. Demetriou, A. Hadjisavvas, M.A. Loizidou, G. Loucaides, I. Neophytou, S. Sieri, E. Kakouri, N. Middleton, P. Vineis, K. Kyriacou, The mediterranean dietary pattern and breast cancer risk in Greek-Cypriot women: a case-control study, BMC Cancer 12 (2012) 113.

[7] F. Visioli, C. Galli, Biological properties of olive oil phytochemicals, Crit Rev Food Sci Nutr 42 (2002) 209-221.

[8] M. Servili, G.F. Montedoro, Contribution of phenolic compounds to virgin olive oil quality, European Journal of Lipid Science and Technology

104 (2002) 602-613.

[9] D. Boskou, Olive oil chemistry and technology, AOCS Press, Champaign IL (USA) (1996).

[10] A.U.R. Rahman, Iridoids and secoiridoids from Oleaceae, Studies in Natural Products Chemistry 32 (2005) 303-363

[11] E. Bourquelot, J.C.R. Vintilesco, Sur l'oleuropein, nouveau principe de nature glucosidique retre de l'olivier (Olea europaea L.), Cmpt. Rend. Herbd. Acad. Sci. 147 (1908) 533-535.

[12] L. Panizzi, M.L. Scarpati, G. Orient, The constitution of oleuropein, a bitter glucoside of the olive with hypotensive action., Gazz Chim Ital 90 (1960) 1449-1485.

[13] F. Gutierrez-Rosales, J.J. Rios, M.L. Gomez-Rey, Main polyphenols in the bitter taste of virgin olive oil. Structural confirmation by on-line high-performance liquid chromatography electrospray ionization mass spectrometry, J Agric Food Chem 51 (2003) 6021-6025.

[14] A. Ranalli, S. Contento, L. Lucera, M. Di Febo, D. Marchegiani, V. Di Fonzo, Factors affecting the contents of iridoid oleuropein in olive leaves (Olea europaea L.), J Agric Food Chem 54 (2006) 434-440.

[15] N. Damak, M. Bouaziz, M. Ayadi, S. Sayadi, M. Damak, Effect of the maturation process on the phenolic fractions, fatty acids, and antioxidant activity of the Chetoui olive fruit cultivar, J Agric Food Chem 56 (2008) 1560-1566.

[16] I. Kruk, H.Y. Aboul-Enein, T. Michalska, K. Lichszteld, A. Kladna, Scavenging of reactive oxygen species by the plant phenols genistein and oleuropein, Luminescence 20 (2005) 81-89.

[17] H.P. Fleming, W.M. Walter, Jr., J.L. Etchells, Antimicrobial properties of oleuropein and products of its hydrolysis from green olives, Appl Microbiol 26 (1973) 777-782.

[18] H.F. Al-Azzawie, M.S. Alhamdani, Hypoglycemic and antioxidant effect of oleuropein in alloxan-diabetic rabbits, Life Sci 78 (2006) 1371-1377.

[19] H. Jemai, A. El Feki, S. Sayadi, Antidiabetic and antioxidant effects of hydroxytyrosol and oleuropein from olive leaves in alloxan-diabetic rats, J Agric Food Chem 57 (2009) 8798-8804.

[20] J.H. Jiang, C.M. Jin, Y.C. Kim, H.S. Kim, W.C. Park, H. Park, Anti-toxoplasmosis effects of oleuropein isolated from Fraxinus rhychophylla, Biol Pharm Bull 31 (2008) 2273-2276.

[21] G. Zhao, Z. Yin, J. Dong, Antiviral efficacy against hepatitis B virus replication of oleuropein isolated from Jasminum officinale L. var. grandiflorum, J Ethnopharmacol 125 (2009) 265-268.

[22] S. Lee-Huang, P.L. Huang, D. Zhang, J.W. Lee, J. Bao, Y. Sun, Y.T. Chang, J. Zhang, Discovery of small-molecule HIV-1 fusion and integrase inhibitors oleuropein and hydroxytyrosol: Part I. fusion [corrected] inhibition, Biochem Biophys Res Commun 354 (2007) 872-878.

[23] S. Lee-Huang, P.L. Huang, D. Zhang, J.W. Lee, J. Bao, Y. Sun, Y.T. Chang, J. Zhang, Discovery of small-molecule HIV-1 fusion and integrase inhibitors oleuropein and hydroxytyrosol: part II. integrase inhibition, Biochem Biophys Res Commun 354 (2007) 879-884.

[24] P.M. Furneri, A. Marino, A. Saija, N. Uccella, G. Bisignano, In vitro antimycoplasmal activity of oleuropein, Int J Antimicrob Agents 20 (2002) 293-296.

[25] H. Zbidi, S. Salido, J. Altarejos, M. Perez-Bonilla, A. Bartegi, J.A. Rosado, G.M. Salido, Olive tree wood phenolic compounds with human platelet antiaggregant properties, Blood Cells Mol Dis 42 (2009) 279-285.

[26] H. Jemai, M. Bouaziz, I. Fki, A. El Feki, S. Sayadi, Hypolipidimic and antioxidant activities of oleuropein and its hydrolysis derivative-rich extracts from Chemlali olive leaves, Chem Biol Interact 176 (2008) 88-98.

[27] A. Ranalli, L. Lucera, S. Contento, Antioxidizing potency of phenol compounds in olive oil mill wastewater, J Agric Food Chem 51 (2003) 7636-7641.

[28] G. Bisignano, A. Tomaino, R. Lo Cascio, G. Crisafi, N. Uccella, A. Saija, On the in-vitro antimicrobial activity of oleuropein and hydroxytyrosol, J Pharm Pharmacol 51 (1999) 971-974.

[29] B. de Roos, X. Zhang, G. Rodriguez Gutierrez, S. Wood, G.J. Rucklidge, M.D. Reid, G.J. Duncan, L.L. Cantlay, G.G. Duthie, N. O'Kennedy, Anti-platelet effects of olive oil extract: in vitro functional and proteomic studies, Eur J Nutr 50 (2011) 553-562.

[30] P.M. Furneri, A. Piperno, A. Sajia, G. Bisignano, Antimycoplasmal activity of hydroxytyrosol, Antimicrob Agents Chemother 48 (2004) 4892-4894.

[31] S. Granados-Principal, J.L. Quiles, C.L. Ramirez-Tortosa, P. Sanchez-Rovira, M.C. Ramirez-Tortosa, Hydroxytyrosol: from laboratory investigations to future clinical trials, Nutr Rev 68 (2010) 191-206.

[32] H.K. Hamdi, R. Castellon, Oleuropein, a non-toxic olive iridoid, is an anti-tumor agent and cytoskeleton disruptor, Biochem Biophys Res Commun 334 (2005) 769-778.

[33] S. Granados-Principal, J.L. Quiles, C. Ramirez-Tortosa, P. Camacho-Corencia, P. Sanchez-Rovira, L. Vera-Ramirez, M.C. Ramirez-Tortosa, Hydroxytyrosol inhibits growth and cell proliferation and promotes high expression of sfrp4 in rat mammary tumours, Mol Nutr Food Res 55 Suppl 1 (2011) S117-126.

[34] C. Manna, P. Galletti, G. Maisto, V. Cucciolla, S. D'Angelo, V. Zappia, Transport mechanism and metabolism of olive oil hydroxytyrosol in Caco-2 cells, FEBS Lett 470 (2000) 341-344.

[35] N.H. Aziz, S.E. Farag, L.A. Mousa, M.A. Abo-Zaid, Comparative antibacterial and antifungal effects of some phenolic compounds, Microbios 93 (1998) 43-54.

[36] D. Zanichelli, T.A. Baker, M.N. Clifford, M.R. Adams, Inhibition of Staphylococcus aureus by oleuropein is mediated by hydrogen peroxide, J Food Prot 68 (2005) 1492-1496.

[37] V. Micol, N. Caturla, L. Perez-Fons, V. Mas, L. Perez, A. Estepa, The olive leaf extract exhibits antiviral activity against viral haemorrhagic septicaemia rhabdovirus (VHSV), Antiviral Res 66 (2005) 129-136.

[38] F. Visioli, G. Bellomo, C. Galli, Free radical-scavenging properties of olive oil polyphenols, Biochem Biophys Res Commun 247 (1998) 60-64.

[39] F. Visioli, C. Galli, Oleuropein protects low density lipoprotein from oxidation, Life Sci 55 (1994) 1965-1971.

[40] E. Coni, R. Di Benedetto, M. Di Pasquale, R. Masella, D. Modesti, R. Mattei, E.A. Carlini, Protective effect of oleuropein, an olive oil biophenol, on low density lipoprotein oxidizability in rabbits, Lipids 35 (2000) 45-54.

[41] P.R. Roberto Fabiani, Angelo De Bartolomeo, Raffaela Fuccelli, Maurizio Servili,, a.G.M. Gian Francesco Montedoro, Oxidative DNA Damage Is Prevented by Extracts of Olive Oil, Hydroxytyrosol, and Other Olive Phenolic Compounds in Human Blood Mononuclear Cells and HL60 Cells, J. Nutr. 138 (2008) 1411–1416.

[42] L. Nousis, P.T. Doulias, N. Aligiannis, D. Bazios, A. Agalias, D. Galaris, S. Mitakou, DNA protecting and genotoxic effects of olive oil related components in cells exposed to hydrogen peroxide, Free Radic Res 39 (2005) 787-795.

[43] J. Han, T.P. Talorete, P. Yamada, H. Isoda, Anti-proliferative and apoptotic effects of oleuropein and hydroxytyrosol on human breast cancer MCF-7 cells, Cytotechnology 59 (2009) 45-53.

[44] Z. Bouallagui, J. Han, H. Isoda, S. Sayadi, Hydroxytyrosol rich extract from olive leaves modulates cell cycle progression in MCF-7 human breast cancer cells, Food Chem Toxicol 49 179-184.

[45] M.H. Elamin, M.H. Daghestani, S.A. Omer, M.A. Elobeid, P. Virk, E.M. Al-Olayan, Z.K. Hassan, O.B. Mohammed, A. Aboussekhra, Olive oil oleuropein has anti-breast cancer properties with higher efficiency on ER-negative cells, Food Chem Toxicol 53C (2013) 310-316.

[46] R. Quirantes-Pine, G. Zurek, E. Barrajon-Catalan, C. Bassmann, V. Micol, A. Segura-Carretero, A. Fernandez-Gutierrez, A metabolite-profiling approach to assess the uptake and metabolism of phenolic compounds from olive leaves in SKBR3 cells by HPLC-ESI-QTOF-MS, J Pharm Biomed Anal 72 (2013) 121-126.

[47] R. Acquaviva, C. Di Giacomo, V. Sorrenti, F. Galvano, R. Santangelo, V. Cardile, S. Gangia, N. D'Orazio, N.G. Abraham, L. Vanella, Antiproliferative effect of oleuropein in prostate cell lines, Int J Oncol 41 (2012) 31-38.

[48] S. Fernandez-Arroyo, A. Gomez-Martinez, L. Rocamora-Reverte, R. Quirantes-Pine, A. Segura-Carretero, A. Fernandez-Gutierrez, J.A. Ferragut, Application of nanoLC-ESI-TOF-MS for the metabolomic analysis of phenolic compounds from extra-virgin olive oil in treated colon-cancer cells, J Pharm Biomed Anal 63 (2012) 128-134.

[49] M. Notarnicola, S. Pisanti, V. Tutino, D. Bocale, M.T. Rotelli, A. Gentile, V. Memeo, M. Bifulco, E. Perri, M.G. Caruso, Effects of olive oil polyphenols on fatty acid synthase gene expression and activity in human colorectal cancer cells, Genes Nutr 6 (2011) 63-69.

[50] R. Fabiani, A. De Bartolomeo, P. Rosignoli, M. Servili, R. Selvaggini, G.F. Montedoro, C. Di Saverio, G. Morozzi, Virgin olive oil phenols inhibit proliferation of human promyelocytic leukemia cells (HL60) by inducing apoptosis and differentiation, J Nutr 136 (2006) 614-619.

[51] J. Anter, Z. Fernandez-Bedmar, M. Villatoro-Pulido, S. Demyda-Peyras, M. Moreno-Millan, A. Alonso-Moraga, A. Munoz-Serrano, M.D. Luque de Castro, A pilot study on the DNA-protective, cytotoxic, and apoptosis-inducing properties of olive-leaf extracts, Mutat Res 723 (2011) 165-170.

[52] R. Fabiani, P. Rosignoli, A. De Bartolomeo, R. Fuccelli, G. Morozzi, Inhibition of cell cycle progression by hydroxytyrosol is associated with upregulation of cyclin-dependent protein kinase inhibitors p21(WAF1/Cip1) and p27(Kip1) and with induction of differentiation in HL60 cells, J Nutr 138 (2008) 42-48.

[53] S.A. Mijatovic, G.S. Timotijevic, D.M. Miljkovic, J.M. Radovic, D.D. Maksimovic-Ivanic, D.P. Dekanski, S.D. Stosic-Grujicic, Multiple antimelanoma potential of dry olive leaf extract, Int J Cancer 128 (2011) 1955-1965.

[54] Y. Son, Y.K. Cheong, N.H. Kim, H.T. Chung, D.G. Kang, H.O. Pae, Mitogen-Activated Protein Kinases and Reactive Oxygen Species: How Can ROS Activate MAPK Pathways?, J Signal Transduct 2011 (2011) 792639.

[55] G.P. Bienert, J.K. Schjoerring, T.P. Jahn, Membrane transport of hydrogen peroxide, Biochim Biophys Acta 1758 (2006) 994-1003.

[56] G.P. Bienert, A.L. Moller, K.A. Kristiansen, A. Schulz, I.M. Moller, J.K. Schjoerring, T.P. Jahn, Specific aquaporins facilitate the diffusion of hydrogen peroxide across membranes, J Biol Chem 282 (2007) 1183-1192.

[57] T. Ozben, Oxidative stress and apoptosis: impact on cancer therapy, J Pharm Sci 96 (2007) 2181-2196.

[58] B. Halliwell, Oxidative stress in cell culture: an under-appreciated problem?, FEBS Lett 540 (2003) 3-6.

[59] L.H. Long, M.V. Clement, B. Halliwell, Artifacts in cell culture: rapid generation of hydrogen peroxide on addition of (-)-epigallocatechin, (-)-epigallocatechin gallate, (+)-catechin, and quercetin to commonly used cell culture media, Biochem Biophys Res Commun 273 (2000) 50-53.

[60] S.C. Roques, N. Landrault, P.L. Teissedre, C. Laurent, P. Besancon, J.M. Rouane, B. Caporiccio, Hydrogen peroxide generation in caco-2 cell culture medium by addition of phenolic compounds: effect of ascorbic acid, Free Radic Res 36 (2002) 593-599.

[61] P. Bellion, M. Olk, F. Will, H. Dietrich, M. Baum, G. Eisenbrand, C. Janzowski, Formation of hydrogen peroxide in cell culture media by apple polyphenols and its effect on antioxidant biomarkers in the colon cell line HT-29, Mol Nutr Food Res 53 (2009) 1226-1236.

[62] P.C. Chai, L.H. Long, B. Halliwell, Contribution of hydrogen peroxide to the cytotoxicity of green tea and red wines, Biochem Biophys Res Commun 304 (2003) 650-654.

[63] T. Lapidot, M.D. Walker, J. Kanner, Can Apple Antioxidants Inhibit Tumor Cell Proliferation? Generation of H2O2 during Interaction of Phenolic Compounds with Cell Culture Media, J. Agric. Food Chem. 50 (2002) 3156-3160.

[64] R.H. Liu, J. Sun, Antiproliferative activity of apples is not due to phenolic-induced hydrogen peroxide formation, J Agric Food Chem 51 (2003) 1718-1723.

[65] R. Fabiani, Sepporta, M. V., Rosignoli, P., De Bartolomeo, A., Crescimanno M., Morozzi G.,, Anti-proliferative and pro-apoptotic activities of hydroxytyrosol on different tumour cells: the role of extracellular production of hydrogen peroxide, Eur J Nutr 51 (2012) 455-464.

[66] G.L. Johnson, R. Lapadat, Mitogen-activated protein kinase pathways mediated by ERK, JNK, and p38 protein kinases, Science 298 (2002) 1911-1912.

[67] P.P. Roux, J. Blenis, ERK and p38 MAPK-activated protein kinases: a family of protein kinases with diverse biological functions, Microbiol Mol Biol Rev 68 (2004) 320-344.

[68] L.A. Hibi M, Smeal T, Minden A, Karin M., Identification of an oncoprotein- and UV-responsive protein kinase that binds and potentiates the c-Jun activation domain Genes Dev. 7 (1993) 2135-2148.

[69] S. Zhang, Y. Lin, Y.S. Kim, M.P. Hande, Z.G. Liu, H.M. Shen, c-Jun N-terminal kinase mediates hydrogen peroxide-induced cell death via sustained poly(ADP-ribose) polymerase-1 activation, Cell Death Differ 14 (2007) 1001-1010.

[70] Y. Xu, S. Huang, Z.G. Liu, J. Han, Poly(ADP-ribose) polymerase-1 signaling to mitochondria in necrotic cell death requires RIP1/TRAF2-mediated JNK1 activation, J Biol Chem 281 (2006) 8788-8795.

[71] J.Y. Son Yo, Shi X, Lee JC., Activation of JNK and c-Jun is involved in glucose oxidase-mediated cell death of human lymphoma cells., Mol Cells. 28 (2009) 545-551.

[72] A. Cuadrado, A.R. Nebreda, Mechanisms and functions of p38 MAPK signalling, Biochem J 429 (2010) 403-417.

[73] L. New, J. Han, The p38 MAP kinase pathway and its biological function, Trends Cardiovasc Med 8 (1998) 220-228.

[74] A. Gutierrez-Uzquiza, M. Arechederra, P. Bragado, J.A. Aguirre-Ghiso, A. Porras, p38alpha mediates cell survival in response to oxidative stress via induction of antioxidant genes: effect on the p70S6K pathway, J Biol Chem 287 (2012) 2632-2642.

[75] A. Porras, S. Zuluaga, E. Black, A. Valladares, A.M. Alvarez, C. Ambrosino, M. Benito, A.R. Nebreda, P38 alpha mitogen-activated protein kinase sensitizes cells to apoptosis induced by different stimuli, Mol Biol Cell 15 (2004) 922-933.

[76] S. Zhuang, R.G. Schnellmann, A death-promoting role for extracellular signal-regulated kinase, J Pharmacol Exp Ther 319 (2006) 991-997.

[77] X. Wang, J.L. Martindale, Y. Liu, N.J. Holbrook, The cellular response to oxidative stress: influences of mitogen-activated protein kinase signalling pathways on cell survival, Biochem J 333 (Pt 2) (1998) 291-300.

[78] T. Kurosaki, H. Ushiro, Y. Mitsuuchi, S. Suzuki, M. Matsuda, Y. Matsuda, N. Katunuma, K. Kangawa, H. Matsuo, T. Hirose, et al., Primary structure of human poly(ADP-ribose) synthetase as deduced from cDNA sequence, J Biol Chem 262 (1987) 15990-15997.

[79] D. D'Amours, S. Desnoyers, I. D'Silva, G.G. Poirier, Poly(ADP-ribosyl)ation reactions in the regulation of nuclear functions, Biochem J 342 (Pt 2) (1999) 249-268.

[80] J.C. Ame, C. Spenlehauer, G. de Murcia, The PARP superfamily, Bioessays 26 (2004) 882-893.

[81] N.A. Berger, Poly(ADP-ribose) in the cellular response to DNA damage, Radiat Res 101 (1985) 4-15.

[82] V.J. Bouchard, M. Rouleau, G.G. Poirier, PARP-1, a determinant of cell survival in response to DNA damage, Exp Hematol 31 (2003) 446-454.

[83] P. Jagtap, C. Szabo, Poly(ADP-ribose) polymerase and the therapeutic effects of its inhibitors, Nat Rev Drug Discov 4 (2005) 421-440.

[84] M. Tewari, L.T. Quan, K. O'Rourke, S. Desnoyers, Z. Zeng, D.R. Beidler, G.G. Poirier, G.S. Salvesen, V.M. Dixit, Yama/CPP32 beta, a mammalian homolog of CED-3, is a CrmA-inhibitable protease that cleaves the death substrate poly(ADP-ribose) polymerase, Cell 81 (1995) 801-809.

[85] M. Germain, E.B. Affar, D. D'Amours, V.M. Dixit, G.S. Salvesen, G.G. Poirier, Cleavage of automodified poly(ADP-ribose) polymerase during apoptosis. Evidence for involvement of caspase-7, J Biol Chem 274 (1999) 28379-28384.

[86] Y.A. Lazebnik, S.H. Kaufmann, S. Desnoyers, G.G. Poirier, W.C. Earnshaw, Cleavage of poly(ADP-ribose) polymerase by a proteinase with properties like ICE, Nature 371 (1994) 346-347.

[87] Z. Herceg, Z.Q. Wang, Failure of poly(ADP-ribose) polymerase cleavage by caspases leads to induction of necrosis and enhanced apoptosis, Mol Cell Biol 19 (1999) 5124-5133.

[88] M.E. Smulson, D. Pang, M. Jung, A. Dimtchev, S. Chasovskikh, A. Spoonde, C. Simbulan-Rosenthal, D. Rosenthal, A. Yakovlev, A. Dritschilo, Irreversible binding of poly(ADP)ribose polymerase cleavage product to DNA ends revealed by atomic force microscopy: possible role in apoptosis, Cancer Res 58 (1998) 3495-3498.

[89] G.M. Shah, R.G. Shah, G.G. Poirier, Different cleavage pattern for poly(ADP-ribose) polymerase during necrosis and apoptosis in HL-60 cells, Biochem Biophys Res Commun 229 (1996) 838-844.

[90] C.A. Casiano, R.L. Ochs, E.M. Tan, Distinct cleavage products of nuclear proteins in apoptosis and necrosis revealed by autoantibody probes, Cell Death Differ 5 (1998) 183-190.

[91] S. Gobeil, C.C. Boucher, D. Nadeau, G.G. Poirier, Characterization of the necrotic cleavage of poly(ADP-ribose) polymerase (PARP-1): implication of lysosomal proteases, Cell Death Differ 8 (2001) 588-594.

[92] R.K. Sodhi, N. Singh, A.S. Jaggi, Poly(ADP-ribose) polymerase-1 (PARP-1) and its therapeutic implications, Vascul Pharmacol 53 (2010) 77-87.

[93] A.M. Gardner, F.H. Xu, C. Fady, F.J. Jacoby, D.C. Duffey, Y. Tu, A. Lichtenstein, Apoptotic vs. nonapoptotic cytotoxicity induced by hydrogen peroxide, Free Radic Biol Med 22 (1997) 73-83.

[94] P. Chambon, J.D. Weill, P. Mandel, Nicotinamide mononucleotide activation of new DNA-dependent polyadenylic acid synthesizing nuclear enzyme, Biochem Biophys Res Commun 11 (1963) 39-43.

[95] K.N. Andrabi SA, Yu SW, Wang H, Koh DW, Sasaki M, Klaus JA, Otsuka T, Zhang Z, Koehler RC, Hurn PD, Poirier GG, Dawson VL, Dawson TM, Poly(ADP-ribose) (PAR) polymer is a death signal., Proc Natl Acad Sci 103 (2006) 18308-18313.

[96] S.W. Yu, S.A. Andrabi, H. Wang, N.S. Kim, G.G. Poirier, T.M. Dawson, V.L. Dawson, Apoptosis-inducing factor mediates poly(ADP-ribose) (PAR) polymer-induced cell death, Proc Natl Acad Sci U S A 103 (2006) 18314-18319.

[97] K.N. Wang Y, Haince JF, Kang HC, David KK, Andrabi SA, Poirier GG, Dawson VL, Dawson TM, Poly(ADP-ribose) (PAR) binding to apoptosis-inducing factor is critical for PAR polymerase-1-dependent cell death (parthanatos), Sci Signal. 4 (2011) 167.

[98] Y.O. Son, Y.S. Jang, J.S. Heo, W.T. Chung, K.C. Choi, J.C. Lee, Apoptosis-inducing factor plays a critical role in caspase-independent, pyknotic cell death in hydrogen peroxide-exposed cells, Apoptosis 14 (2009) 796-808.

[99] N. Modjtahedi, F. Giordanetto, F. Madeo, G. Kroemer, Apoptosis-inducing factor: vital and lethal, Trends Cell Biol 16 (2006) 264-272.

[100] S.A. Susin, H.K. Lorenzo, N. Zamzami, I. Marzo, B.E. Snow, G.M. Brothers, J. Mangion, E. Jacotot, P. Costantini, M. Loeffler, N. Larochette, D.R. Goodlett, R. Aebersold, D.P. Siderovski, J.M. Penninger, G. Kroemer, Molecular characterization of mitochondrial apoptosis-inducing factor, Nature 397 (1999) 441-446.

[101] S.A. Susin, N. Zamzami, M. Castedo, T. Hirsch, P. Marchetti, A. Macho, E. Daugas, M. Geuskens, G. Kroemer, Bcl-2 inhibits the mitochondrial release of an apoptogenic protease, J Exp Med 184 (1996) 1331-1341.

[102] S.W. Yu, H. Wang, M.F. Poitras, C. Coombs, W.J. Bowers, H.J. Federoff, G.G. Poirier, T.M. Dawson, V.L. Dawson, Mediation of poly(ADP-ribose) polymerase-1-dependent cell death by apoptosis-inducing factor, Science 297 (2002) 259-263.

[103] Y. Wang, N.S. Kim, X. Li, P.A. Greer, R.C. Koehler, V.L. Dawson, T.M. Dawson, Calpain activation is not required for AIF translocation in PARP-1-dependent cell death (parthanatos). J Neurochem. 110 (2009) 687-696.

[104] A.S. David KK, Dawson TM, Dawson VL., Parthanatos, a messenger of death., Front Biosci. 14 (2009) 1116-1128.

[105] Y. Wang, V.L. Dawson, T.M. Dawson, Poly(ADP-ribose) signals to mitochondrial AIF: a key event in parthanatos, Exp Neurol 218 (2009) 193-202.

[106] M.J. Berridge, Inositol trisphosphate and calcium signalling, Nature 361 (1993) 315-325.

[107] A. Galat, S.M. Metcalfe, Peptidylproline cis/trans isomerases, Prog Biophys Mol Biol 63 (1995) 67-118.

[108] T.T. Lynda J. Kieffer, and Robert E. Handschumachern, Isolation and characterization of a 40-kDa cyclophilin-related protein, J Biol Chem 267 (1992) 5503-5507.

[109] T. Nakagawa, S. Shimizu, T. Watanabe, O. Yamaguchi, K. Otsu, H. Yamagata, H. Inohara, T. Kubo, Y. Tsujimoto, Cyclophilin D-dependent mitochondrial permeability transition regulates some necrotic but not apoptotic cell death, Nature 434 (2005) 652-658.

[110] C.P. Baines, R.A. Kaiser, N.H. Purcell, N.S. Blair, H. Osinska, M.A. Hambleton, E.W. Brunskill, M.R. Sayen, R.A. Gottlieb, G.W. Dorn, J. Robbins, J.D. Molkentin, Loss of cyclophilin D reveals a critical role for mitochondrial permeability transition in cell death, Nature 434 (2005) 658-662.

[111] K. Andrabi, N. Kaul, N.K. Ganguly, J.B. Dilawari, Altered calcium homeostasis in carbon tetrachloride exposed rat hepatocytes, Biochem Int 18 (1989) 1287-1295.

[112] A.P. Halestrap, G.P. McStay, S.J. Clarke, The permeability transition pore complex: another view, Biochimie 84 (2002) 153-166.

[113] M. Crompton, H. Ellinger, A. Costi, Inhibition by cyclosporin A of a Ca2+-dependent pore in heart mitochondria activated by inorganic phosphate and oxidative stress, Biochem J 255 (1988) 357-360.

[114] A.P. Halestrap, S.J. Clarke, S.A. Javadov, Mitochondrial permeability transition pore opening during myocardial reperfusion--a target for cardioprotection, Cardiovasc Res 61 (2004) 372-385.

[115] G. Weissmann, Analytical Review: Lysosomes, blood 24 (1964) 594-606.

[116] C. De Duve, B.C. Pressman, R. Gianetto, R. Wattiaux, F. Appelmans, Tissue fractionation studies. 6. Intracellular distribution patterns of enzymes in rat-liver tissue, Biochem J 60 (1955) 604-617.

[117] C. de Duve, Lysosomes revisited, Eur J Biochem 137 (1983) 391-397.

[118] P. Boya, G. Kroemer, Lysosomal membrane permeabilization in cell death, Oncogene 27 (2008) 6434-6451.

[119] K. Ollinger, U.T. Brunk, Cellular injury induced by oxidative stress is mediated through lysosomal damage, Free Radic Biol Med 19 (1995) 565-574.

[120] T. Kurz, B. Gustafsson, U.T. Brunk, Intralysosomal iron chelation protects against oxidative stress-induced cellular damage, FEBS J 273 (2006) 3106-3117.

[121] H.J.H. Fenton, The oxidation of tartaric acid in presence of iron J. Chem. Soc. Proc. 10 (1894) 157-158.

[122] F. Haber, J. Weiss, The catalytic decomposition of hydrogen peroxide by iron salts Proc. Roy. Soc. 147 (1934) 332-351.

[123] C.C. Winterbourn, Toxicity of iron and hydrogen peroxide: the Fenton reaction, Toxicol Lett 82-83 (1995) 969-974.

[124] M. Dizdaroglu, G. Rao, B. Halliwell, E. Gajewski, Damage to the DNA bases in mammalian chromatin by hydrogen peroxide in the presence of ferric and cupric ions, Arch Biochem Biophys 285 (1991) 317-324.

[125] A. Barbouti, P.T. Doulias, B.Z. Zhu, B. Frei, D. Galaris, Intracellular iron, but not copper, plays a critical role in hydrogen peroxide-induced DNA damage, Free Radic Biol Med. 31 (2001) 490-498.

[126] T. Kurz, A. Leake, T. Von Zglinicki, U.T. Brunk, Relocalized redox-active lysosomal iron is an important mediator of oxidative-stress-induced DNA damage, Biochem J 378 (2004) 1039-1045.

[127] T. Kurz, A. Leake, T. von Zglinicki, U.T. Brunk, Lysosomal redox-active iron is important for oxidative stress-induced DNA damage, Ann N Y Acad Sci 1019 (2004) 285-288.

[128] N. Festjens, T. Vanden Berghe, P. Vandenabeele, Necrosis, a well-orchestrated form of cell demise: signalling cascades, important mediators and concomitant immune response, Biochim Biophys Acta 1757 (2006) 1371-1387.

[129] G. Kroemer, L. Galluzzi, P. Vandenabeele, J. Abrams, E.S. Alnemri, E.H. Baehrecke, M.V. Blagosklonny, W.S. El-Deiry, P. Golstein, D.R. Green, M. Hengartner, R.A. Knight, S. Kumar, S.A. Lipton, W. Malorni, G. Nunez, M.E. Peter, J. Tschopp, J. Yuan, M. Piacentini, B. Zhivotovsky, G. Melino, Classification of cell death: recommendations of the Nomenclature Committee on Cell Death 2009, Cell Death Differ 16 (2009) 3-11.

[130] N.A. Thornberry, Y. Lazebnik, Caspases: enemies within, Science 281 (1998) 1312-1316.

[131] S.K.a.A. Kikuchi, DNA topoisomerase: the key enzyme that regulates DNA super structure Nagoya J. Med. Sci. 61 (1998) 11-26.

[132] M.-C.C. Gálvez M, Ayuso MJ, Iridoids as DNA topoisomerase I poisons, J Enzyme Inhib Med Chem. 20 (2005) 389-392.

[133] Y. Pommier, DNA topoisomerase I inhibitors: chemistry, biology, and interfacial inhibition, Chem Rev 109 (2009) 2894-2902.

[134] J.L. Nitiss, Targeting DNA topoisomerase II in cancer chemotherapy, Nat Rev Cancer 9 (2009) 338-350.

[135] I.S. Wood, P. Trayhurn, Glucose transporters (GLUT and SGLT): expanded families of sugar transport proteins, Br J Nutr 89 (2003) 3-9.

[136] M. Grover-McKay, S.A. Walsh, E.A. Seftor, P.A. Thomas, M.J. Hendrix, Role for glucose transporter 1 protein in human breast cancer, Pathol Oncol Res 4 (1998) 115-120.

[137] D.L. Betz AL, Gilboe DD, Inhibition of glucose transport into brain by phlorizin, phloretin and glucose analogues, Biochimica et Biophysica Acta (BBA) - Biomembranes 406 (1975) 505–515.

[138] J.A. Nelson, R.E. Falk, Phloridzin and phloretin inhibition of 2-deoxy-D-glucose uptake by tumor cells in vitro and in vivo, Anticancer Res 13 (1993) 2293-2299.

[139] T.E. Wood, S. Dalili, C.D. Simpson, R. Hurren, X. Mao, F.S. Saiz, M. Gronda, Y. Eberhard, M.D. Minden, P.J. Bilan, A. Klip, R.A. Batey, A.D. Schimmer, A novel inhibitor of glucose uptake sensitizes cells to FAS-induced cell death, Mol Cancer Ther 7 (2008) 3546-3555.

[140] A. Agalias, P. Magiatis, A.L. Skaltsounis, E. Mikros, A. Tsarbopoulos, E. Gikas, I. Spanos, T. Manios, A new process for the management of olive oil mill waste water and recovery of natural antioxidants, J Agric Food Chem 55 (2007) 2671-2676.

[141] A.J. Raffo, A.L. Kim, R.L. Fine, Formation of nuclear Bax/p53 complexes is associated with chemotherapy induced apoptosis, Oncogene 19 (2000) 6216-6228.

[142] H. Babich, E.J. Liebling, R.F. Burger, H.L. Zuckerbraun, A.G. Schuck, Choice of DMEM, formulated with or without pyruvate, plays an important role in assessing the in vitro cytotoxicity of oxidants and prooxidant nutraceuticals, In Vitro Cell Dev Biol Anim 45 (2009) 226-233.

[143] L.H. Long, B. Halliwell, Artefacts in cell culture: pyruvate as a scavenger of hydrogen peroxide generated by ascorbate or epigallocatechin gallate in cell culture media, Biochem Biophys Res Commun 388 (2009) 700-704.

[144] M. Akagawa, T. Shigemitsu, K. Suyama, Production of hydrogen peroxide by polyphenols and polyphenol-rich beverages under quasi-physiological conditions, Biosci Biotechnol Biochem 67 (2003) 2632-2640.

[145] T. Ozbay, R. Nahta, Delphinidin Inhibits HER2 and Erk1/2 Signaling and Suppresses Growth of HER2-Overexpressing and Triple Negative Breast Cancer Cell Lines, Breast Cancer (Auckl) 5 (2011) 143-154.

[146] K. Landis-Piwowar, D. Chen, T.H. Chan, Q.P. Dou, Inhibition of catechol-Omicron-methyltransferase activity in human breast cancer cells enhances the biological effect of the green tea polyphenol (-)-EGCG, Oncol Rep 24 (2010) 563-569.

[147] N.C. Yang, C.H. Lee, T.Y. Song, Evaluation of resveratrol oxidation in vitro and the crucial role of bicarbonate ions, Biosci Biotechnol Biochem 74 (2010) 63-68.

[148] M. Chen, Z. Zsengeller, C.Y. Xiao, C. Szabo, Mitochondrial-to-nuclear translocation of apoptosis-inducing factor in cardiac myocytes during oxidant stress: potential role of poly(ADP-ribose) polymerase-1, Cardiovasc Res 63 (2004) 682-688.

[149] S. Sperandio, K. Poksay, I. de Belle, M.J. Lafuente, B. Liu, J. Nasir, D.E. Bredesen, Paraptosis: mediation by MAP kinases and inhibition by AIP-1/Alix, Cell Death Differ 11 (2004) 1066-1075.

[150] A.J. Watson, J.N. Askew, R.S. Benson, Poly(adenosine diphosphate ribose) polymerase inhibition prevents necrosis induced by H2O2 but not apoptosis, Gastroenterology 109 (1995) 472-482.

[151] M.X. Filipovic DM, Reeves WB, Inhibition of PARP prevents oxidant-induced necrosis but not apoptosis in LLC-PK1 cells., Am J Physiol. 277 (1999) 428-436.

[152] W.L. Liu, X. Guo, Z.G. Guo, Effects of p38 and p42/p44 CCDPK signaling on H2O2-induced apoptosis in bovine aortic endothelial cells, Acta Pharmacol Sin 21 (2000) 991-996.

[153] S.M. Chuang, G.Y. Liou, J.L. Yang, Activation of JNK, p38 and ERK mitogen-activated protein kinases by chromium(VI) is mediated through oxidative stress but does not affect cytotoxicity, Carcinogenesis 21 (2000) 1491-1500.

[154] S.A. Andrabi, N.S. Kim, S.W. Yu, H. Wang, D.W. Koh, M. Sasaki, J.A. Klaus, T. Otsuka, Z. Zhang, R.C. Koehler, P.D. Hurn, G.G. Poirier, V.L. Dawson, T.M. Dawson, Poly(ADP-ribose) (PAR) polymer is a death signal, Proc Natl Acad Sci U S A 103 (2006) 18308-18313.

[155] V. Borutaite, G.C. Brown, Caspases are reversibly inactivated by hydrogen peroxide, FEBS Lett 500 (2001) 114-118.

[156] M.B. Hampton, S. Orrenius, Dual regulation of caspase activity by hydrogen peroxide: implications for apoptosis, FEBS Lett 414 (1997) 552-556.

[157] O.I. Aruoma, B. Halliwell, B.M. Hoey, J. Butler, The antioxidant action of N-acetylcysteine: its reaction with hydrogen peroxide, hydroxyl radical, superoxide, and hypochlorous acid, Free Radic Biol Med 6 (1989) 593-597.

[158] T. Vanden Berghe, N. Vanlangenakker, E. Parthoens, W. Deckers, M. Devos, N. Festjens, C.J. Guerin, U.T. Brunk, W. Declercq, P. Vandenabeele, Necroptosis, necrosis and secondary necrosis converge on similar cellular disintegration features, Cell Death Differ 17 (2010) 922-930.

[159] J.A. Menendez, A. Vazquez-Martin, R. Colomer, J. Brunet, A. Carrasco-Pancorbo, R. Garcia-Villalba, A. Fernandez-Gutierrez, A. Segura-Carretero, Olive oil's bitter principle reverses acquired autoresistance to trastuzumab (Herceptin) in HER2-overexpressing breast cancer cells, BMC Cancer 7 (2007) 80.

[160] J.A. Menendez, A. Vazquez-Martin, R. Garcia-Villalba, A. Carrasco-Pancorbo, C. Oliveras-Ferraros, A. Fernandez-Gutierrez, A. Segura-Carretero, tabAnti-HER2 (erbB-2) oncogene effects of phenolic compounds directly isolated from commercial Extra-Virgin Olive Oil (EVOO), BMC Cancer 8 (2008) 377.

[161] R. Fabiani, P. Rosignoli, A. De Bartolomeo, R. Fuccelli, M. Servili, G.F. Montedoro, G. Morozzi, Oxidative DNA damage is prevented by extracts of olive oil,

hydroxytyrosol, and other olive phenolic compounds in human blood mononuclear cells and HL60 cells, J Nutr 138 (2008) 1411-1416.

[162] Z.P. Vissers MN., Katan MB.,, Bioavailability and antioxidant effects of olive oil phenols in humans: a review, European Journal of Clinical Nutrition 58 (2004) 955-965.

[163] E. Miro-Casas, M.I. Covas, M. Farre, M. Fito, J. Ortuno, T. Weinbrenner, P. Roset, R. de la Torre, Hydroxytyrosol disposition in humans, Clin Chem 49 (2003) 945-952.